Document made available under the Patent Cooperation Treaty (PCT)

International application number: PCT/US05/006692

International filing date: 04 March 2005 (04.03.2005)

Document type: Certified copy of priority document

Document details: Country/Office: US
Number: 60/550,816
Filing date: 05 March 2004 (05.03.2004)

Date of receipt at the International Bureau: 04 July 2005 (04.07.2005)

Remark: Priority document submitted or transmitted to the International Bureau in compliance with Rule 17.1(a) or (b)

THE UNITED STATES OF AMERICA

TO ALL TO WHOM THESE PRESENTS; SHALL COME:

UNITED STATES DEPARTMENT OF COMMERCE

United States Patent and Trademark Office

June 24, 2005

THIS IS TO CERTIFY THAT ANNEXED HERETO IS A TRUE COPY FROM THE RECORDS OF THE UNITED STATES PATENT AND TRADEMARK OFFICE OF THOSE PAPERS OF THE BELOW IDENTIFIED PATENT APPLICATION THAT MET THE REQUIREMENTS TO BE GRANTED A FILING DATE.

APPLICATION NUMBER: *60/550,816*
FILING DATE: *March 05, 2004*
RELATED PCT APPLICATION NUMBER: *PCT/US05/06692*

Certified by

Jon W. Dudas

Under Secretary of Commerce
for Intellectual Property
and Director of the United States
Patent and Trademark Office

PROVISIONAL APPLICATION FOR PATENT COVER SHEET

This is a request for filing a PROVISIONAL APPLICATION FOR PATENT under 37 CFR 1.53(c).

Express Mail Label No.	EL 179781578US

INVENTOR(S)

Given Name (first and middle [if any])	Family Name or Surname	Residence (City and either State or Foreign Country)
James F.	Leary	Galveston, Texas
Tarl W.	Prow	Baltimore, Maryland

☐ Additional inventors are being named on the _____ separately numbered sheets attached hereto

TITLE OF THE INVENTION (500 characters max)

Molecular Programming of Nanoparticle Systems for an Ordered and Controlled Sequence of Events for Gene-Drug Delivery

Direct all correspondence to:	**CORRESPONDENCE ADDRESS**	
☑ Customer Number	22904 ⟶	Place Customer Number Bar Code Label here
OR	Type Customer Number here	

☐	Firm or Individual Name	
Address		
Address		
City		State		ZIP	
Country		Telephone		Fax	

ENCLOSED APPLICATION PARTS (check all that apply)

☑ Specification Number of Pages		☐ CD(s), Number	
☑ Drawing(s) Number of Sheets		☑ Other (specify)	post card
☐ Application Data Sheet. See 37 CFR 1.76			

METHOD OF PAYMENT OF FILING FEES FOR THIS PROVISIONAL APPLICATION FOR PATENT

		FILING FEE AMOUNT ($)
☑ Applicant claims small entity status. See 37 CFR 1.27.		
☐ A check or money order is enclosed to cover the filing fees		
☑ The Commissioner is hereby authorized to charge filing fees or credit any overpayment to Deposit Account Number:	12-1322/021101-00400	$80.00
☐ Payment by credit card. Form PTO-2038 is attached.		

The invention was made by an agency of the United States Government or under a contract with an agency of the United States Government.
☐ No.
☑ Yes, the name of the U.S. Government agency and the Government contract number are: NAS 02059
  National Aeronautics and Space Administration

Respectfully submitted,	Date 3/5/04
SIGNATURE _____	
TYPED or PRINTED NAME D. Brit Nelson	REGISTRATION NO. 40,370
	(if appropriate)
TELEPHONE 713.226.1361	Docket Number: 021101-00400

USE ONLY FOR FILING A PROVISIONAL APPLICATION FOR PATENT

INVENTORS: JAMES F. LEARY, TARL W. PROW

TITLE: MOLECULAR PROGRAMMING OF NANOPARTICLE SYSTEMS
FOR AN ORDERED AND CONTROLLED SEQUENCE OF
EVENTS FOR GENE-DRUG DELIVERY

SPECIFICATION

FIELD OF THE INVENTION

The present invention relates to the delivery of one or more drugs to an organism. More particularly, the present invention relates to a nanoparticle system for a selective delivery of the drugs.

BACKGROUND OF THE INVENTION

Usually targeted delivery of drugs or genes to a cell only concerns itself with the first stage of targeting to the cell surface. But that is only the first stage of a multi-stage process of drug-gene delivery which must occur in a controlled sequence to be successful and/or effective. There must also be a multi-step intracellular molecular targeting process. These drugs or genes must survive the different intracellular microenvironments on the way to their site of action within the cell and must be guided by physical or molecular mechanisms to the site of action within a cell. Since delivery of a drug to a cell in-vivo is a "rare-event", there must be error-checking within the system in addition to the molecular targeting since it is difficult or impossible to not make mistakes in targeting. In order to perform a controlled drug or gene delivery inside single living cells, it is necessary to have feedback control in the drug-gene

delivery system. There are many ways to accomplish this. One way is through the use of molecular biosensors which are connected to the nanosystems. These biosensors can not only sense targets but also respond in feedback loops to the relative amount of cellular molecular responses to the drug or gene delivery. Since it is difficult to deliver enough drug or gene therapy contained in or on the nanoparticle, the idea is to send nanoparticles containing the molecular machinery (e.g. gene sequences that can be transcribed by the host cell or enzymes) for reorganizing or synthesizing therapeutic molecules from raw materials within the cells.

Competing systems have only gone as far as use of initial targeting molecules on nanoparticles and further refinements in encapsulation of drugs or genes. The concept that nanodelivery of drugs or genes is a multistep process that must be done in a controlled sequence of events, including error-checking, intracellular positioning and feedback control is not obvious to those with ordinary skill in the art working in this area.

Therefore, there remains a need for such a system and process.

SUMMARY OF THE INVENTION

The present invention provides method, apparatus, and system to produce multifunctional and multi-step nanoparticle systems that follow a predictable and well defined sequence of events ("molecular programming") as laid out by a molecular chain of events. These events include, but are not limited to, events such as initial cell targeting, facilitation of cell entry, intracellular re-targeting, intracellular anchoring to the site of drug/gene delivery, drug or gene delivery, and controlled delivery of the drugs or genes within single cells through feedback loops facilitated by molecular biosensors and other molecules.

In one or more embodiments, the invention can provide:

A multifunctional and multi-step nanodelivery system consisting of targeting molecules, entry facilitating molecules, re-targeting molecules, anchoring molecules, drugs or genes that are either driven or controlled through molecular biosensor feedback loops for controlled drug-gene delivery

A nanodelivery system with molecular error-checking based on desired or permissible Boolean logic conditions (based on presence or absence of specific molecules on or within the cell) to reduce false positive targeting which then lowers undesired, adverse bystander side reactions

A nanosystem having molecules that use, create or reorganize molecules already within individual living cells such that a single nanoparticle can manufacture enough drugs or genes to have a therapeutic response. This can solve the problem of how to deliver enough drugs or genes to single cells in-vivo to achieve therapeutic value.

A nanosystem that positions itself at the active site of importance for subsequent drug-gene delivery within a single living cell through the use of localization or anchoring sequences.

A nanosystem that uses feedback loop molecules, such as molecular biosensors, to provide for controlled drug-gene delivery in continuous response to single cell drug-gene delivery at earlier timepoints.

BRIEF DESCRIPTION OF THE DRAWINGS

A more particular description of the invention, briefly summarized above, may be had by reference to the embodiments thereof which are illustrated in the appended drawings of the documents attached to this application and described therein. It is to be noted, however, that the

appended drawings illustrate only some embodiments of the invention and are therefore not to be considered limiting of its scope, because the invention may admit to other equally effective embodiments.

The figures are described below at each relevant point of the disclosure with cross references to other figures.

DETAILED DESCRIPTION OF A PREFERRED EMBODIMENT

Figure 1 is a schematic diagram of the present invention illustrating the targeted programmed sequence of events that can be used in conjunction therewith. The use of a programmed sequence of events, including Boolean combinations of targeting molecules, re-targeting, intracellular localization and feedback control of drugs in nanosystems through the use of molecular biosensors or other molecules, and molecular error checking, is novel and nonobvious as an integrated nanosystem.

1. The present invention can provide a multifunctional and multi-step nanodelivery system consisting of targeting molecules, entry facilitating molecules, re-targeting molecules, anchoring molecules, drugs or genes that are either driven or controlled through molecular biosensor feedback loops for controlled drug-gene delivery

The multilayered nanoparticles are constructed in reverse "molecular programming" order. The innermost layers of the multilayered nanoparticle contain molecules which occur latest in the order of events (e.g. biosensing and drug delivery molecules). The outermost layer of the multilayered nanoparticle contains the events which must occur first (e.g. cell targeting and entry molecules). Intermediate layers may contain molecules for intermediate steps (e.g.

intracellular localization molecular sequences for intermediate re-targeting to sites of action for drug/gene delivery). The process of molecular programming of nanoparticles systems involves layer-by-layer disassembly by any one or more of processes including, but not limited to: catalysis of molecules, conformational changes, protein digestion, ... The overall situation is depicted in **Figure 1** and as described briefly in the closing paragraph 8.8.2 of the Tarl Prow thesis (p. 207):

Figure 1

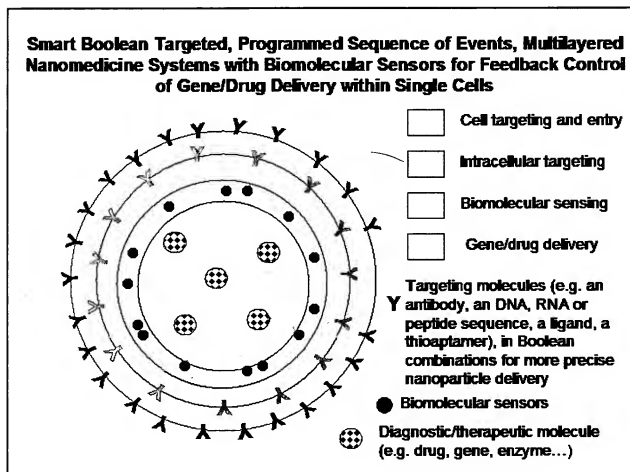For the purposes of this provisional application and for a more detailed explanation of the invention, the following documents are included with this application and form part of the disclosure herein and are otherwise incorporated herein by reference:

1.   **TITLE:** Nanomedicine: Targeted Nanoparticles For The Delivery Of Biosensors And Therapeutic Genes (Thesis)

     AUTHOR: Tarl W. Prow

NANOMEDICINE:
TARGETED NANOPARTICLES FOR THE DELIVERY OF BIOSENSORS AND THERAPEUTIC GENES

APPROVED BY THE SUPERVISORY COMMITTEE

James Leary, Ph.D.
Nicholas Kotov, Ph.D.
Massoud Motamedi, Ph.D.
Norbert Herzog, Ph.D.
Rene Rynbrand, Ph.D.

Dean, Graduate School

NANOMEDICINE:
TARGETED NANOPARTICLES FOR THE DELIVERY OF BIOSENSORS
AND THERAPEUTIC GENES

by

Tarl W. Prow

DISSERTATION

Presented to the Faculty

of

THE UNIVERSITY OF TEXAS
GRADUATE SCHOOL OF BIOMEDICAL SCIENCES AT GALVESTON

in partial fulfillment

of the requirements

for the degree of

Doctor of Philosophy

THE UNIVERSITY OF TEXAS MEDICAL BRANCH
AT GALVESTON

December 2003

To my family for giving me this life so full of joy, wonder, and inspiration.

ACKNOWLEDGMENTS

I would like to first thank my mentor, Dr. James Leary. I am forever indebted to him for all of his patience, support, and advice. My life is truly richer for having spent time with him. I must also thank him for his friendship during those difficult times we all face. This dissertation and my career in science would have not been possible had I not been able to follow my dreams, for those opportunities I am greatly appreciative. I must also thank Dr. Leary for all of those late night history lessons, he taught me to learn from the past, one of my most valuable lessons.

This work would have suffered greatly without the guidance and friendship of Dr. Rene Rijnbrand. During this dissertation I faced many technical challenges and through many of these periods we worked side by side to meet and overcome those trials. Equally important to the science was your friendship and belief in this project, thank you.

I would like to express my deepest gratitude to Dr. Norbert Herzog for all of his time, effort, and patience. Your humble and enthusiastic nature has not only comforted me during trying times, but has also motivated me throughout many adventures over the last 4 years. Whenever needed, Dr. Herzog was always willing to listen and share his ideas and for that I am

genuinely appreciative. I am also deeply grateful to Harriet Ross for saving me on too many occasions to count. Thank you for being my guardian angel, I really do appreciate everything you have done for me.

Dr. Nicholas Kotov, I would like to thank you for spending time with me. As a scientist, I am very grateful for the time and support you have given to me and this project. It has been an honor and a pleasure to work and interact with you.

I want to thank Dr. Massoud Motamedi and the biomedical engineering group, including Brent Bell, Gracie Vargas, and Todd Papas, for their time and efforts spent on me and my multiple projects. I would also like to personally thank Dr. Motamedi for playing a vital role in this project and supporting the animal studies. Finally I would like to thank Mohammad Eghtedari for his rotation in our laboratory. Ardi it was a pleasure having you here.

Two other researchers central to this dissertation are Dr. Yuri Lvov and Amish Patel. They have given many hours and graciously helped pursue the development of nanomedicine technology. Thank both of you for all of your time, ideas, and dedication to this project.

To my lab family, I give a very special thanks, primarily for putting up with me and my many projects. Nan Wang and I spent many hours side by side in the lab and for that I am grateful. We collected both good and bad data, but she always had a smile, thanks. To Jacob Smith, a valued friend and coworker, your advice was always suspect, but never boring. Thank you for all your help and undying support. To Jose Salazar, thanks for going the distance and never giving up. Thanks to Lisa Reece, Andrea Fontenot, Peter Szaniszlo, and William Rose for your support and hard work.

Finally, I would like to thank my family for listening and inspiring me. Your encouragement and enthusiasm for life makes me what I am. Thank you.

NANOMEDICINE:
TARGETED NANOPARTICLES FOR THE DELIVERY OF BIOSENSORS AND THERAPEUTIC GENES

Publication No. _____ *

Tarl Prow, M.S.

The University of Texas Medical Branch
at Galveston, 2003

Supervising Professor   James Leary, Ph.D.

Nanomedicine is a concept that embodies a multidisciplinary approach to treating disease that enables individual cells to treat themselves in response to a pathogenic stimuli. The goal of this dissertation was to design and test the three major components of nanomedicine: targeted nanoparticle gene delivery; pathogen activated biosensor; and inducible therapeutic genes. These components were to be tested individually, *in vitro*. To this end, three nanoparticle systems were developed: layer by layer, semiconductor based, and magnetic nanoparticles. Layer by layer constructed nanoparticles were capable of targeted gene delivery via sugar coated outer layers. Inner layers contained alternating charged species, including DNA. Non-targeted gene delivery via lipid coated nanoparticles was found to be more efficient, but also more sensitive to nanoparticle cluster size. Semiconductor based nanocrystals were used as fluorescent markers during targeting studies. These <20 nm particles could be found within cells even without targeting molecules, but targeting with arginine rich peptides and antibodies showed the greater cellular penetration. Magnetic nanoparticles were easy to purify and bioconjugate. Amplified DNA fragments containing a 5' biotin were easily bioconjugated to the surface of these particles (~50 nm). Lipid coating the DNA tethered magnetic nanoparticles greatly facilitated transfection. Gene expression from these nanoparticles was similar to transfected DNA fragments. Additional experiments demonstrated that the DNA tethered magnetic nanoparticle could be extracted and purified from an individual cell. Hepatitis C virus biosensors were able to detect and report the presence of a subgenomic replicon. A reactive oxygen species sensitive promoter based biosensor was obtained and a stable cell line produced. This cell line was found to be sensitive to chemical induction of reactive oxygen species. A targeted

ribozyme gene therapy was constructed and tested *in vitro*. This ribozyme was targeted to the hepatitis C virus internal ribosome entry site. The ribozyme cassette was cloned downstream of a tetracycline response element repeat. This construct appeared to cleave a hepatitis C virus internal ribosome entry site that was transcribed *in vitro*. Later studies with a subgenomic hepatitis C virus replicon showed promising results.

TABLE OF CONTENTS

LIST OF ILLUSTRATIONS

xi

LIST OF TABLES

CHAPTER 1.   INTRODUCTION

1.1.   NANOMEDICINE OVERVIEW

The focus of this project was to develop novel platform technologies that can be used to treat a range of complications and diseases via gene directed therapy. The two major biological models that were chosen as vehicles for development during this project were: 1) the Hepatitis C virus (HCV) and 2) cellular radiation damage accumulated during long term/deep space missions. The approach described in this dissertation uses techniques which have engineered targeted nanoparticles seeking out cells that could possibly be affected by a particular pathology. The nanoparticles developed have specific molecule(s) coupled to the outer surface, thereby targeting the cell types potentially affected by a particular pathogen or environmental insult. Once bound, these nanoparticles will be able to enter the cell through endocytosis and degrade in a pH dependant manner within the endosome. At this stage endosomallytic agents will be released and will lyse the endosome, thereby releasing the payload into the cytoplasm. This payload will contain specific molecular biosensors and anti-viral or DNA repair gene therapy constructs (**Figure 1.1**).
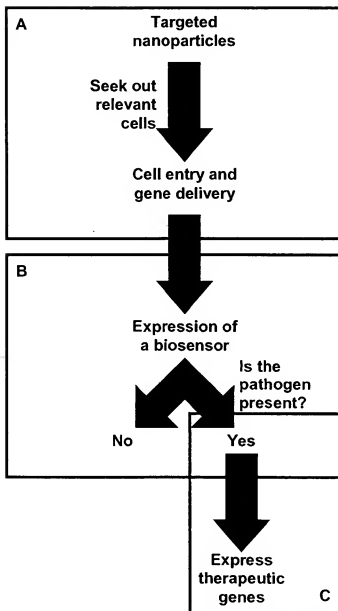
Figure 1.1. Overview of nanomedicine. The concept of nanomedicine can be broken into three steps: gene delivery (A), biosensor detection (B), and gene therapy (C).

In the case of HCV, one expression product of these constructs, the biosensor will be targeted to the same sub-cellular location as the HCV translation machinery and will monitor for the presence of the HCV. Only when detected, the expression of an anti-HCV gene product be triggered. The experiments described in this dissertation will discuss how the anti-HCV construct is engineered to express a hammerhead ribozyme with a nuclear export signal which is directed to the internal ribosome entry site (IRES), a highly conserved region of the HCV genome which controls translation and viral replication.

For the DNA repair component of this project, the aim was to develop a gene therapy technique which would provide increased *in vivo* protection against radiation damage to the blood and bone marrow of astronauts who experience long term/deep space missions. The primary goal was to develop an *in vivo,* intra-cellular DNA repair system for radiation damaged cells in astronauts before they progress to radiation induced leukemia. This system would therefore use a promoter based sensor which could detect the presence of reactive oxygen species (ROS). When ROS are present, the sensor would trigger the transcription of foreign DNA repair enzymes, which may be more efficient and effective than our innate DNA repair system.

The approaches described are advantageous for the following reasons: (1) these techniques have the ability to deliver genes with targeted particles that cannot replicate and are biodegradable; (2) the therapeutic gene generated can be silenced at any time by the addition of tetracycline; (3) the amount and duration of the gene therapy developed can be controlled without having to treat the individual with extremely high non-physiological doses of harmful drugs, as is currently administered with ribavirin/interferon therapies and chemotherapy for cancer; (4) the gene therapy products are only specifically expressed when the pathogen or radiation damage is present in the cell; (5) the anti-HCV treatment is highly specific for HCV, thereby minimizing side effects.

The scope of this dissertation was to develop and test the individual components of the nanomedicine system *in vitro* (**Figure 1.2**). Nanoparticles capable of delivering DNA payloads were to be developed from different core components. Targeted delivery was secondary to the payload delivery due to the importance of developing an *in vitro* model with which to develop the remaining technologies. Biosensor platform technology was to be developed in a way that facilitates the rapid development of biosensors for other applications. *In vitro* experiments were designed to test the feasibility of a protease activated biosensor platform technology. A ribozyme based gene therapy system was proposed and later constructed. This concept was to be

4

tested with a hepatitis C virus replicon system. The overall scope of this dissertation was to develop and test these technologies *in vitro*.

Tier 1 ——————— **Tier 2** ——————— **Tier 3** ——————— **Tier 4** ——————— **Tier 5**

targeted nanoparticle that can deliver multilayered payloads containing molecular programming genes to cell populations — Component optimization: *in vitro*

targeted biosensor that can induce gene expression only in the presence of a pathological process (irradiation, viral infection, etc.) — Component optimization: *in vitro*

a specifically **targeted gene therapy** system capable of silencing pathogenic mRNA — Component optimization: *in vitro*

Component integration: *in vitro*

Component optimization: *in vivo*

Component integration: *in vivo*

Figure 1.2. The nanomedicine project plan. This schematic represents a tiered project plan to develop nanomedicine applications for use in vivo. The scope of the current dissertation is through Tier 1. Later studies in this same laboratory will continue the research through the remaining tiers until a useful in vivo nanomedicine application has been developed.

6

1.2. SPECIFIC AIMS

The three major aims of this dissertation are:

Specific Aim 1: To develop novel nanoparticle based gene delivery systems. These nanoparticles will be assessed for DNA transfer capabilities and biocompatibility.

Specific Aim 2: To develop molecular biosensors which are activated in the presence of certain pathogen associated activities.

Specific Aim 3: To design and construct an inducible ribozyme based gene therapy targeted to silence a specific mRNA.

It was hypothesized that:

A novel nanoparticle and biosensor system with minimal cytotoxic effects can be developed and tested *in vitro*. These systems should be able to deliver biosensor encoding DNA to cells *in vitro*. Once activated, the biosensor should be capable of inducing the expression of a therapeutic gene product.

1.3. NANOMEDICINE BACKGROUND AND SIGNIFICANCE

This proposal is based on a novel nanomedicine concept, that each cell should be given the capability to induce or inhibit gene therapy depending on the presence of a pathogen or pathogenic processes. By tailoring specific gene therapies to be non-toxic, yet effective, it was hoped that a novel system could be created to treat HCV infection or radiation induced DNA damage without administering large quantities of potentially toxic chemicals. Viral infections are currently difficult for clinicians to detect and are usually identified only after irreparable damage has occurred. In diseases such as HCV infection and leukemia, patients are then given a variety of drug cocktails, which are somewhat effective, yet are highly toxic (Cripe and Hinton 2000; Gutfreund and Bain 2000). The side effects of this treatment ultimately result in poisoning of normal cells during the elimination of abnormal cells. Furthermore, these undesirable side effects lead to severe pain and debilitation in the patients, even when therapies are effective (Cripe and Hinton 2000; Gutfreund and Bain 2000). In both HCV infection and cancer, there are significant numbers of individuals in whom the infection or cancer relapses (Cripe and Hinton 2000; Gutfreund and Bain 2000). Therefore, there is now a need for a non-invasive treatment which enables the target cells to be detected and the particular pathology eliminated or suppressed. Ideally, this

new treatment should then cease and exist at non-detectable levels only when the pathology has been cleared.

Existing gene delivery systems have a variety of limitations (De Smedt, Demeester, and Hennink 2000). These systems are designed to eliminate an infection by transferring a therapeutic gene to host cells, however, they have been largely unsuccessful since only low doses of genetic material can reach the specific infected cell types. Increased side effects also include the treatment of non-infected cells with high levels of genes and the host cells reacting to the carrier molecules associated with their delivery. The current gene delivery systems contain retroviral vectors, are liposome based. Genes (naked DNA, RNA and modified RNA) have also been injected directly into the blood stream. All of these delivery methods can produce many undesirable side effects which can compromise the treatment of patients. Retroviral vectors have potentially dangerous side effects which include incorporation of the virus into the hosts immune system and hence, have been less successful than originally hoped (De Smedt, Demeester, and Hennink 2000). Liposome based gene transfer methods have relatively low transfection rates, are difficult to produce in a specific size range, can be unstable in the blood stream, and are difficult to target to specific tissues (De Smedt, Demeester, and Hennink 2000). Injection of naked DNA, RNA, and modified RNA directly into the blood stream leads to clearance of the injected nucleic acids with minimal beneficial

outcome (Sandberg et al. 2000). As such, there is currently a need for a gene delivery system which has minimal side effects but high affectivity and efficiency. One such system could be that of the self-assembled nanoparticles coated with targeting biomolecules (Lvov and Caruso 2001).

1.4.   GENE DELIVERY

Three different kinds of particles are relevant to the work described in this dissertation: layer by layer nanoparticles, nanocrystals, and magnetic nanoparticles. Each type of nanoparticle has pros and cons. The overall goal of using nanoparticles is to deliver genes first *in vitro*, and then *in vivo*.

Some or the first attempts at delivering genes *in vivo* were carried out with naked DNA coupled to reporter enzymes (Cristiano et al. 1993; Cristiano, Smith, and Woo 1993; Kay et al. 1992; Wu and Wu 1991). In the early 1990s several researchers were developing viral based systems to deliver therapeutic genes to specific cell populations (Flotte 1993; Fraser 1994; Geller et al. 1990; Kennedy and Steiner 1993; Kotin 1994). For the most part, these and latter studies utilized Herpes virus or Adenovirus for gene delivery. These viral vectors were chosen partly because of their targeting capabilities, but more importantly for their ability to efficiently deliver a genetic payload. Specifically, the Herpes simplex virus vectors were chosen because of their

ability to infect neuronal cells and deliver relatively large payloads of genetic material (Kennedy and Steiner 1993; Latchman 1994). The Adenovirus vectors were chosen based on their ability to infect a wide variety of cells and were initially developed for use in humans to treat cystic fibrosis (Flotte and Carter 1995). Although these and other viral based vectors were tested in humans, they all had major drawbacks. One of these disadvantages was that the delivered genes did not persist in the host cells and gene expression was too brief. Viral based gene delivery in humans met with some successes but those achievements were overshadowed by unexpected side effects (Ghosh et al. 2000). Some of the specific problems that were encountered by these patients included a fatal immune reaction and a subsequent leukemia like disease due to uncontrolled DNA integration (Check 2002; Hacein-Bey-Abina et al. 2003; Kaiser 2003; Marshall 1999). Although these tragic events showed that viral based gene therapy was not feasible for the masses, there was significant progress made. In 2000, viral based gene therapy recorded its first success in which three children were cured of a severe immune deficiency illness (Cavazzana-Calvo et al. 2000). Throughout the short history of gene therapy there have been two consistant problems: DNA integration and gene delivery (Brenner 1995; Emery and Stamatoyannopoulos 1999; Fischer 2001; Ghosh et al. 2000; Herrmann 1995; Pfeifer and Verma 2001; Romano et al. 1998; Strauss 1994; Thomas, Ehrhardt, and Kay 2003). The lack of excellent

vectors is the core hindrance for gene therapy researchers. Therefore, non-traditional means of gene delivery have been explored in recent years.

1.5. LAYER BY LAYER NANOPARTICLES

There are currently many DNA transfer technologies being developed for gene therapy. One of the most novel and exciting areas being developed for this application is nanotechnology. Specifically tailored nanoparticles are currently being developed for gene delivery applications. One of the earliest examples of this technology was reported in 1997 by Maruyama and colleagues. (Maruyama et al. 1997). This study detailed the construction of a biodegradable nanoparticle capable of binding DNA (**Figure 1.3**) (Maruyama et al. 1997). Later studies showed that this and similar methods could be used to generate DNA containing nanoparticles that were capable of delivering genes to living cells (Heng et al. 2002; Prabha et al. 2002; Reynolds, Moein Moghimi, and Hodivala-Dilke 2003).

6.8kb
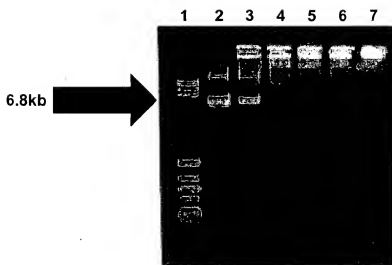
Figure 1.3. Construction of DNA coated nanoparticles. Gel electrophoresis of plasmid DNA (pSV) and NPs mixtures (1% agarose): (**lane 1**) MW marker; (**lane 2**) pSV alone (1 μg); (**lanes 3-7**) mixtures of pSV (1 μg) and increasing amounts of PLL-Dex (7-2600) NPs (10, 30, 50, 80, or 120 μg). Before electrophoresis, these mixtures were incubated in PBS for 1 h at room temperature. Plasmid DNA was detected as ultraviolet fluorescence after ethidium bromide staining. PLL-Dex (7-2600) NPs were prepared by the diafiltration method from 10 mL of DMSO solution containing 25 mg of PLA and 9 mg of PLL-Dex (7-2600). (Maruyama et al. 1997, Copyright ACS Publications)

The majority of the nanoparticle based gene delivery tools in the current literature are based on DNA complexes. These complexes are mixtures of biopolymers, for example poly-L lysine and chitosan, and DNA (De Smedt, Demeester, and Hennink 2000; Nishikawa et al. 2000). Once mixed in the proper proportions, these components yield nanometer size particles and can be titrated to form particles of a particular size. Solid nanoparticles composed of biologically inert polymers are well defined in various biological applications and can be commercially purchased (De Smedt, Demeester, and Hennink 2000; Nishikawa et al. 2000). The majority of work in this field has been done with particles in the 100 nm size range composed of poly-L lysine (De Smedt, Demeester, and Hennink 2000). Fluorescent dyes incorporated into the polymer matrix of these particles may help to track them during the targeting stage. Special coatings have also been used to help nanoparticles target and enter specific cell populations (De Smedt, Demeester, and Hennink 2000; Nishikawa et al. 2000). There has been much data gathered on the ability of these particles to target and transfer genes into living cells (De Smedt, Demeester, and Hennink 2000; Nishikawa et al. 2000). The particles have been reported to enter the cell via endocytosis and then degrade due to the subsequent decrease in pH (De Smedt, Demeester, and Hennink 2000; Nishikawa et al. 2000).

Particle size has been shown to greatly influence the transfection efficiency (Prabha et al. 2002). It is generally accepted that there is an optimal nanoparticle size range for transfection that resides somewhere between 20 and 200 nm. The smaller the nanoparticle, the easier the particle can enter the cell, but if the particle is too small the reticular endothelial system will efficiently clear the particles (Tiefenauer, Kuhne, and Andres 1993). Alternately, the larger nanoparticles, the more likely the particle will be excluded from the cell or caught in the cell membrane (Prabha et al. 2002). Therefore, this dissertation has focused on the development of nanoparticles between 20 and 200 nm.

The diverse requirements for a nanoparticle based system led to the exploration of three different types of nanoparticles. These were chosen as potential gene vectors: layer by layer, semiconductor based, and super paramagnetic nanoparticles. Each of these particles has advantages and disadvantages.

Layer by layer nanoparticles are formed around a core particle with the layers being held together by the charge of the individual molecules, thus they are composed of alternating positive and negative charged species (**Figures 1.4 and 1.5**) (Lvov et al. 2001; Lvov and Caruso 2001). One benefit of using this type of particle is that once constructed, the particle core can be

suspended and then made porous by changing solvents without damaging the outer layers. Incubating these porous nanocapsules with dissolved chemicals, one can load the nanocapsules through diffusion. Once loaded, the nanocapsules can be made non-porous by changing the solvent, thereby encapsulating the chemical of choice. Through this technique one can encapsulate fluorescent dyes and possibly other molecules (Lvov et al. 2001; Lvov and Caruso 2001). Reporter genes may also be used as an interior layer because of the inherently negative charge of DNA. Additional layers of targeting molecules may then be added to help direct the particle to the correct cell types (Lvov et al. 2001; Lvov and Caruso 2001). One disadvantage to this type of particle is that this technology is new and not well defined in the biological arena.
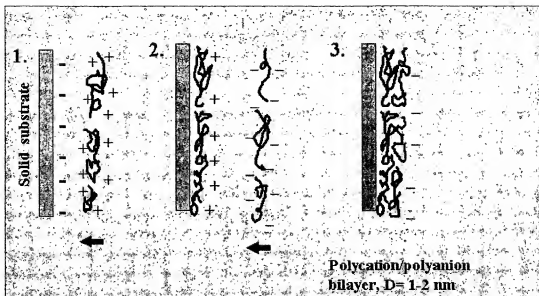
Figure 1.4. Layer by layer assembly. The core particle is composed of silica and is negatively charged (**Panel 1.**). The addition of a positive charged moiety causes the layer to pack tightly onto the surface of the particle (**Panel 2.**). Alternate layers are thereby deposited onto the surface of the particle (**Panels 1. to 3.**). Lvov, personal communication.

~300 nm of protein layers
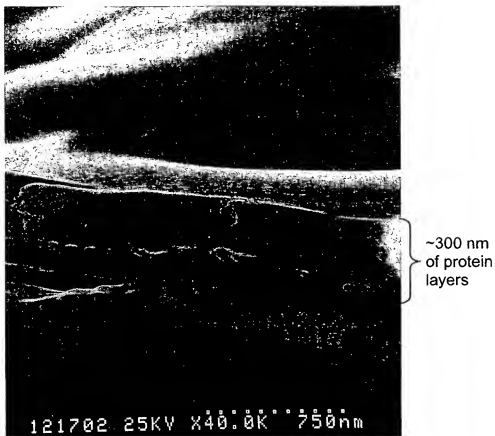
Figure 1.5. Protein assembly by alternate adsorption with linear polylons. Glucose oxidase, urease, arginase, and myoglobin were used in the layer by layer assembly of this multilayer assembly. SEM was used to photograph this cross section of the layered film. Lvov, unpublished data.

This dissertation builds on the concept of creating synthetic viruses. In other words, the following chapters describe nanoparticles that were developed with their viral counterparts in mind. Basing nanoparticle design on viruses is not a new concept, but is difficult to realize, even *in vitro*. Wagner and colleagues described a system in which nanoparticles were coupled to replication deficient adenovirus (Wagner et al. 1992). This publication described a synthetic system devised to increase transfection efficiency *in vitro*. Simply put, viral particles coupled to poly-L lysine particles containing DNA. These complexes were tested for transfection efficiency and shown to transfect cells at a very high level. Each of the components serves a valuable purpose. Transferrin bound nanoparticles were shown in an earlier study, to be taken up by cells with transferrin receptors (Neutra et al. 1985). Additionally, transferrin is known to be endocytosed through the transferrin receptor (Dautry-Varsat 1986; Morgan and Baker 1988; Qian et al. 2002). This receptor has also shown promise as a gateway non-viral gene vectors (Qian et al. 2002). This publication shows gene delivery that utilizes multiple components can prove to be very efficient. For this reason, multilayered nanoparticles were very attractive non-viral gene delivery vectors and were developed for *in vitro* use in this dissertation.

Wagner et al. had the right concept, but the implementation was cumbersome (Wagner et al. 1992). The results from this multi-component system were effective and therefore deserve recognition. The concept of a multi-component system for targeted gene delivery is best executed by viruses. This is where the concept of multi-component layer by layer nanoparticles for this dissertation was derived. Creation of a nanoparticle with the ability to seek and bind to a receptor, positively charged sugars and peptides, were used for this dissertation. The asialoglycoprotein receptor was targeted because it is a liver specific protein that binds and internalizes glycoproteins that end in galactose. This receptor is used as a classical example of endosomal sorting. The glycoproteins are internalized in endosomes and rapidly transferred to lysosomes. After that, the receptors are then recycled back to the surface of the cell (Stockert 1995; Weigel 1993). Additionally, researchers have found that the asialoglycoprotein receptor is capable of internalizing relatively large particles and can be used to transfer genes into a cell (Teradaira et al. 1983; Thurnher et al. 1994).

1.6. SEMICONDUCTOR NANOCRYSTALS

Small size and fluorescent properties make semiconductor based nanoparticles attractive for targeting and cell entry studies. These nanocrystals are composed of a semiconductor core that self assembles and is brightly

fluorescent. These nanoparticles have two unique characteristics that lend them to targeting studies: the excitation and emission spectra have a very broad stokes shift and the emission wavelengths can be tuned by changing the size of the semiconductor core (Rogach et al. 2000). Because of these novel fluorescent characteristics, researchers have been able to make up to 14 resolvable colors of nanoparticles that can all be excited by a single UV wavelength (Chan et al. 2002; Mamedov et al. 2001). The semiconductor cores can be coated with a number of biologically inert substances including sulfur and bovine serum albumin. These coatings can then be used to bioconjugate targeting molecules, such as antibodies through a number of conjugation techniques (i.e. NHS conjugation).

Because nanocrystals are composed of materials that alone are toxic, many believe the particles themselves should also be toxic. The current *in vitro* and *in vivo* data shows that there are no overt toxicities associated with nanocrystals (Dubertret et al. 2002; Jaiswal et al. 2003; Wu et al. 2003). Studies using nanocrystals to label cells in a developing *Xenopus* embryo over the course of several days showed no toxicity or developmental abnormalities (**Figure 1.6**) (Dubertret et al. 2002). During the embryo stage, the liver, kidney, and brain are not fully developed and therefore long term toxicities could not be determined. These data support the idea that the nanocrystals are stable for at least days within the intracellular milieu. This is most likely due to the chemical capping and conjugating of biological materials to the nanocrystal core particles. These may help to buffer and protect the nanocrystals from the harsh environment of the cell. Recent studies have also shown that semiconductor nanocrystals can be used as gene transfer vectors (Paunesku et al. 2003).

4. The present invention can provide a nanosystem that positions itself at the active site of importance for subsequent drug-gene delivery within a single living cell through the use of localization or anchoring sequences.

Molecules can be localized within a site (e.g. at the desired site for drug/gene delivery) by a variety of mechanisms. Three examples have been demonstrated in section 6.3.1.5 of the Tarl Prow dissertation. Results are shown in **Figure 5** (Figure 6.7 of Tarl Prow dissertation; and Figure 6 of the JMH paper):
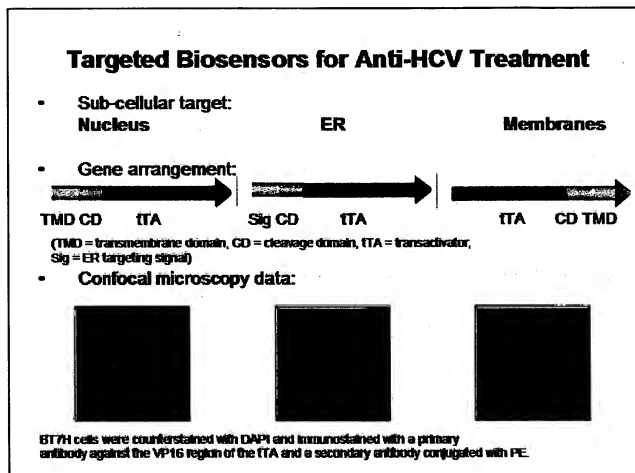
Figure 5

5. The present invention can provide a nanosystem that uses feedback loop molecules, such as molecular biosensors, to provide for controlled drug-gene delivery in continuous response to single cell drug-gene delivery at earlier timepoints.

This feature involves continuous control of any drug/gene therapy to deliver the proper therapeutic amount for each single cell. While we have not yet done a complete drug/gene therapy of a single cells we have demonstrated that this control mechanism is possible by linking a biosensor to an expression vector of a green fluorescent protein reporter molecule. This example is cited only as one demonstrating feasibility. While the present invention may make no claim on either the specific reporter gene (owned by others) or the HCV replicon (owned by others) or West Nile replicon (owned by others), the present invention may claim applications of the basic invention to these application areas. There are many other possible applications. There are many ways these feedback loops can be done. One specific example is the delivery of an HCV biosensor linked to a GFP reporter molecule which transcribes the reporter gene as long as the HCV replicon is detected. This is shown in Figures 6 and 7 (sections 6.3.1.7 and 6.3.1.8 and Figures 6.10 and 6.11 of the Tarl Prow dissertation):
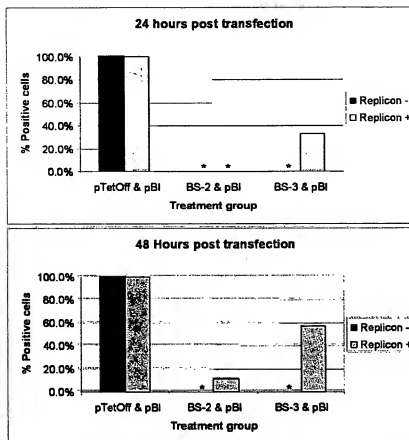
Figure 6

Figure 6.10. Hepatitis C replicon activated biosensor flow cytometry data. Values were calculated as the percent of GFP positive cells normalized to the pTet-Off/pBI values. Huh7 cells are protease/replicon negative and Huh7-RG cells are protease/replicon positive. * indicates 0%.
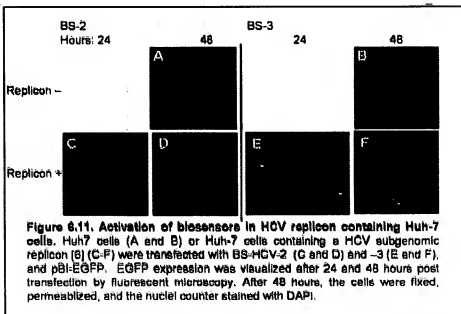
Figure 7

Figure 6.11. Activation of biosensors in HCV replicon containing Huh-7 cells. Huh7 cells (A and B) or Huh-7 cells containing a HCV subgenomic replicon (B) (C-F) were transfected with BS-HCV-2 (C and D) and –3 (E and F), and pBI-EGFP. EGFP expression was visualized after 24 and 48 hours post transfection by fluorescent microscopy. After 48 hours, the cells were fixed, permeablized, and the nuclei counter stained with DAPI.

A second example of a nanoparticle system with feedback is shown in collaborative work we have been doing with Dr. Peter Mason (not an inventor of the present application) with his West Nile virus systems.
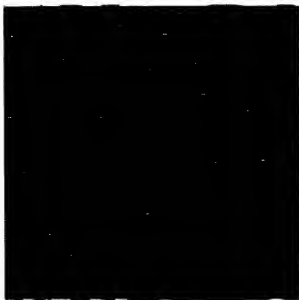
This image shows cells (nuclei are stained blue with Hoechst 33342) treated with multilayered nanoparticles coated with cell entry facilitating molecules. One of the inner layers contained the gene encoding for EGFP (green). The presence of green cells indicated the nanoparticles have reached the nucleus of the cell. These are all BS-3 biosensors specific for West Nile virus.

Demonstration of a feedback loop: When there is no viral protease present, the biosensor remains tethered in the cytoplasmic membranes. The presence of the viral protease induces cleavage of the biosensor from the anchor and the free protein fragment is localized to the nucleus via a VP16 nuclear localization signal. Once in the nucleus, the protein fragment binds

to the tetracycline response element and induces the expression of any gene downstream (in this case EGFP reporter genes).

Data for the system described in Figure 8 in shown below in Figure 9. The expression of the biosensor/ reporter gene complex is driven by the West Nile virus infection.
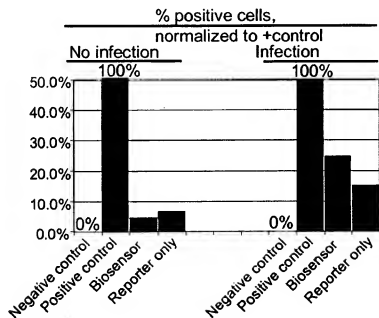
Figure 9
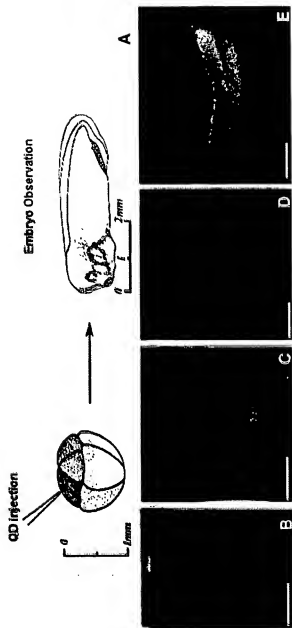
Figure 1.6. Nanocrystal (QD) labeling of *Xenopus* embryos at different stages and specific QD intracellular localizations. (A) Schematic showing the experimental strategy. QD-micelles, as in Fig. 2, were injected into an individual blastomere during very early cleavage stages. Between 1.5 and 3 nl of a 2.3 μM suspension of QDs were injected, corresponding to 2.1 × 109 to 4.2 × 109 injected particles per cell. Embryos were then cultured until they reached different stages of development, and imaging was done as in Fig. 2. In (B) to (E), transmission and fluorescence images have been superposed. (B) Injection of one cell out of an eight-cell-stage embryo resulted in labeling of individual blastomeres. (C) Same embryo shown 1 hour later. The daughter cells of the injected blastomere are labeled (D) and at a later stage (E) show two neurula embryos, which were injected into a single cell at the eight-cell-stage in the animal pole. (Dubertret et al. 2002)

These situations are discussed in different places of the papers and dissertation included as further information herein. An example of targeting and entry steps are given in **Figure 2** (Figure 4.14 of Tarl Prow dissertation, mentored by Dr. James Leary; and Figure 10 of the Journal of Molecular Histology (JMH) paper):
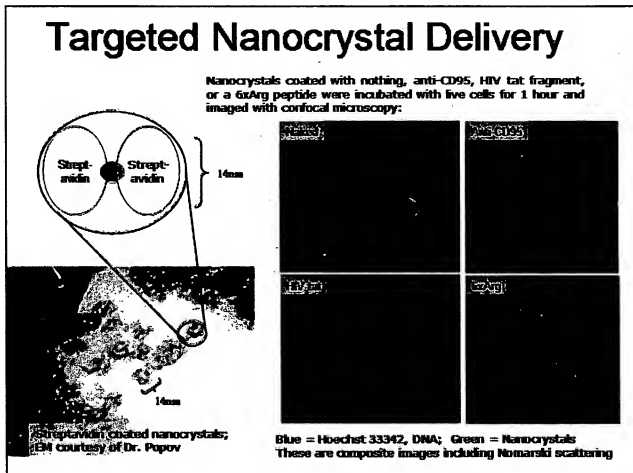
Figure 2

2. The present invention can provide a nanodelivery system with molecular error-checking based on desired or permissible Boolean logic conditions (based on presence or absence of specific molecules on or within the cell) to reduce false positive targeting which then lowers undesired, adverse bystander side reactions

The importance of Boolean combinations of targeting molecules to correctly identify rare cells (the usual in-vivo targeting situation) is well known and documented, including in previous work by one of the inventors (Leary, 1994). For the reasons given in this reference, the preferred Boolean combination is to have two "positive selectors", for example A and B, which must be simultaneously present (Boolean AND) and one "negative selector", for example C, which must be absent (Boolean NOT). This Boolean logic condition of "(A AND B) AND (NOT C)" has been demonstrated to provide good target selection down to frequencies of more than 10^{-6} in at least some applications where each targeting molecule, A or B may only be individually accurate to frequencies of 10^{-2}. The non-specifically binding C target molecule, which should not bind to the correct cells, is used to eliminate cells which may also bind A or B. Targeting molecule C can also be used to eliminate all dead/damaged and other cells which non-specifically bind molecule C. As discussed in the reference (Leary, 1994), A, B and C can also consist of cocktails of targeting molecules. All of this has been done previously by others at the molecular labeling level using fluorescent antibodies of different colors. Thus a cell of interest may be identified at A+B+C- . Nanoparticles of different colors can obviously be similarly used for in-vitro, ex-vivo, and in-vivo diagnostic purposes.

Nanoparticles for in-vivo drug/gene delivery are more complicated, since it is difficult, but not impossible, to construct a similar Boolean targeting scheme on a single nanoparticle. A simpler way to accomplish the objectives is to have a drug delivery system which is binary, i.e. it

requires that two different nanoparticles with different targeting molecules (e.g. nanoparticle type 1 with targeting molecule A, and nanoparticle type 2 with targeting molecule B) bind to the cell. The intermediate steps bring two different components of the drug/gene delivery system together to form a process that can only be completed if both drug/gene prerequisite molecules are present. The non-specific targeting molecule C can have a nanoparticle with a "suppressor" molecule which blocks the completion of the assembled drug/gene delivery system. This combination of three different targeting molecules A, B and C on separate nanoparticles can then be used to create the Boolean logic system of (A AND B) AND (NOT C) for a complete targeted drug/gene delivery system.

This claim area, invented by JFL, will require further effort to reduce the Boolean requirement for ht drug/gene delivery to practice. But we have demonstrated the idea that two different types of nanoparticles can be co-localized to the same place within a cell as shown in **Figure 3** (JMH paper figure 11):
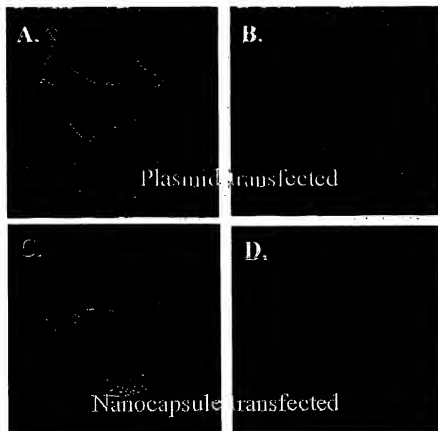
Figure 3

3. The present invention can provide a nanosystem having molecules that use, create or reorganize molecules already within individual living cells such that a single nanoparticle can manufacture enough drugs or genes to have a therapeutic response. This solves the problem of how to deliver enough drugs or genes to single cells in-vivo to achieve therapeutic value.

It will be difficult to deliver enough drugs to a cell in-vivo to be of therapeutic value. This feature of the present invention suggests that the problem can be overcome by delivering drug/gene manufacturing capability to the cell. Then any amount of desired drug or gene can be manufactured in-situ. If combined with a molecular biosensor, the drug can be manufactured and delivered until the biosensor shuts down the manufacturing. The biosensor can either be sensitive to drug concentration or better yet, be sensitive to the single cell's response to the previously delivered drug or gene therapy.

An example is given in **Figure 4** (Figure 6.2 in the dissertation of Tarl Prow; also figure 5 of the JMH paper):
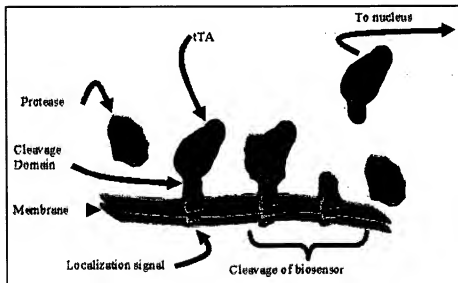
Figure 4

1.7. MAGNETIC NANOPARTICLES

Magnetic nanoparticles have also been targeted to cell populations *in vivo*. In fact, magnetic particles have been used to enhance virus mediated gene transfer for gene therapy applications (Scherer et al. 2002). In this case the nanoparticles were used to concentrate the viral vectors to a specific location and thereby increase the likelihood of transfection (Scherer et al. 2002). This application of magnetic nanoparticles is a departure from the norm. Most researchers use magnetic particles as contrast agents (Bonnemain 1998; Mitchell 1997; Petersein, Saini, and Weissleder 1996; Violante 1990; Wang, Hussain, and Krestin 2001). Because these agents are used primarily in diagnostic imaging, many of the particle formulations are already approved for use in humans. Although there is no current data on gene delivery by magnetic nanoparticles, this dissertation explores that application both *in vitro* and *in vivo*. The magnetic properties of these particles are quite favorable for layered construction of a non-viral based gene delivery vector. One of the most difficult challenges facing researchers constructing layered nanoparticles is the purification of the particles after each step. With magnetic particles that utilize superparamagnetic iron oxide cores, the purification is generally simple and utilizes off the shelf products.

1.8. HEPATITIS C VIRUS

Hepatitis C virus is a positive stranded RNA virus that has no known DNA intermediate. The genome of the virus is approximately 9.5 kb and is replicated through a double stranded RNA intermediate by a virally encoded RNA polymerase with no proofreading capabilities (Beard et al. 2001). The lack of proof reading during replication accounts for the great variation known to exist in various isolates of HCV (Rice and Hagedorn 2000). The genome codes for three structural proteins: core, E1, E2 and several nonstructural proteins: NS2, NS3, NS4A, NS4B, NS5A, and NS5B (Beard et al. 2001). This genome is translated as a single polyprotein that is cleaved by host and viral proteases, such as the virus specific NS3 protease (**Figure 1.7**) (Rice and Hagedorn 2000). The coding sequence is flanked by the 5' and 3' non-translated regions (NTR) that controls viral translation and replication. The 5' NTR contains the internal ribosomal entry site (IRES) that directs the ribosome to the AUG initiation codon (Rijnbrand et al. 2001). While, the E2 glycoprotein is located on the surface of the viral particle and is thought to contribute to virus binding (Rice and Hagedorn 2000). The target for the E2 glycoprotein has been suggested to be CD81, however, this is still a point of controversy among HCV researchers (Allander et al. 2000; Flint et al. 1999; Forns et al. 2000; Pileri et al. 1998; Wunschmann et al. 2000). There is however convincing evidence that CD81 plays a role in HCV particle binding (Allander

et al. 2000; Flint et al. 1999; Forns et al. 2000; Pileri et al. 1998; Rice and Hagedorn 2000).
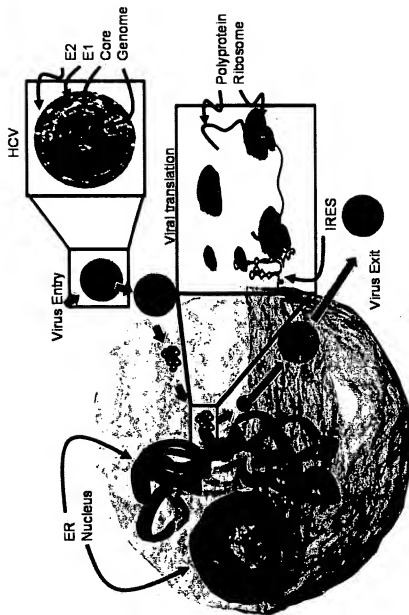
Figure 1.7. Hepatitis C virus life cycle. The Hepatitis C virus is composed of a mRNA genome, core, E1, and E2 glycoproteins (Top right panel, HCV). The virus enters the cell and replicates near the endoplasmic reticulum, never entering the nucleus. Viral translation occurs via an internal ribosome entry site and results in the production of a polypeptide (Lower right panel, Viral translation). The polypeptide is processed by host/viral factors and then forms a viral particle that exits the cell.

There are, as yet, no fully protective vaccines for Hepatitis C while existing therapies such as interferon and ribavirin therapies are 50% effective and very expensive (Gutfreund and Bain 2000). Of the patients that present with acute HCV infection, only 10-40% eventually clear HCV (Barrera et al. 1995; Hino et al. 1994). The closest curative therapy for HCV infection is a liver transplant. Even if interferon/ribavirin treatment is successful, HCV infection can reoccur and could cause cirrhosis and/or loss of hepatic allograft (Bizollon et al. 1999; Feray et al. 1999; Ghobrial et al. 1999). The first generation of HCV chemotherapeutic agents was an interferon based therapy that used various types of targeted interferon, such as interferon alpha-2a, alpha-2b and consensus interferon. These anti-viral and immunomodulatory drugs resulted in only 15-20% viral clearance for at least 6 months (Poynard et al. 1996). The next generation of anti-HCV therapy was α-interferon in combination with ribavirin a nucleoside analog, was found to be more beneficial as it improved the sustained (>6 months of non-detectable HCV levels by PCR) antiviral response of interferon to 40% in previously untreated patients (Gutfreund and Bain 2000). Furthermore, relapsing HCV positive patients previously treated with interferon monotherapy were able to achieve up to a 50% sustained response with this combined therapy (Gutfreund and Bain 2000). However, at least half of those treated with this strategy remained infected with HCV (Gutfreund and Bain 2000). One other disadvantage is that the high price of combination therapy severely limits world wide use. Side

effects from this interferon/ribavirin combination therapy can also be severe enough to stop the therapy. For example, in a recent 24- and 48-week combination therapy study, 8% and 19% of the patients had to stop therapy due to adverse effects (Gutfreund and Bain 2000). Among the major side effects of both interferon and ribavirin are hemolytic anemia, teratogenic effects, depression, and congestive heart failure (Gutfreund and Bain 2000). Currently, PEGylated interferon and ribavirin are being used with higher success rate than the non-PEGylated therapies (40-45%), but response rates with persistent infections are still disappointing and the side effects are significant (Cornberg, Wedemeyer, and Manns 2002). Therefore, a more effective and less toxic anti-HCV therapy is needed.

1.9. ANTI-HCV RIBOZYME

Hammerhead ribozymes (HH) are small catalytic RNA molecules that bind to and cleave a specific RNA sequence. The HCV IRES plays a vital role in viral replication by initiating the translation of the viral polyprotein (Rice and Hagedorn 2000). IRES activity depends wholly on the primary, secondary, and tertiary structure. Controlling the level and duration of ribozyme treatment can be achieved by driving the expression of the anti-HCV RNA segment with a sensor which activates an inducible promoter. Traditional ribozyme therapy strategies have shown promising results in cell free systems and in vitro,

however the results were largely disappointing in clinical trials (Sullenger and Gilboa 2002). Two main issues that may have contributed to these disappointing outcomes are the method of delivery and its final localization. Delivery via injection of massive quantities of modified RNA into the blood stream has resulted in a poorly targeted and very limited system (Lee et al. 2000).

In gene therapy strategies, hammerhead ribozymes are expressed and retained in the nucleus, which may be effective for some mRNA targets, but not for HCV as the genome is localized outside of the nucleus. Recently, Kuwabara and Warashina have shown that the problem of sub-cellular localization can be solved by the addition of a nuclear export signal to the 5' terminus of the HH . This study went on to use several versions of this strategy in a combination of systems ranging from cell free systems to *ex vivo* experiments and to also engineer fusions which are able to cleave a variety of cellular and viral targets. The studies reported by this group are based on a tRNA promoter driving the transcription of a tRNA-HH (Kuwabara et al. 2001). Further modification of this model has contributed to the development of the experimental systems proposed in this dissertation.

1.10. RADIATION DAMAGE

To date there have been limited studies which have focused on the development of new generation therapies for *in vivo* prevention, detection and repair of DNA damage triggered by radiation. Such a system is needed to treat astronauts which receive unpreventable radiation exposure during long duration spaceflight (Ohnishi, Takahashi, and Ohnishi 2001).

A significant challenge to the implementation of manned, long duration space travel and exploration is the maintenance of human health in deep space (Cucinotta et al. 2001). The zero gravity environment can cause many complex health issues such as weakening of the immune system, increased risk of infectious diseases and cancers, and exposure to high levels of ionizing radiation (IR) and thereby DNA damage (Cucinotta et al. 2001; Ohnishi, Takahashi, and Ohnishi 2001). If not repaired, these DNA lesions can produce permanent genetic changes that ultimately can lead to carcinogenesis (Cucinotta et al. 2001; Ohnishi, Takahashi, and Ohnishi 2001). Previous studies have reported significantly accelerated rates of cancer onset due to gene inactivation and higher than "normal" exposure to DNA damaging agents (Ohnishi, Takahashi, and Ohnishi 2001). These data suggest that humans possess little "extra" DNA repair capacity, hence long-term space travel and IR exposure are likely to have severe health consequences (Cucinotta et al. 2001; Ohnishi, Takahashi, and Ohnishi 2001). There is now a need to develop

31

methodologies which can engineer human cells to detect major IR induced DNA damage and if possible, enhance the DNA repair capacity in human cells thus rendering them less susceptible to the detrimental effects of IR. One other method would be to increase the resistance of human cells to UV radiation by genetic engineering. This may be via the augmentation of the existing human base excision repair pathway and the introduction of prokaryotic DNA repair genes into cells hence increasing both the quantity and specificity of the repair process in humans.

CHAPTER 2.   MATERIALS AND METHODS

2.1.   LAYER BY LAYER NANOPARTICLE CONSTRUCTION

2.1.1.   Layer by layer nanoparticle construction

Layer by layer nanoparticles were constructed by using a charged silica core particles between 60-100nm in diameter (Nissan Chemical, Inc., Houston, TX). Alternately charged layers were added using polyethylimine (Sigma-Aldrich Chemical, Inc., St. Louis, MO) as a positive layer and DNA, sugars (Sigma-Aldrich Chemical, Inc. , St. Louis, MO), or poly(allylamine hydrochloride) PAH (Sigma-Aldrich Chemical, Inc. , St. Louis, MO) as negative layers. Deposition of each layer was monitored though sizing and zeta potential with a ZetaPlus instrument (New Haven Instruments, Inc., New Haven, CT). DNA, including pEGFP-C1 (APPENDIX 2.01.1.) and pDsRed2-C1 were initially obtained from Clontech, Inc., San Jose, CA. The electrical potential drops off exponentially with distance from the particle and reaches a uniform value in the solvent outside the diffuse double layer. The zeta potential is the voltage difference between a plane a short distance from the particle surface and the solvent beyond the double layer. Quantities of DNA were obtained from transforming *E. coli* with the appropriate plasmid and growing them to 1 L. The bacteria were lysed and the DNA isolated through cesium chloride gradients at the UTMB core facility for molecular biology. All DNAs were then concentrated and kept frozen in water. Linear DNA containing the

CMV promoter and EGFP gene was obtained by large scale PCR reactions using pEGFP-C1 (Clontech, Inc., San Jose, CA.) as the template and the following oligos: forward 5' - TAG TTA TTA ATA GTA ATC AAT TAC GGG GTC ATT AG - 3' and reverse 5' - TAC ATT GAT GAG TTT GGA CAA ACC ACA ACT AGA AT - 3'. After the PCR reactions, the resulting DNA was isolated using commercial PCR product purification kits (Qiagen, Inc., Valencia, CA). The outer coatings including, galactosamine, protamine, and poly-arginine were purchased from Sigma-Aldrich Chemical, Inc., St. Louis, MO. Lipid coatings were deposited on DNA coated particles just prior to exposure to cells. Lipofectamine™ 2000 (Invitrogen, Inc., Carlsbad, CA) was used to coat the nanoparticles in a method identical for DNA transfections as directed by the manufactures instructions.

Specifically, the layered nanoparticles were coated with Lipofectamine™ 2000 by combining 2 µl of Liofectamine 2000 with 50 µl of Optimem™ (Gibco BRL, Burlington ON, Canada). This mixture was incubated at room temperature for 5 minutes. DNA coated nanoparticles (15 µl) was gently mixed with 50 µl of Optimem™, inverted gently several times, and incubated for 5 minutes at room temperature. After incubation with Optimem™, the Lipofectamine™ 2000 and layer by layer nanoparticle mixtures were mixed and incubated at room temperature for 20 minutes. After

20 minutes, 117 μl of coated layer by layer nanoparticles were added to a single well in a 24 well plate containing 1x10^5 adherent cells.

2.1.2. TUNEL analysis

TUNEL analysis was used to detect late phase apoptosis in a variety of cell types. The TUNEL reaction utilizes a terminal deoxynucleotidyl transferase to mediate a dUTP end labeling of nicks. Therefore, the more nicks are present in cellular DNA, the more labeling will be transferred. Increased DNA fragmentation caused by apoptosis is labeled by the TUNEL reaction, resulting in apoptotic cells with brightly labeled nuclei. The *in situ* cell death kit, TMR red was purchased from Roche-Diagnostics, Indianapolis, IN. The cells were washed 3 times in PBS and fixed in 4% paraformaldehyde with PBS at pH 7.4. The cells were then permeabilized with 0.1% Triton X-100 in 0.1% sodium citrate that was freshly prepared. Then 50 μl of TUNEL reaction mixture was added to cells in a single well of a 4 well slide. The slide was then incubated for 60 minutes at 37°C in the dark. After incubation, the slide was rinsed 3 times with PBS. The sample was then analyzed by fluorescence microscopy.

2.1.3. Trypan blue dye exclusion assay

This assay helps to identify cells with leaky or damaged cell membranes. A cell suspension (50 µl) was mixed with 50 µl of trypan blue dye (Sigma-Aldrich Chemical, Inc., St. Louis, MO). The cells were then gently mixed and viewed with a light microscope. Healthy and intact cells were clear, while cells with damaged membranes appear blue.

2.1.4. Cell culture and transfections

Cells were incubated at 37°C in 5% CO_2. BT7-H, Huh7, Vero, and BHK cell lines were cultured in DMEM supplemented with 10% FBS (Sigma-Aldrich Chemical, Inc., St. Louis, MO) and Penicillin/Streptomycin (Sigma-Aldrich Chemical, Inc., St. Louis, MO). Cells were transiently transfected with Lipofectamine™ 2000 (Invitrogen, Inc., Carlsbad, CA) using the manufacturer's instructions. Negative controls used in biosensor experiments included untreated, reporter only treated, and protease free groups. pTet-Off in combination with an appropriate reporter was used as a positive control.

2.1.5. Confocal microscopy

Cells were examined with a Zeiss 510 META confocal microscope (Carl Zeiss Microlmaging, Inc., Thornwood, NY). Excitation wavelengths included

UV, 488, 514, 546, and 633 nm depending on the fluorescent probes used. Appropriate emission wavelengths were determined and used for each fluorochrome used. Cells were analyzed with either 20, 40, 63, or 100X objectives. A 20X objective was used for imaging large numbers of cells for analysis.

2.1.6. Flow cytometry

Samples were analyzed by flow cytometry with either a FACScan (BD Biosciences, Inc., San Jose, CA) or a home built high speed cell sorter. Briefly, treated cells were trypsinized to attain a single cell suspension. Then, the cells were fixed in 4% formalin or paraformaldehyde (Fisher Scientific, Inc.) in PBS for 10 minutes. The cells were then washed three times with PBS. If the cells required intracellular staining prior to flow, the cells were then premeabilized and stained. These cells were permeabilized with 0.25% Triton X-100 (Fisher Scientific, Inc., Houston, TX) for 5-10 minutes. After treatment with Triton X, the cells were washed three times prior to staining. After staining the cells were filtered with a 70 μm mesh cell strainers (Fisher Scientific, Inc., Houston, TX) and analyzed by flow cytometry. EGFP samples were excited using an Argon ion laser tuned to 488 nm and detected after 488 nm band reject and 530 nm band pass optical filters (Omega Optical, Inc., Brattleboro, VT).

2.2. NANOCRYSTAL METHODS

Nanocrystals were constructed in the Kotov laboratory. Their construction is both complicated and lengthy. The protocols for the construction will be presented elsewhere by Kotov et al. As of Spring 2003, some nanocrystals are recently commercially available (Quantum Dot, Corp., Hayward, CA).

2.2.1. Cell culture

Cells, including MOLT4, BJAB, and BHK-S lines, were exposed to various nanocrystal preparations and subsequently imaged. Generally, 5 μl of nanocrystals were added to 10^5 cells and placed on a microscope for viewing while alive. Briefly, nanocrystals were introduced to the cell media and incubated at 37°C for up to 48 hours. Because of the variability in the construction and bioconjugation of the nanocrystals, it was not feasible to determine the number of nanocrystals in each preparation. In fact, only rough estimations of the quantity of nanocrystals in a preparation were possible and were entirely based on the estimated size of the crystals and the amount of starting chemicals. The question of the abount of nanocrystals per volume is further complicated by the clumping of these particles with time. Because the formation of these complexes is not well understood and appears to vary from

batch to batch as well as with time, it was extremely difficult to determine the concentration of these nanocrystals.

2.2.2. Transmission electron microscopy

Electron microscopy was carried out under the supervision of Dr. Popov, University of Texas Medical Branch. Samples were prepared by putting 5 µl of nanocrystal mixture onto a gold electron microscopy grid. The droplet was allowed to dry for 10 minutes and then the sample was viewed with either a Phillips 410 or CM 100 electron microscope (Phillips Electron Optics, Eindhoven, The Netherlands) at 60 kV. Representative photos were taken and the magnification calculated. The size of objects was determined by measuring the object of interest over the power of magnification.

2.3. PROTEASE ACTIVATED BIOSENSORS

2.3.1. Biosensor construction

Biosensor constructs were created using common cloning techniques. Briefly, the TA region of the pTet-Off (Clontech, Inc., San Jose, CA.) vector was amplified by PCR using the following primers: forward 5' – ATT CGG AAT GTC TAG ATT AGA TAA AAG TAA AGT – 3' and reverse 5' – CAT TGA

CTA CCC ACC GTA CTC GTC AAT TCC AAG GGC – 3'. See Appendix for primer locations and map. The PCR fragment was then purified (Qiagen, Inc., Valencia, CA.) and concentrated. This fragment was then used as a template for subsequent PCR reactions designed to add localization and cleavage domains. Three different biosensor constructs were initially made, BS-1, BS-2, and BS-3 using the TA template. Overlapping 100 base primers were used to PCR the BS-1, BS-2, and BS-3 (see Appendix for gene sequences). Specifically, the TA region of pTet-Off was obtained from PCR reactions using the primers described above. This PCR product was then purified with a PCR product purification kit from Qiagen, Inc., Valencia, CA. The resulting DNA fragment was then resuspended in purified water and spectrally quantified with an Eppendorf Biophotometer (Eppendorf, Inc., Westbury, NY). From this stock 50 ng was used as a template for the first primer based elongation reaction using the same forward oligo described above. The reverse oligo contained a 30 base overlap with the 3' terminus of the TA gene followed by the cleavage domain sequence. This PCR reaction was carried out and the procedure repeated until the complete gene was synthesized. This method gave fast and reliable results and was used repeatedly to produce multiple biosensors. For those biosensors that required appending sequences to the 5' region of the TA gene, the same procedure was used except that the elongating oligos were forward primers and the reverse oligo described above was used. Variants of BS-3 were developed with cleavage domains specific

for other proteases; one example of this is Caspase-3 whose cleavage domain is KRKGDEVDGVDF. Once constructed, the biosensors were cloned into the pCMV-Script vector (Stratagene, Inc., La Jolla, CA) and transformed into bacteria (Super competent E. coli, Stratagene, Inc., La Jolla, CA). Colonies were selected based on kanamycin resistance. Selected colonies were grown in LB broth and the plasmid DNA isolated (Qiagen, Inc., Valencia, CA). Restriction digests and PCR were used to confirm the presence and orientation of the PCR insert.

2.3.2.   Immunocyochemistry

Cells were fixed and permeabilized as described in 2.01.4. Biosensor protein was detected by immunostaining with anti-VP16 raised in rabbit (Clontech, Inc., San Jose, CA.). Active Caspase-3 was detected with anti-active Caspase-3 raised in rabbit (Cell Signaling Technology, Inc., Beverly, MA). Secondary antibodies were purchased from Molecular Probes, Inc. and were conjugated to Alexa-fluor 488, 546, or 596. Cells were also counterstained with one or more of the following, Hoechst 33342, 4',6-diamidino-2-phenylindole, dihydrochloride (DAPI). (DAPI emits blue fluorescence upon binding to AT regions of DNA) and Phalloidin 546 (Molecular Probes, Inc., Eugene, OR).

CHAPTER 3.   DEVELOPMENT OF LAYER BY LAYER CONSTRUCTED NANOPARTICLES

3.1.   INTRODUCTION

The proposed goal for this chapter is to develop multilayered nanoparticle delivery systems. This chapter discusses different approaches used in the development of these particles, including modification of commercially available fluorescent nanoparticles and the construction of "layer by layer" nanoparticles.

For the first set of experiments, commercially available fluorescent nanoparticles (Spherotech, Inc., Libertyville, IL) with bioconjugated anti-mouse IgG on the surface were used to test targeting strategies. In order to determine which targeting strategy would be most accurate, efficient, and cost effective three modalities were considered for these particles: specific antibodies (anti-CD95), recombinant protein, and sugar molecules.

The second set of experiments involved the development of layer by layer nanoparticles using alternating charged layers coated on a solid core particle. These layered nanoparticles were developed to enable the delivery of a payload to specific populations of cells. Initial experiments were created to test the toxicity of these components and their effectiveness for gene delivery.

3.2. METHODS

3.2.1. Coating of commercially available nanoparticles

Anti-CD95 was used to target commercially available nanoparticles (Spherotech, Inc., Libertyville, IL) to BJAB cells (CD95 positive). This was achieved by first incubating BJAB cells with mouse anti-human CD95 antibodies (Southern Biotech, Inc., Birmingham, AL) for 1 hour in PBS. Cells were then incubated for a further 1 hour at 37°C with the purchased fluorescent green-nanoparticles (Spherotech, Inc., Libertyville, IL) with anti-mouse IgG conjugated to the surface. Cells were counterstained for 10 minutes with Hoechst Dye 33342 (Molecular Probes, Inc., Eugene, OR) and then washed three times with PBS, to detect nuclei. This mixture was washed three times with PBS. The experiments were then analyzed by fluorescent microscopy, where the results were visualized and photographed.

In a separate experiment, CD95 positive BJAB cells were co-cultured with CD95 negative MOLT4 cells. The BJAB cells were labeled with mouse anti-human CD95 and exposed to green fluorescent nanoparticles (~520 nm) coated with anti-mouse IgG while the MOLT4 cells were labeled with a blue fluorescent tracking dye, CMAC (Molecular Probes, Inc., Eugene, OR). The CMAC tracking dye stains the cell membrane and is trapped there. Once

cells are stained and washed, the tracking dye will not bleed out. This is one simple method for differentiating cell types during mixed culture experiments. Cells stained with antibodies conjugated to fluorochromes were used as positive controls. Cells not containing the receptor target were used as negative controls.

3.3. RESULTS

3.3.1. Fluorescent polystyrene layered nanoparticles for targeting

The priority of this project was to develop techniques to successfully target layered nanoparticles to specific cell populations. **Figure 3.1** demonstrates the labeling and counterstaining of Live BJAB cells with Hoechst 33342 (Panel A, blue) and anti-CD95 (Panel A, green), respectively. Importantly, FITC labeled nanoparticles coated with anti-mouse IgG F(ab) fragment (Panel B, green particles) were able to attach themselves to the targeted BJAB cells which expressed CD95. This experiment demonstrates that antibody coated particles can target cells containing CD95 on their surface, but did not explore nanoparticle entry into the cell.
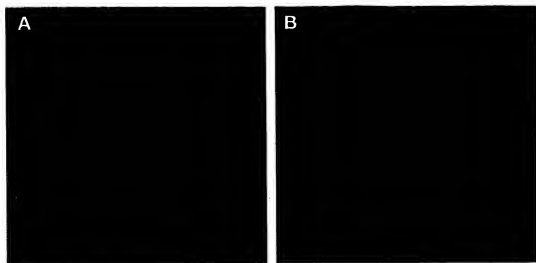
Figure 3.1. Nanoparticle targeting of CD95 positive cells. Live BJA cells were labeled with anti-CD95 FITC (Panel A). BJAB cells labeled wit anti-CD95 and exposed to FITC labeled nanoparticles coated wit secondary antibodies specific for the Fc portion of anti-huma CD95antibodies (Panel B). All nuclei are counterstained with Hoechs 33342.

Cells without CD95 on their surface were used as negative controls during a mixed population test of the CD95 targeting strategy. **Figure 3.2** depicts the successful binding of nanoparticles conjugated to anti-mouse IgG to BJAB cells which expressed the CD95 antigen on its cell surface (Panel A and B green FITC cells). These nanoparticles were however unable to bind to the CD95 negative MOLT4 cells which were labeled with CMAC, a blue fluorescent tracking dye (panel B, blue cells). These results indicate that particles can indeed target via conjugated antibodies in our hands, confirming data shown by others (Spherotech, Inc., Libertyville, IL).
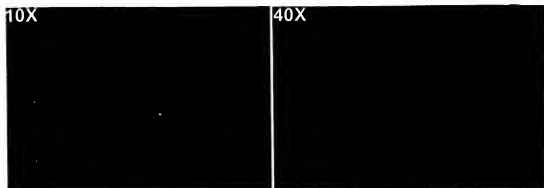
Figure 3.2. Nanoparticles target CD95 positive cells in a 1:1 cel mixture. MOLT4 cells were stained blue with a cell tracking dye (CMAC) washed and mixed with BJAB cells. The MOLT4 cells were used as negative control because they do not normally express CD95 on thei surface. BJAB cells constitutively express CD95 on their surface. This liv cell mixture was first exposed to an anti-CD95 antibody raised in mice Green fluorescent particles conjugated to anti-mouse IgG were then adde to the culture in an attempt to target to only the CD95 positive BJAB cells As shown in both panels, none of the blue MOLT4 cells were targeted by th green particles. Only the BJAB (unstained) cells, that are CD95 positive were bound to the green particles.

3.3.2. Cytotoxicity of layer by layer nanoparticles

The previous experiments gave practical knowledge of using antibodies to target commercial nanoparticles to cells in culture. To construct layered nanoparticles *de novo* that could carry multiple payloads. The toxicities of different core particles, onto which discrete layers would be deposited, were tested using markers for membrane integrity and apoptosis. Initial experiments determined the toxicities of 20 µl several different core particles in cell culture. The actual concentration of core nanoparticles in each sample was not determined due to a lack of methods. So, a 20 µl dose for 1×10^5 cells was chosen as a starting point for these initial toxicity studies. In total, three core particles were evaluated and these consisted of two silica (Si and Si2, both silica particles from different preparations) and one latex product (LA). The different nanoparticle cores were gifts from the Lvov laboratory. Both the Si2 and LA preparations were found to be highly toxic as they markedly increased apoptosis and loss of membrane integrity in BJAB cells (**Figures 3.3 and 3.4**). **Figure 3.3** also shows that high levels of apoptosis were also observed in BJAB cells treated with core nanoparticles containing one if the silica based core preparations. These results are typical of those seen in repeated experiments of this nature.

The most promising nanoparticle core, Si, was also tested on Huh7 cells for hepatitis C virus based studies (**Figure 3.5**). These cells were derived from a human hepatoma and are use in these studies because they were derived from human liver cells. It was observed that a 10 μl dose, per 1×10^5 cells, of the Si nanoparticles induced apoptosis in about 10% of the cells. A dose response experiment was conducted with the silica particles (**Figure 3.5 Bottom panel**). This study also utilized dialysis to rule out the possibility of a toxic component in the nanoparticle solution. The results of this experiment showed that the there was indeed a nontoxic concentration of nanoparticles and that there was no dialyzable toxic component in this mixture. This strongly suggests that the nanoparticles themselves are responsible for the toxicity issues observed. The nanoparticles tested in this experiment were not washed, resulting in a much higher concentration of particles per cell. Importantly, this concentration was found to be less toxic as the BJAB cells did not show any detectable membrane damage. As a result, the Si core was chosen as the preferred particle for the remaining experiments reported in this thesis. In conclusion, there are three main results from these experiments:

1. Si2 and LA both killed all of the cell types extremely well and were therefore not chosen for future studies.

2. Si was the least toxic nanoparticle core and was therefore chosen for future experiments.

Panel A. Trypan blue dye assay for membrane integrity
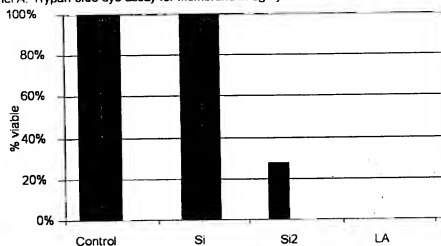
Panel B. TUNEL assay for late stage apoptosis
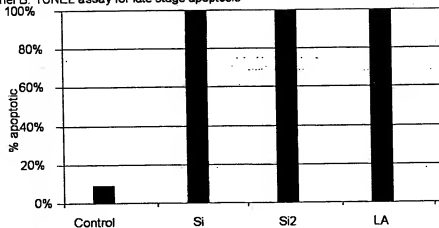
Figure 3.3. Determination of nanoparticle core toxicity. Three core particles, two silica particles (Si and Si2) and a latex (LA) particle were evaluated for toxicity with trypan blue dye exclusion (Panel A) at 1 and 24 hours (black and gray bars, respectively). Cells exposed for 24 hours were also assayed for apoptosis with the TUNEL assay (Panel B).
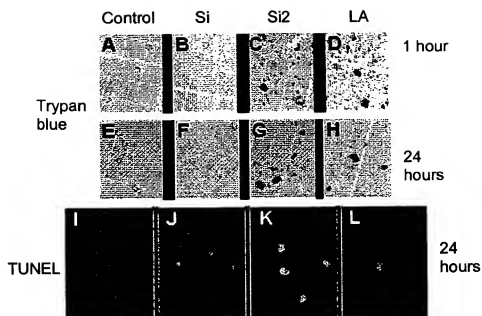
Figure 3.4. Cytotoxicity of three nanoparticle core preparations in BJAB cells. Cells were harvested at 1 (top row) and 24 (middle and bottom rows) hours. Trypan blue dye exclusion was used to determine membrane integrity (top two rows) and TUNEL analysis (bottom row) to determine the number of apoptotic cells in each treatment group. Cells were treated with nothing (panels A, E, and I), two silica Si (panels B, F, and J) and Si2 (panels C, G, and K), and a latex (panels D, H, and L) cored particles. Panel L only contains one apoptotic cell because there were only a handful of intact cells remaining in the samples, therefore only one intact nucleus could be captured in a single frame.
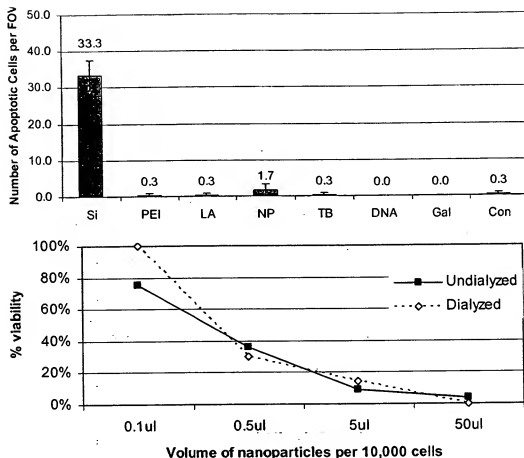
Figure 3.5. Effect of individual LBL components on apoptosis in Huh7 cells. Top Panel: Huh7 cells were treated with the individual components used to construct LBL; silica core partricles (Si), Polyethylimine (PEI), Lipofectamine™ 2000 (LA), complete nanoparticle (NP), Tris buffer (TB), pEGFP (DNA), Galactosamine (Gal), and untreated (Con). The cells were incubated for 24 hours and then assayed for apoptosis with the TUNEL assay. Only the silica core particles appeared to induce apoptosis (Si). The error bars indicate the standard variation between fields of view. Each field of view contains approximately 300 cells and 3 FOV for each sample. Bottom Panel: Huh7 cells were treated with different volumes of silica nanoparticles and viability was determined by trypan blue dye exclusion. The nanoparticles were either untreated or dialyzed against PBS for 24 hours.

Layered nanoparticles containing the Si core were found to be the least toxic, therefore, these cores were selected for further development of the layer by layer nanoparticles containing payloads in the form of alternating charged layers. **Figure 3.5** shows a toxicity study on each of the potential layers. These results indicate that the individual components that will comprise each layer in the layer by layer nanoparticles are not toxic, except for the core particles. The individual components were tested for toxicity once with the exception of the Si and NP groups. Because of their importance, the Si and NP groups were evaluated for toxicity several more times with very similar results. These preliminary experiments were used to determine which components were the cause of toxicities seen during pilot studies. The toxicity studies, while not extensive, clearly showed that the only toxic component was the silica nanoparticle. These particles, while somewhat toxic, were acceptable for use in early experiments. The principal reason for using these particular components was that the Lvov laboratory has considerable experience assembling layered components using these particular silica particles, PEI (poly(ethyleneimine)), PAH (poly(allylamine hydrochloride)), etc. The components tested are also the minimal layers necessary to build layered silica particles bound to DNA and a targeting layer.

Multilayered nanoparticles were constructed with the idea that they would eventually be used for molecular programming. Molecular programming is a concept that describes giving an individual cell a set of instructions. These instructions are similar in concept to a software program that allows the cell to effectively deal with a pathogenic process. This endpoint requires the deposition of many layers on a single particle. Therefore particles with multiple layers were constructed. For example, the overall negative charge of DNA was used to bind to the positively charged polymer and this effect was used to construct 16 layered nanoparticles which had increasing particle size (**Figure 3.6**). **Figures 3.6 and 3.7** outline the composition of each layer and their respective thickness. Simple layered nanoparticles (**Figure 3.7**) were constructed to test the efficiency of outer coatings used to facilitate cell entry. By using the minimal number of layers (3 with one layer of DNA and 5 with two layers of DNA), the number of variables could be minimized. Additionally, minimizing the number of layers, maximizes the probability that it will be correctly constructed. **Figure 3.6** shows a decrease in layered nanoparticle diameter after the addition of the first BSA layer. This is due to the washing of the particles after each layer deposition. The BSA forms a thick layer of which the most is removed through washing.
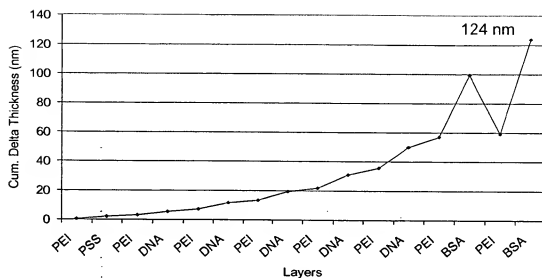
Figure 3.6. Nanoparticle growth, diameter. Graph shows the cumulative thickness (y axis in nm) as layers are added (x axis) resulting in approx. 124nm particles. Size was measured with a zeta potential/sizing. Layers include polyethylimine (PEI), poly (sulfonate styrene) (PSS), pEGFP-C1 (DNA), and bovine serum albumin (BSA). Done in collaboration with the laboratory of Dr. Lvov.
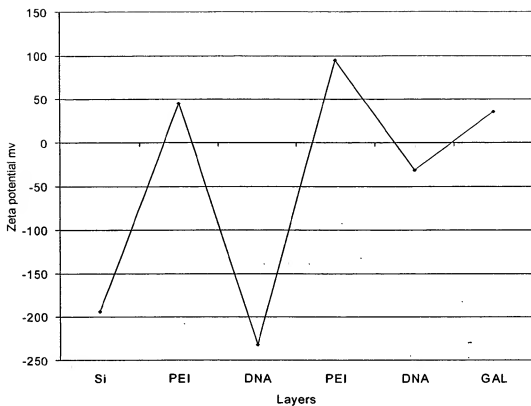
Figure 3.7. Nanoparticle growth, zeta potential. Chart showing the zeta potential of layer by layer as charged layers are deposited on the silica core particle, where each point is a layer. Done in collaboration with the laboratory of Dr. Lvov.

The shape and size distribution of 5 layered nanoparticles were determined using Atomic Force Microscopy (AFM) and Transmission Electron Microscopy **(Figures 3.8** (panel A and B)**; and 3.9)**. Atomic force microscopy was done at Louisiana Tech University by the Lvov group and gives information about the size, shape, and clustering of these layered nanoparticles. The electron microscopy data gives similar data and was done at UTMB. Both of these techniques were used to confirm the presence and physical characteristics of these novel layered nanoparticles. There appears to be one prominent group of layered nanoparticles, approximately 106 nm in diameter (~30%), which was similar to the estimated size of 126 nm found by zeta sizing. Based on TEM images the diameters of the layered nanoparticles was estimated to range from 64 to 117 nm **(Figures 3.8,** panels B and C) show a histogram of the diameter data gathered from the TEM images. From these data we conclude that this batch of layer by layer nanoparticles has a large population of ~106 nm particles, but also contains populations of larger and smaller layered nanoparticles ranging in size from 124 nm to 70 nm. Seventy nanometers is the average size of the core silica particles used for these studies. The atomic force microscopy data shown in **Figure 3.9** shows both small and large clusters of layered nanoparticles. These data also show layered nanoparticles within the same size range (70-130 nm). Unfortunately there was no way to purify the complete particles. These layered nanoparticles were then used in later experiments despite the obvious heterogeneity of the

particles produced.   These data show that constructing a population of homogenous layered nanoparticles without aggregates is not possible using this technique unless the protocols were extensively optimized. Some of these issues are addressed in later chapters, particularly in **CHAPTER 5**. Once a rudimentary layered nanoparticles construction technique was established experiments with the targeting outer layer began.
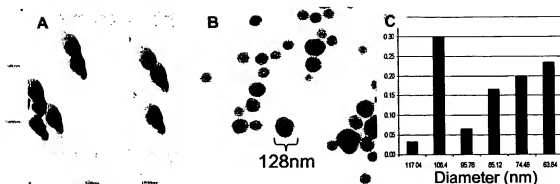
Figure 3.8. Structural analysis of nanoparticles. Panel A represents AFM of layer by layer particles constructed with DNA layers and a BSA outer coat, with 6 layers in total. Panel B shows the same particles analyzed by TEM, while Panel C shows a bar graph containing a histogram showing nanoparticle diameter data based on the TEM data. These data show aggregates, suggesting that the overall size is much larger than the individual particles. Done in collaboration with the Lvov and Popov laboratories.
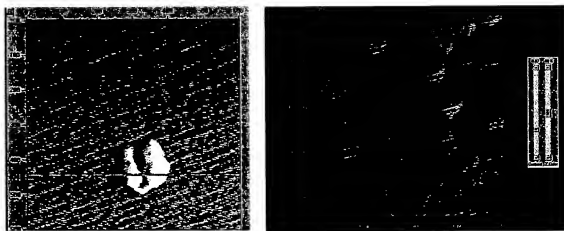
Figure 3.9: **Atomic force microscopy (AFM) of six layered nanocapsules with two internal pEGFP-C1 DNA layers coated with nothing or galactosamine.** Nanoparticles were visualized and measured with AFM to determine the size distribution of the particles. The average size of these clusters is ~160 nm and there appeared to be little variation in the size distribution. The left panel is a small cluster of nanoparticles. The right panel shows large clusters of nanoparticles. Done in collaboration with the laboratory of Dr. Lvov.

3.3.3.   Development of sugar coated layered nanoparticles for targeted delivery of DNA

To be able to use layered nanoparticles to deliver genes, at least *in vitro*, layered nanoparticles were tested with various outer coatings that were chosen to enhance the uptake of the layered nanoparticles by cells. Galactosamine was chosen to test a receptor mediated endocytosis method of cell entry. This strategy is based on the presence of asialoglycoprotein receptors on the surface of liver derived cells, thus facilitating entry of layered nanoparticles into the cell (Schwartz 1984). In addition, lipid coating was tested as an non-targeting method of delivery. After the initial construction of the layered nanoparticles, several batches of six different groups of layered nanoparticles (**Table 3.1.**) were produced with layers of pEGFP-C1 (Clontech, Inc., San Jose, CA). The underlying layers were identical to those layered nanoparticles described in **Figure 3.7.** These layered nanoparticles were then used to transfect a small number of Huh7 liver cells in culture (**Figure 3.10**).

LBL	Approx. Size (nm)	Outer coating
1	1500	Galactosamine
2	1500	Lipid
3	300	Galactosamine
4	300	Lipid
5	100	Galactosamine
6	100	Lipid

Table 3.1. Size and outer coat composition of layered nanoparticles. Six nanoparticle samples were constructed in order to determine the effect of size and outer coating on transfection efficiency and cell viability. Nanoparticle clusters 1500, 300, 100 nm were constructed. These particles had one of two outer coatings: galactosamine or Lipofectamine™ 2000 (Lipid). Done in collaboration with the laboratory of Dr. Lvov.
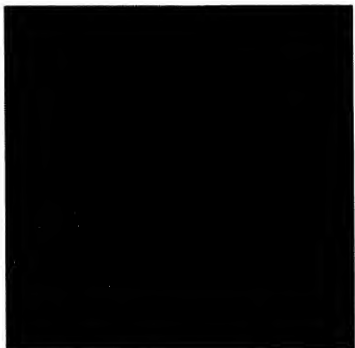
Figure 3.10. Nanoparticle mediated transfection of EGFP DNA. Huh7 cells were exposed to sugar coated nanoparticles with pEGFP DNA sub-layers. EGFP protein was expressed from the DNA transferred by the nanoparticles in a small population of cells, <1%, therefore only one cell per FOV could be photographed.

Efficiency of layered nanoparticles transfections were determined by assessing the expression of pEGFP-C1 in Huh7 cells exposed to several different types of layered nanoparticles which were of varying sizes and outer coatings. Fluorescence and confocal microscopy were used to evaluate the expression of EGFP and the overall viability of the cells during the experiment. Cell health was observed by viewing cellular shape and nuclear morphology. Initial studies showed that galactosamine coated layered nanoparticles were much less efficient for transfecting cells than those layered nanoparticles coated with Lipofectamine™ 2000. Therefore, later experiments utilized more of the lipid coated layered nanoparticles than galactosamine coated layered nanoparticles. **Figure 3.11** demonstrates data from a series of experiments which were set up to determine the effects of layered nanoparticles size on the delivery of pEGFP-C1 by lipid coated layered nanoparticles. The left panel of **Figure 3.11** reports the transfection efficiency (y-axis) of different amounts (0, 0.01, 0.5, and 1.0 ul) of layered nanoparticles to Huh7 cells. Three different sizes of layered nanoparticles clusters were utilized for these studies, ~100, 300, and 1500 nm diameter. Cells exposed to layered nanoparticles >100 nm were in poor health and showed signs of decreased membrane integrity and apoptotic nuclei; although some cells did express EGFP. The cells exposed to the 100 nm layered nanoparticles appeared healthy and did not show any visible signs of toxicity (**Figure 3.11**, right panel). Very few cells exposed to lipid coated layered nanoparticles >100 nm showed visible expression of

EGFP. Data from Huh7 cells exposed to galactosamine coated layered nanoparticles of varying diameters is shown in **Figure 3.12**. The left panel of **Figure 3.12** shows that 100 nm and 300 nm layered nanoparticles were capable of delivering EGFP to cells, but not 1500 nm layered nanoparticles. Again, the cells exposed to larger layered nanoparticles (>100 nm) showed overt visual signs of toxicity including blebbing, compartmentalization, and apoptosis (data not shown). The cells exposed to 100 nm layered nanoparticles remained healthy throughout the experiments and never showed any signs of increased apoptosis (**Figure 3.12**, right panel). Comparisons between the lipid and galactosamine layered nanoparticles showed that while lipid coated layered nanoparticles were more effective gene delivery agents, they were also more sensitive to size. Cells exposed to galactosamine coated layered nanoparticles were more likely to express EGFP from larger layered nanoparticles than those cells treated with lipid coated layered nanoparticles, 10% versus 1%. Additional studies are necessary to confirm this trend and testing more coatings has the potential to yield more efficient gene transfer.
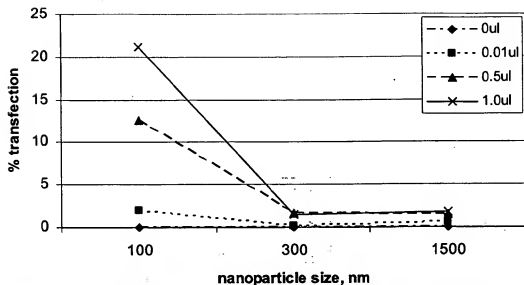
Figure 3.11. Effect of size on lipid coated, nanoparticle transfection. Left panel. Graph of transfection efficiency (y axis) versus nanoparticle size (x axis) with different amounts of nanoparticle solution (inset). Right panel. Fluorescent micrograph of cells transfected with lipid coated pEGFP-C1 (EGFP protein is green) containing nanoparticles. All cells were counterstained with DAPI (blue).
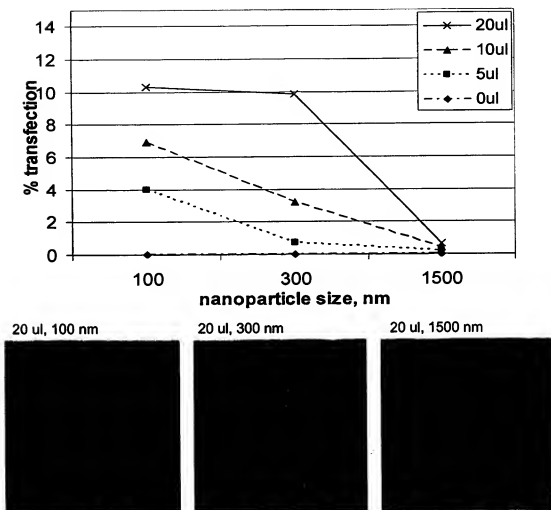
Figure 3.12. Effect of size on galactosamine coated, nanoparticle transfection. Left panel. Graph of transfection efficiency (y axis) versus nanoparticle size (x axis) with different amounts of nanoparticle solution (inset). Right panel. Fluorescent micrograph of cells transfected with lipid coated pEGFP-C1 (EGFP protein is green) containing nanoparticles. All cells were counterstained with DAPI (blue).

3.3.4. Dual gene delivery by layer by layer nanoparticles

Next, dual gene layering was used to determine the capability of these layered nanoparticles to deliver more than one type of DNA to an individual cell. A solution of equal molar proportions of pEGFP-C1 and pDSRed2-C1 DNA was mixed to create a simple three layered nanoparticle mixture with a silica core coated with PEI (poly(ethyleneimine)) and finally with the DNA mixture. One microliter of these layered nanoparticles were then further coated with a lipid (Lipofectamine™ 2000) and used to transfect Huh7 cells. Lipofectamine coated layered nanoparticles were used instead of other coatings because of the higher transfection efficiency. It was found that lipid coated layered nanoparticles were able to deliver two types of DNA, pEGFP-C1 and pDSRed2-C1 to these cells (**Figure 3.13**). We also observed dual labeling in a small fraction of cells (<1%) which were found in clusters and were similar to that seen in **Figure 3.13.** This could be due to large clusters of layered nanoparticles settling on the cells. Clustering could also lead to decreased transfection efficiency. The poor transfection efficiency of these layered nanoparticles precluded quantification. The majority of fluorescent cells were green, but as mentioned above there were so few cells transfected that quantification was not necessary. These cells were counterstained with DAPI.
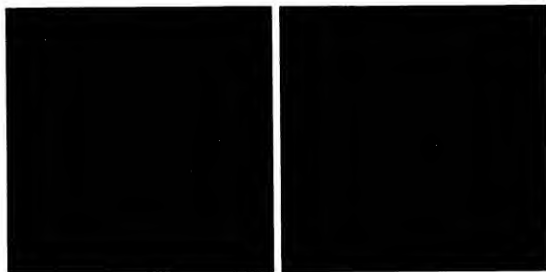
Figure 3.13. Dual gene delivery by layer by layer nanoparticles
Fluorescent microscopy images of Huh7 cells exposed to lipid coated laye
by layer nanoparticles containing a layer of a mixture of pEGFP-C1 an
pDSRed2 DNA. Left panel shows cells positive for EGFP (green). Righ
panel shows cells positive for dsRed (Red). Less than 1% of cells wer
fluorescent and of those only a few were double positive. In fact, the grea
majority of cells were positive for EGFP but not dsRed. All cells wer
counterstained with DAPI (blue). Images were taken with a 40X objective.

3.3.5. Imaging of single fluorescent beads as a surrogate for biosensor positive white blood cells

If successful, injected layered nanoparticles would yield EGFP positive cells. *In vivo* imaging was used to determine if there were large quantities of EGFP positive cells. One of the goals of this project was to develop means of detecting the level of radiation damage experienced by astronauts during space travel. To accomplish this we chose to focus on blood cells as these cells flow through the eye and near the skin where they can be assessed for biosensor activity. To visualize the individual blood cells *in vivo* in, the eye, the mucosa of oral cavity, and the skin, three distinct optical approaches with various degrees of spatial resolution were employed. A fundus scope was modified to allow the detection and visualization of EGFP labeled fluorescence beads which were mixed with blood and circulated through capillary tubes. From the optical point of view, the eye provided the optimum location for the detection and visualization of transfected individual blood cells. **Figures 3.14 and 3.15** show our ability to see the presence of EGFP loaded beads in blood within a capillary tube. This line of experiments will lead to the ability to monitor nanoparticle transfected cells *in vivo*.

Figure 3.14. Imaging of fluorescent beads in blood at a 1:20 dilution in a capillary tube. For 20 times dilution (5% Beads, 95% Blood) individual beads were visible as bright green spots using Slit Lamp with 10 seconds of scanning time. Done in collaboration with the Motamedi laboratory.

Figure 3.15. Imaging of fluorescent beads in blood at a 1:100 dilution i a capillary tube. For 100 times dilution (1% Beads, 99% Blood), individua beads were visible as bright green spots using Slit Lamp with 10 seconds o scanning time. Done in collaboration with the Motamedi laboratory.

3.4. DISCUSSION

The initial studies with the commercial particles served two purposes, the first to start experiments with simple well characterized particles prior to working with novel layered nanoparticles. The second use of these studies was to determine if antibody mediated targeting was a practical approach for nanomedicine applications. From these experiments, we learned that while these particles were easy to use, but would require large quantities of antibodies for scaled up use *in vivo*. This was valuable information that was considered throughout the remainder of this dissertation.

We focused on developing layer by layer constructed nanoparticles that are capable of delivering multiple payloads to specific populations of cells *in vivo*. The first experiments towards this end were designed to test antibody mediated cell targeting. These targeting experiments yielded positive results and were succeeded by the development of actual layer by layer nanoparticles in collaboration with the help of Dr. Lvov's laboratory, Louisiana Tech University, Rustin, LA.

The layer by layer nanoparticle experiments proceeded from the core of the layered nanoparticles outwards. This logical approach gave rise to a fundamentally stable layered nanoparticles with which used in several follow

up experiments. First, layers were deposited on a silica core particle in such that there was built in flexibility with respect to what layer was deposited. In fact, up to 16 layers were deposited onto a single core particle. The next studies were focused on the outer coating of the layered nanoparticles. Naked, galactosamine, and lipid coated particles were tested for gene delivery *in vitro* and *in vivo*.

The initial studies focused on delivering these particles to liver derived cells, instead of CD95 expressing cells. This is because the layer by layer deposition requires a large amount of materials (grams) and using antibodies for the development stage was not practical. Therefore, we turned to sugars, which can be purchased in large quantities. Galactosamine was initially chosen based on its affinity for the asialoglycoprotein receptor on the surface of liver cells.

The development of these layered nanoparticles began at the core of the layered nanoparticles. Three core particles made of either silica or latex were tested for toxicity. Of those, only one core particle did not cause immediate destruction of the cell membrane, Si. Although this particle did induce apoptosis, it was the least toxic of the three tested. Future experiments in this lab will focus on developing less toxic core particles for payload delivery

to cells. None of the other layered nanoparticles constituents were found to be toxic.

Although layered nanoparticles with many layers (up to 16) were constructed, the smaller and less complex layered nanoparticles were found to be the most effective vectors for gene transfer. The two most important aspects of gene transfer with these layered nanoparticles are (1) size and (2) outer coat. An enhanced green fluorescent protein plasmid (pEGFP-C1) was used to detect successful transfection. The most effective means for transfecting cells appears to be coating small layered nanoparticles (<100 nm) with lipid (Lipofectamine™ 2000, Invitrogen, Inc., Carlsbad, CA). The small layered nanoparticles had the highest transfection efficiency (~30%). The size of these lipid coated layered nanoparticles was very critical for transfection. There was virtually no transfection with lipid coated layered nanoparticles greater than or equal to 300 nm in diameter. On the other hand, transfection with sugar coated layered nanoparticles seemed less dependant on size, but never achieved a transfection efficiency over 15%. These results could be strengthened by testing other sugar coatings with the same method of entry.

The next step was to attempt to deliver genes *in vivo* with these layered nanoparticles. Briefly, a mouse was injected with six layered nanoparticles containing pEGFP-DNA. No EGFP fluorescence could be detected in the

major organs with *in vivo* imaging. This was likely due to a very low level of transfection efficiency that was below the limit of detection for this *in vivo* imaging system. Furthermore, PCR of the targeted tissue, liver, showed no clear evidence of the presence of EGFP DNA. These results clearly show that more efficient and better targeted layered nanoparticles are needed for gene transfer *in vivo*. Another contributing factor could be the amount of layered nanoparticles injected. More layered nanoparticles and smaller clusters could help to increase the transfection efficiency. A higher transfection efficiency will also be needed to visualize EGFP positive white blood cells. The preliminary data shown in the previous section illustrates that a modified fundus scope can be used to detect fluorescent particles the size of cells in a solution of blood. Viewing these same solutions *in vivo* will be more difficult and will require large numbers of positive cells. In the end, only a fraction of the white blood cells will be successfully transfected with layered nanoparticles; of those only a fraction will trigger the biosensor and of those only fraction will be bright enough for the detection system to see. For these reasons, it is imperative that future experiments need to be focused on the optimization of these technologies.

CHAPTER 4. DEVELOPMENT OF SEMICONDUCTOR BASED NANOCRYSTALS

4.1. INTRODUCTION

The previous chapter described both *in vitro* and *in vivo* experiments with layered nanoparticles constructed by charged layer deposition. These experiments resulted in both positive and negative data. Some of the problems with these layered nanoparticles included core toxicity, relatively impure particles, no nanoparticle fluorescence, large size, and outer layer assembly. Semiconductor nanocrystals were used in the following experiments as part of an ongoing collaboration with the Kotov lab from Oklahoma State University. These nanocrystals have properties that were used to solve some of the problems mentioned above.

Nanocrystals are relatively non-toxic despite the toxicities of their core components. There are likely substantial differences between the toxicities of the raw materials and the crystalline structures used in these studies. To date there have been no publications that compare the toxicity of the raw semiconductor materials and their crystalline counterparts. *In vivo* developmental studies with similar particles showed neither toxicity nor developmental problems, even after long term exposure (Dubertret et al. 2002; Jaiswal et al. 2003). The nanocrystals are also highly fluorescent and have

excellent spectral properties, such as the absence of photobleaching. These nanocrystals are also far smaller than their layer by layer counterparts. The size of these nanocrystals suggests that they will easily traverse the cell membrane. Finally, streptavidin can be bioconjugated to the surface of these nanocrystals. The bound streptavidin gives great flexibility with surface coatings. Construction of these nanocrystals is fairly straight forward and is depicted in **Figure 4.9**.

4.2. METHODS

4.2.1. Targeting molecule conjugation to nanocrystals

Multiple targeting and cell entry molecules were tested on streptavidin coated nanocrystals. In all cases, the targeting molecule was biotin labeled. Several biotin labeled targeting agents were evaluated for use with streptavidin coated nanocrystals, including anti-CD95 (Southern Biotech, Inc., Birmingham, AL), anti-CD81 (Southern Biotech, Inc., Birmingham, AL), and two arginine rich synthetic peptides. The synthetic peptides were synthesized at UTMB and both contained N terminal biotin tags. One peptide was composed of an 8 residue segment (GRKKRRQRRR) of the HIV tat protein and was called HIV-tat. The other peptide was a 6x arginine repeat. The targeting molecules were incubated with the nanocrystals at 10:1 volume:volume with the targeting molecule in excess (5 µl antibody to 0.5 µl

nanocrystals). This volume based method cannot be translated to a concentration and was intended as a way to begin to address the problem of nanoparticle concentration. This mixture was incubated at 37°C for 30 minutes prior to cell treatment. Cells were treated with 5 μl of this mixture for times that varied from 30 minutes to 24 hours.

4.3. RESULTS

4.3.1. CdTe nanocrystals

The first step towards developing these nanocrystals for biological use was testing their targeting capacity. Nanocrystal preparations containing a CdTe core and anti-human CD95 or anti-human CD81 outer coatings were initially tested by incubation with cell lines known to express either CD81 or CD95. CD95 was chosen as it expressed on the surface of cells shortly after radiation exposure. CD81 has been implicated to be involved in viral targeting of hepatitis C virus to hepatocytes (Rice and Hagedom 2000). Therefore, CD81 was used to target the same cells as the hepatitis C virus. The nanocrystal preparations were most stable at pH>8, and after these experiments, considered to be incompatible with media designed for cell culture (pH=7.5). Initial data showed that uncapped CdTe nanocrystals (**Figure 4.1**) were not stable in media with pH<8. This proved to be problematic when experimenting with live cells. Even coating the particles with

BSA or antibodies did not appear to help. CdTe nanocrystals were microinjected into T24 cells to assess the possibility of using these nanocrystals for intracellular targeting. T24 cells are derived from a transitional cell carcinoma, these cells were chosen because they constitutively expresses CD95 on the surface (Mizutani et al. 1997). Once inside the cells, the nanocrystals were assayed for their ability to fluoresce within the cellular compartment (**Figure 4.2**). The particles did retain their fluorescent properties within the cytoplasm of cells and were photographed shortly after injection (~1 minute).
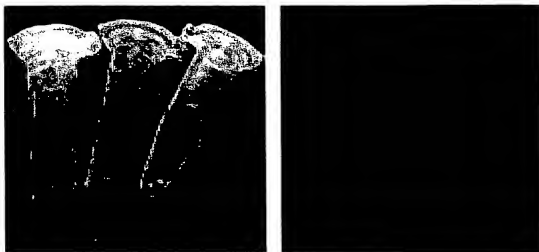
Figure 4.1. Nanocrystals under white and UV light. Tube contents (fro left to right): Dry CdTe nanocrystals coated with BSA/Avidin; CdT nanocrystals coated with BSA/Avidin in PBS (pH=7.4); same particles bu diluted 1:10 in PBS.
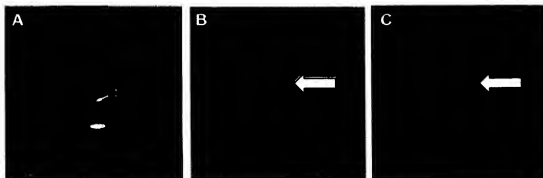
Figure 4.2. CdTe nanocrystals coated with BSA/Avidin in PBS. Panel shows CdTe nanocrystals loaded into a pipette prior to microinjection. T2 cells were microinjectd with nanocrystals and photographed under light fiel (Panel B) and fluorescence conditions (Panel C).

These particles were in suspension until injected into the cell culture media. When injected into the cell culture media the solution immediately became viscous. Because of the unstable nature of these particles at physiological pH, we worked to design a more stable particle that had stabilizing outer layers. We settled on a particle (from the core out) with a semiconductor core for fluorescence, a sulfur cap for stability at physiological pH, and an outer shell of streptavidin. The final coat of streptavidin gives flexibility with respect to attaching targeting molecules to the surface of the particle. We initially used biotin labeled antibodies to target cells. Since antibodies are not cost effective for bulk preparation, other more cost effective biotin labeled moieties could be used without changing the particle preparation.

4.3.2. Sulfur capped nanocrystal construction and cytotoxicity

To improve the stability of the particle under physiological conditions nanocrystals were produced with a sulfur cap. The presence and size of these particles were confirmed by electron microscopy (**Figure 4.3**). The size of the particles present was determined to be ~14 nm and roughly spherical. The particles were used in a number of experiments, the first of which were toxicity studies. The endpoints examined in these studies were membrane integrity and apoptosis (**Figures 4.4 and 4.5**). MOLT4 cells, expressing CD81 on their surface, were exposed to nanocrystals for 24 hours and cells harvested at 1

and 24 hours for cytotoxicity assays. Harvested cells were assayed for membrane integrity after exposure to nanoparticles at both 1 and 24 hours. Cells harvested at 24 hours were also assayed for late stage apoptosis by the TUNEL assay. There were no notable differences in membrane integrity after 1 hour, with respect to the control samples however, after 24 hours, there was a remarkable increase in cells showing compromised membranes. There was also a modest increase in late stage apoptotic cells, represented as an increase in percent apoptotic in the bar graph below.
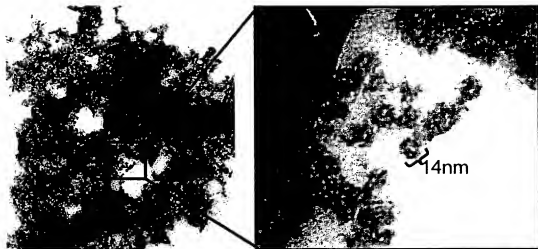
Figure 4.3. TEM data on CdTe nanocrystals coated with S, BSA, and streptavidin. CdTe nanocrystals were evaluated for size and consistency. The particles appeared to be uniform and about 14 nm in diameter and form large clusters.
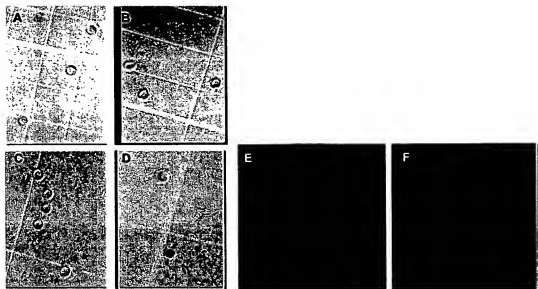
Figure 4.4. Cell viability and TUNEL assays in cells exposed t nanocrystals. BJAB cells were incubated with nanocrystals and cell harvested at 1 (Panels A and B) and 24 hours (Panels C, D, E, and F) fo both trypan blue dye exclusion (Panels A, B, C, and D) and TUNEL assay (Panels E and F). In all time points examined, there were very few cells wit compromised membrane integrity. After 24 hours, there appeared to be modest increase in TUNEL positive (apoptotic) cells (Panel F) and a larg increase in membrane compromised cells (Panel D).

Panel A. Trypan blue dye assay for membrane integrity
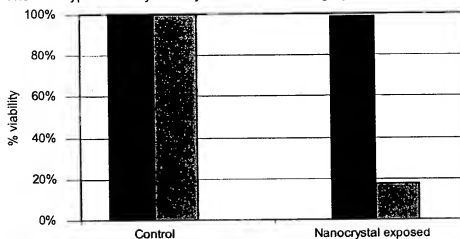
Panel B. TUNEL assay for late stage apoptosis
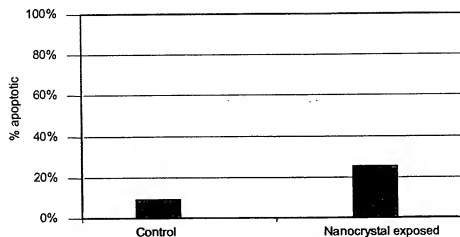
Figure 4.5. Membrane integrity and TUNEL positive cell counts. Control and nanocrystal exposed cells were evaluated for toxicity with trypan blue dye exclusion (Panel A) at 1 and 24 hours (black and gray bars, respectively). Cells exposed for 24 hours were also assayed for apoptosis with the TUNEL assay (Panel B).

4.3.3. Coating nanocrystals for targeting and cell entry

The next step towards targeted delivery of nanocrystals is the addition of targeting moieties to the streptavidin coated outer surface. Therefore, streptavidin coated nanocrystals were assayed for their ability to bind biotin conjugated antibodies. Protein A coated non-fluorescent 5 μm beads were used to bind antibodies either bound or unbound to nanocrystals. Protein A is a surface receptor expressed by *Staphylococcus aureus* and is capable of binding the Fc portion of immunoglobulins, especially IgGs, from a large number of species (Boyle et al. 1985). One protein A molecule can bind at least 2 molecules of IgG simultaneously (Sjoquist, Meloun, and Hjelm 1972). Thus, if the streptavidin on the nanocrystals can bind antibodies, incubation of this complex with protein A coated beads should yield fluorescent 5 μm beads with the same spectral characteristics as the nanocrystals. In fact, this experiment did show fluorescent 5 μm beads, and as expected, nanocrystals without antibody did not fluoresce (**Figure 4.6**). Confocal microscopy data from this application showed that the nanocrystals were able to remain photostable after prolonged exposure (10 minutes) to high intensity excitation wavelengths from a laser light source.
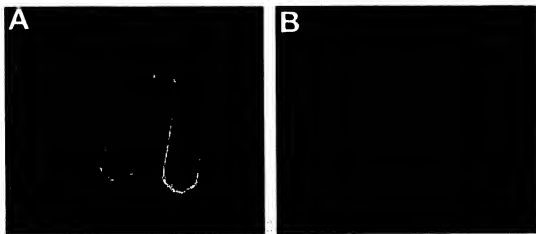
Figure 4.6. Verification of antibody conjugation to CdTe/ nanocrystals. CdTe particles made of: CdTe core, S, BSA, an streptavidin are illuminated with UV light (Panel A, from left dry BSA coate particles, BSA coated, and streptavidin coated nanocrystals). Protein binds the Fc portion of antibodies. CdTe/S nanocrystals conjugated to anti-CD95 bound to non-fluorescent Protein A coated beads (5 μm) (Panel B).

4.3.4. Nanocrystals targeted to live human cells

Human cells, BJAB line, constitutively express CD95 on their surface. Since CD95 is an early indicator of radiation damage, we conjugated anti-human CD95 antibodies to the surface of CdTe/S nanocrystals. This complex was then incubated with BJAB cells for 1 hour at 37°C. The resulting cell/nanocrystal mixture was then washed three times prior to examination by confocal microscopy. Nanocrystal clusters were found on the surface of the live human cells and were much brighter than background fluorescence (**Figure 4.7**). In most instances, the nanocrystals appeared to cluster when bound to the cells, even more so then when in suspension. Thus, more experiments are needed to determine the optimal ratio of nanocrystals to antibody. These experiments were not possible because of the lot to lot variability of the nanocrystals. Not only were there lot variabilities, but the shelf life of these nanocrystals was variable. Some of these issues could be addressed by optimizing the storage buffers. These studies are difficult because the nanocrystal synthesis is not well characterized at the time of this writing. The synthesis protocols are still being optimized as well as the storage buffers. These factors make this technology difficult to use, but developing this technology for use in biology is very exciting because of the potential uses of nanocrystals.
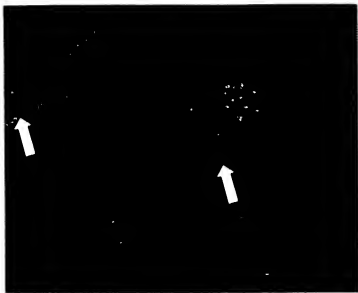
Figure 4.7. Anti-human CD95 coated CdTe nanocrystals targeted to human cells. BJAB cells, which normally express CD95, were labeled with clusters of nanocrystals previously coated with anti-human CD95. The cells were exposed to the nanocrystals for 1 hour prior to viewing with a confocal microscope and appeared in good condition throughout the experiment.

4.3.5. Photostability of semiconductor nanocrystals attached to human cells

Prolonged exposure (10 minutes) of semiconductor based nanocrystals with high intensity UV laser light has been shown to increase fluorescence intensity over that of briefly pulsed nanocrystals (**Figure 4.8**). This property of nanocrystals is important for nanomedicine during the developmental stage. The increased photostability of these particles should allow long term and repeated visualization of nanoparticles within cells. To confirm photostability, we conducted an experiment that utilized nanocrystals bound to living cells. In this system, the entire field of view was exposed to a high intensity UV laser beam and images taken in regular intervals for >630 seconds. Areas on the resulting images containing nanocrystals or unlabeled cell or background were selected and intensity over time calculated. The background fluorescence (dark red and black lines, at the bottom of the graph) quickly decreased, while the intensity of the nanocrystals (orange and blue) initially increased, then reached a plateau.
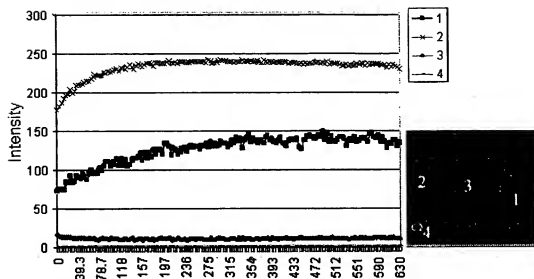
Figure 4.8. Effect of prolonged UV exposure on nanocrysta
fluorescence intensity. The fluorescence intensity of nanocrystal
increased with prolonged UV laser beam exposure (Areas 1 and 2; orang
and blue lines). Background and autofluorescence intensities (Areas 3 an
4; dark red and black lines) decreased initially and then reached a lo
intensity plateau.

4.3.6. Optimization of nanocrystal conjugation methods

The streptavidin coating is critical for these experiments, therefore binding of streptavidin coated nanocrystals to biotin coated 800nm non-fluorescent polystyrene beads were tested. Nanocrystals were constructed as depicted in **Figure 4.9**. The success of these reactions was evaluated with confocal microscopy (**Figure 4.10**). In **Figure 4.10** the black arrow indicates a polystyrene bead. From these data we were also able to obtain the emission spectra of the particles bound to the biotin coated beads (**Figures 4.10 and 4.11**). By using our own custom image analysis software written by Jacob Smith, we were able to determine several critical measurements. Firstly, we determined the relative fluorescence intensity of only those nanocrystals bound to beads (**Figure 4.12**). Of those, Sample B, E, and F stood out as the brightest of the bound particles. **Figure 4.13** was derived from a histogram that describes not only intensity, but also the relative binding ability of each nanocrystal sample. Therefore, the number of beads bound with nanocrystals is represented on the y-axis. Therefore, the greater the y-axis value, the more beads bound to nanocrystals. The x-axis represents the relative intensity of the nanocrystals bound to beads. The larger the intensity value, the brighter the bead. The nanocrystal preparation of choice would be the highest of both x and y values. With these data in mind we chose sample B (cysteine stabilized BSA coated nanocrystals coated with glutaraldehyde conjugated streptavidin)

and E (cysteine stabilized nanocrystals coated with NHS conjugated streptavidin in EDC) as the most optimal methods for bioconjugation. Additionally, sample E appeared to stay in suspension longer, with respect to sample B. Although we do not know why these particles fall out of suspension, this phenomena is ameliorated by coating the particles with proteins like BSA and streptavidin. Because of this clumping problem, the solution of nanocrystals contains at least two populations of crystals: monodisperse/small clusters and large clumps of nanocrystals that had different spectral properties.

Construction of DNA Tethered Nanocrystals
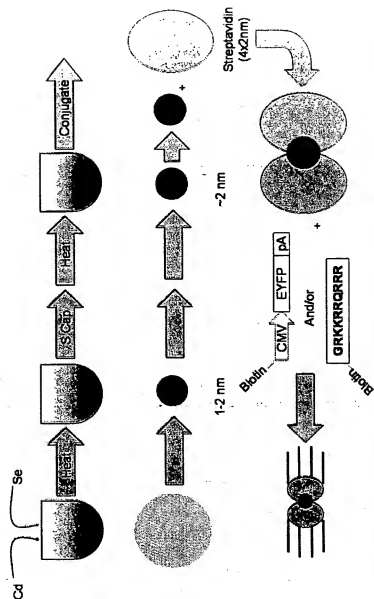
Figure 4.9. Construction of DNA tethered semiconductor nanocrystals. Schematic showing the construction of CdSe core particles, capped with sulfur and conjugated to streptavidin. The streptavidin coated particles are then coated with biotin labeled DNA encoding EYFP and/or biotin labeled peptide targeting sequence.
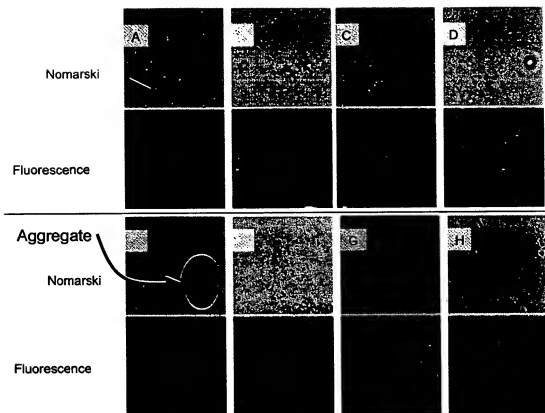
Figure 4.10. Nanocrystal/streptavidin conjugation methods. Top Pane
are nomarsky scattering images, bottom Panel are fluorescence emissio
from 514nm laser light. Panel A, shows beads alone, arrow indicates 1μ
biotin coated bead; Panel B, cysteine stabilized BSA coated nanocrystal
coated with glutaraldehyde conjugated streptavidin; Panel C, BSA coate
nanocrystals coated with glutaraldehyde conjugated streptavidin dialyzed
Panel D, nanocrystals coated with glutaraldehyde conjugated streptavidin
Panel E, cysteine stabilized nanocrystals coated with NHS conjugate
streptavidin in EDC; Panel F, cysteine stabilized BSA coated nanocrystal
coated with NHS conjugated streptavidin in EDC; Panel G, citrate stabilize
nanocrystals coated with NHS conjugated streptavidin in EDC; Panel H
citrate stabilized BSA coated nanocrystals coated with NHS conjugate
streptavidin in EDC. The large green spots are large aggregates o
nanocrystals. Some clusters cannot be seen with Nomarski scattering.
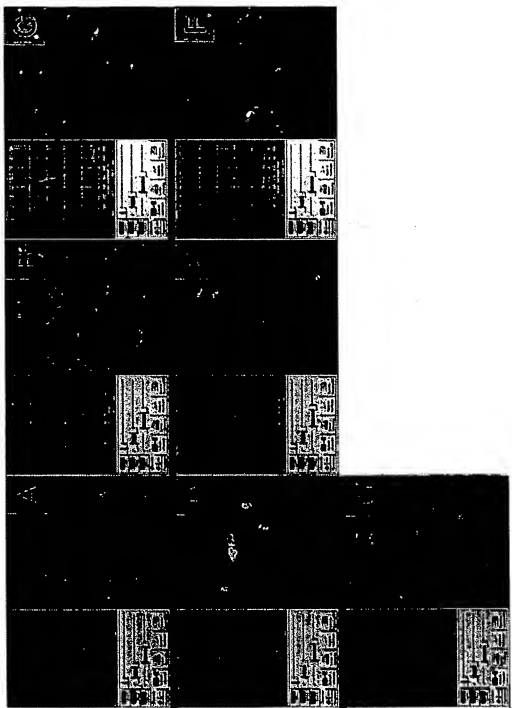
Figure 4.11. Emission spectra of conjugated nanocrystals. Panel A cysteine stabilized BSA coated nanocrystals coated with glutaraldehyde conjugated streptavidin; Panel B BSA coated nanocrystals coated with glutaraldehyde conjugated streptavidin dialyzed; Panel C nanocrystals coated with glutaraldehyde conjugated streptavidin; Panel D cysteine stabilized nanocrystals coated with NHS conjugated streptavidin in EDC; Panel E cysteine stabilized BSA coated nanocrystals coated with NHS conjugated streptavidin in EDC; Panel F citrate stabilized nanocrystals coated with NHS conjugated streptavidin in EDC; Panel G citrate stabilized BSA coated nanocrystals coated with NHS conjugated streptavidin in EDC.
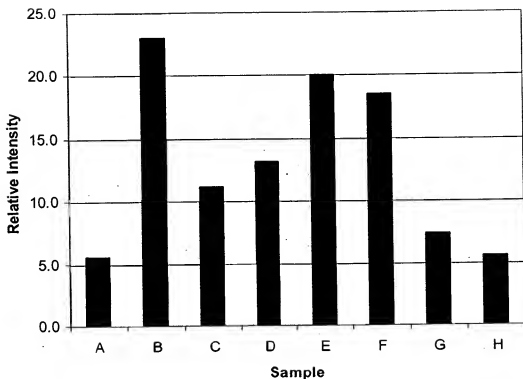
Figure 4.12. Nanocrystal bound biotin bead fluorescence. Average intensity of biotin coated beads exposed to streptavidin conjugated nanocrystals. Sample A, beads alone; Sample B, cysteine stabilized BSA coated nanocrystals coated with glutaraldehyde conjugated streptavidin; Sample C, BSA coated nanocrystals coated with glutaraldehyde conjugated streptavidin dialyzed; Sample D, nanocrystals coated with glutaraldehyde conjugated streptavidin; Sample E, cysteine stabilized nanocrystals coated with NHS conjugated streptavidin in EDC; Sample F, cysteine stabilized BSA coated nanocrystals coated with NHS conjugated streptavidin in EDC; Sample G, citrate stabilized nanocrystals coated with NHS conjugated streptavidin in EDC; Sample H, citrate stabilized BSA coated nanocrystals coated with NHS conjugated streptavidin in EDC.
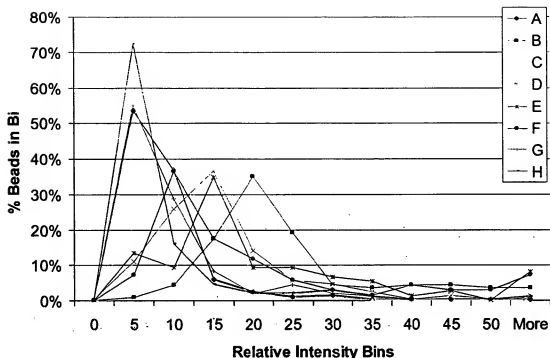
Figure 4.13. Data from an intensity histogram of biotin coated bead exposed to streptavidin coated CdSe/CdS nanocrystals. Line A, bead alone; Line B, cysteine stabilized BSA coated nanocrystals coated wit glutaraldehyde conjugated streptavidin; Line C, BSA coated nanocrystal coated with glutaraldehyde conjugated streptavidin dialyzed; Line D nanocrystals coated with glutaraldehyde conjugated streptavidin; Line E cysteine stabilized nanocrystals coated with NHS conjugated streptavidin i EDC; Line F, cysteine stabilized BSA coated nanocrystals coated with NH conjugated streptavidin in EDC; Line G, citrate stabilized nanocrystal coated with NHS conjugated streptavidin in EDC; Line H, citrate stabilize BSA coated nanocrystals coated with NHS conjugated streptavidin in EDC This graph shows that the nanocrystal preparation B is the brightes nanocrystal that also binds to beads well.

99

4.3.7. Recombinant peptide and antibody targeted nanocrystals

We tested several nanocrystal targeting strategies *in vitro* (**Figure 4.14**) These data suggested that by using a biotinylated fragment of the HIV tat protein, we could target the nanocrystals to the nucleus of a living human white blood cell (BJAB cell line; **Figure 4.14** panel C). To a lesser extent, a biotin labeled peptide containing a six arginine repeat could target nanocrystals to the nucleus (**Figure 4.14** panel D). Based on confocal imaging data, the streptavidin coated particles alone were capable of entering the cell (**Figure 4.14** panel B). Labeling the particles with an anti-CD95 antibody resulted in both outer membrane and strong nuclear staining (**Figure 4.14** panel E).
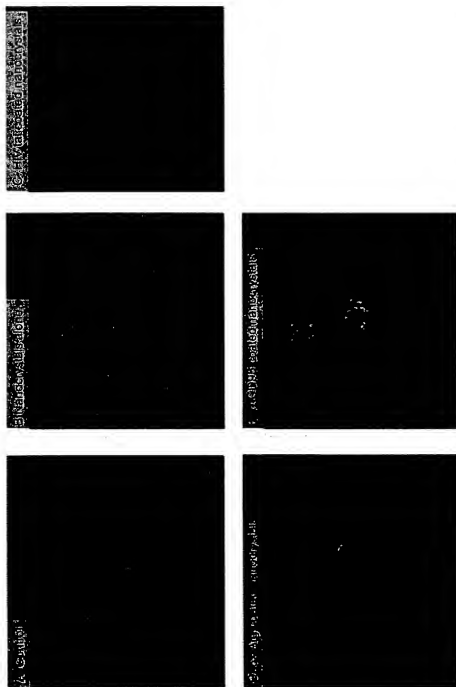
Figure 4.14. Nanocrystal targeting. BJAB cells exposed to A. nothing; B. nanocrystals alone; C. HIV Tat coated nanocrystals ; D. 6x Arg coated nanocrystals ; E. anti-CD95 coated nanocrystals. All cells are counterstained with Hoechst 33342 (blue), nanocrystals are green.

4.3.8. Photostability of recombinant peptide targeted nanocrystals compared to a traditional nuclear dye, Hoechst 33342, to nanocrystal stained nuclei

To verify the presence and photostability of the nanocrystals, a photobleaching experiment was carried out **(Figure 4.15)**. During this experiment, which lasted >400 seconds, the fluorescence of the nanocrystals was far more resistant to photobleaching than the AT binding DNA dye Hoechst 33342 (Molecular Probes, Inc., Eugene, OR). These studies are important for tracking nanoparticle containing cells over multiple time points and for detailed nanoparticle targeting studies. In the future, these nanocrystals will be used to target intracellular locations and their ability to resist photobleaching will be crucial for repeated confocal and flow cytometric analyses.
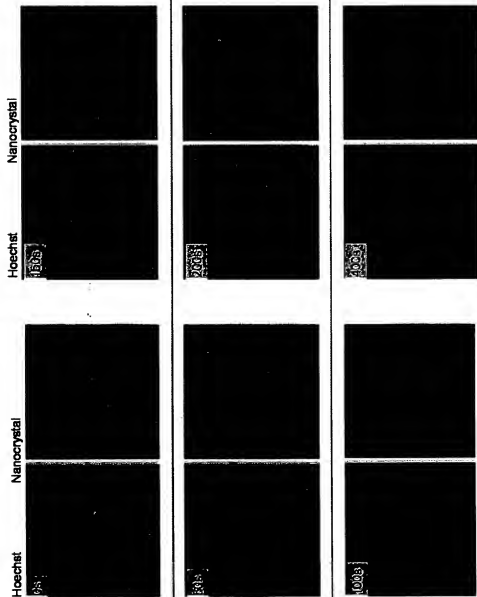
Figure 4.15. Photostability of intracellular targeted nanocrystals. Live BJAB cells were stained with tat tagged nanocrystals (right panels, green) and counterstained with Hoechst 33342 (left panels, blue). Photobleaching from 0 to 400 seconds (inset).

In conclusion, nanocrystals that remain stable in physiological conditions have been developed. These particles were coated with streptavidin, so that multiple targeting/functional agents could be tethered to the outer surface. The coated particles were then used in multiple experiments using live human derived cells. These experiments showed that nanocrystals can enter cells with or without coatings.

4.4. DISCUSSION

Semiconductor cored nanocrystals are currently being developed for the field of biology in many different laboratories. These nanocrystals have extraordinary spectral properties that have the potential to revolutionize fluorescent imaging. Although these particles hold promise, there were some substantial hurdles during their development for use under physiological conditions. Our first few batches of nanocrystals from Dr. Kotov's laboratory, composed of CdTe were stable at pH>8. These nanocrystals had excellent spectral characteristics and were easy to bioconjugate. Unfortunately, the pH requirement precluded their use in tissue culture. The next series of particles, constructed by the Kotov laboratory, were composed of a CdSe core particle that was stable at physiological pH. These particles were optimized by the Kotov laboratory in collaboration with the Leary laboratory and used for the remainder of this dissertation.

The problems encountered during the previous chapter using polystyrene and silica based particles due to the size and structure of these particles were overcome in part by the semiconductor nanocrystals. The small size of the nanocrystals was probably the biggest factor contributing to their ability to enter the BJAB cells. This cell line was repeatedly exposed to commercial lipid/DNA cocktails and could never be transfected (data not shown), but nanocrystals were able to enter these cells without any special coating. Therefore, further experiments that explore the ability of these nanocrystals to transfer genes are necessary before concluding that nanocrystals are superior to traditional methods of gene delivery. Interestingly, when these cells were exposed to nanocrystals, regardless of coating, some of the cells contained large amounts of particles while other cells took up no detectable nanocrystals. Our original hypothesis was that most cells would take up nanocrystals in a dose dependant manner. This hypothesis was false, in low dose cases only a few cells would take up the nanocrystals. Although there is no data, these results suggest to a cell regulated uptake of nanocrystals. By treating cells with different concentrations of nanocrystals, one could better determine if there is a cell dependant uptake of nanocrystals. This would help differentiate between cell or nanocrystal mediated uptake. Currently, there is very little known about the uptake of these particles. The cell density and cell cycle phase may also influence the uptake of

nanocrystals. The internalization of nanocrystals appears to not be limited to the monodisperse nanocrystals, but also to nanocrystal clusters. This cellular characteristic could then be exploited to enhance the uptake of these small particles in cells that are notoriously difficult to transfect.

The next logical step would be to target these particles *in vivo*. The small size and excellent fluorescent properties would be very beneficial during these studies. Unfortunately, the CdSe based nanocrystals fluoresce in the green wavelengths. Biological material absorbs this region of the spectrum, making green fluorescent probes very difficult, if not impossible to use *in vivo*. Recently, through collaboration with the Kotov and Leary laboratories, a new nanocrystal, (CdHg/Te) has been developed for biological use. This nanocrystal has spectral properties similar to the clinical indocyanin dyes that were developed to fluoresce at wavelengths in the near infrared. Although these experiments with these particles will not be discussed in this dissertation, they are the next step in nanocrystal technology.

CHAPTER 5.   DEVELOPMENT   OF   SUPERPARAMAGNETIC NANOPARTICLES FOR INTRACELLULAR PAYLOAD DELIVERY AND RECOVERY.

5.1.   INTRODUCTION

The third and final type of particle to be developed for payload delivery was based on a superparamagnetic iron oxide core. These magnetic nanoparticles were coated with streptavidin and used to deliver genes to cells *in vitro* and *in vivo*. Later studies provided evidence that the magnetic properties of these nanoparticles could be used to rescue the DNA tethered magnetic nanoparticles intact.

This section outlines a simple magnetic nanoparticle based system that was modified from a commercially available product. Superparamagnetic nanoparticle cores were coated with streptavidin and used for gene transfer as they were easily obtainable, simple to construct and the magnetic nanoparticles could be purified from the layer components. The layer by layer construction of these coated magnetic nanoparticles is shown in **Figures 5.1.** The delivery and recovery of these magnetic nanoparticles is depicted in **Figure 5.2.** Later experiments characterize the purification and analyze the completed magnetic nanoparticles. These magnetic nanoparticles were found

to have reasonably high expression profiles when compared to the positive, DNA alone, and negative, no DNA, controls. Next, fluorescence microscopy was used to determine the relative transfection efficiency of these magnetic nanoparticles *in vitro*. Data were then analyzed using a customized image analysis software program, written by Jacob Smith which compared the relative gene expression between DNA tethered to magnetic nanoparticles and free DNA. It was found that intact magnetic nanoparticles could be recovered from populations of nanoparticle exposed cells through purification and PCR analysis. These magnetic nanoparticles showed promising results during *in vivo* gene delivery experiments.
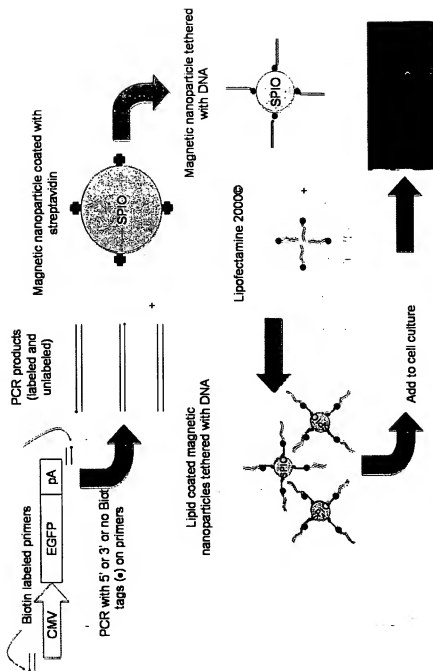
Figure 5.1. Schematic of gene delivery with magnetic nanoparticles. Biotin labeled primers are used to generate labeled PCR products encoding EGFP that are mixed with streptavidin coated magnetic nanoparticles. These DNA coated particles are washed and then coated with lipid. Lipid coated particles are then added to cell culture.

Lyse cells

Magnetically separate particles from lysate

Concentrate

PCR

(1,500bp)

CMV | EGFP | pA

Confirm by gel electrophoresis

Sequence purified PCR fragment

```
        10              20
        |               |
TGGCCCGAACA AAGACAGAATT
        60              70
        |               |
GACTGTTTTT TGATTAGAGA
        110             120
        |               |
```
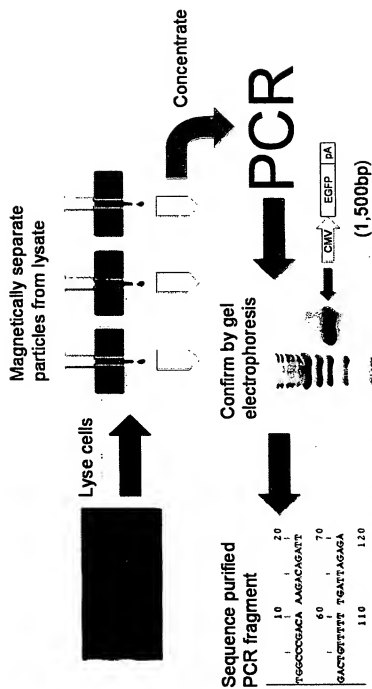
Figure 5.2. **Isolation and purification of magnetic nanoparticles from within cells.** Cells containing nanoparticles are lysed and the magnetic nanoparticles isolated via magnetic columns. The DNA bound to the nanoparticles can be amplified by PCR and then sequenced.

110

5.2. MATERIALS AND METHODS

5.2.1. Biotin labeled DNA fragment preparation

PCR amplification was used to create biotin labeled DNA fragments. Oligonucleotide primers were purchased from Integrated DNA Technologies, Inc. For initial studies, oligos were ordered with a single biotin tag either the 5' or 3' termini. Later studies used only forward oligos labeled with biotin at the 5' terminus. These oligos were then used as PCR primers. A typical reaction would include 25 μl Red Taq, (Sigma-Aldrich Chemical, Inc., St. Louis, MO), 1 μl 5' biotinylated primer (20 pM), 1 μl 20 pM 3' primer (20 pM), 1 ul template (50 ng), to 50 μl with water. The primers were at 200 pM and the template at 50 ng/μl. A typical reaction for DNA tethering to magnetic nanoparticles would include about 25 of these reactions. Typical PCR cycles would include ~35 cycles of denaturing temperature at 94°C for 30 seconds, annealing temperature at 65°C for 30 seconds and extension for 2 minutes at 72°C.

5.2.2. DNA tethered magnetic nanoparticle construction

Biotin labeled PCR products were tethered to streptavidin coated magnetic nanoparticles (Miltenyi Biotec, Inc., Auburn, CA). DNA tethered magnetic nanoparticles were constructed as per the manufacturer's instructions. The magnetic nanoparticles were incubated with the biotin

111

labeled PCR fragments at the ratio prescribed by Miltenyi Biotech, Inc. The ratio of DNA to nanoparticles is 100 µl of magnetic nanoparticles to 100 pmol of biotinylated DNA fragments. Therefore, X µg of DNA binds 100 µl of magnetic nanoparticles, such that X=the length of DNA (basepairs) x 0.066. There are approximately 10 streptavidin moieties per particle, resulting in ~40 biotin binding sites on each magnetic nanoparticle. In all experiments the amount of DNA remained constant between the DNA only and DNA- magnetic nanoparticle treatment groups. Normalizing to the amount of DNA was the best way to keep the treatments consistent. This is because the concentration of nanoparticles would likely change during the construction phase and there was no procedure for quantifying nanoparticles in solution. The mixture was allowed to incubate at room temperature for 30 minutes. During that time, the magnetic column was prepared by washing once with 100 µl of the included nucleic acid buffer and three times with 100 µl Optimem™ (Gibco BRL, Burlington ON, Canada). Once washed, the column was loaded with the DNA magnetic nanoparticles mixture. The column was then washed three times with 100 µl Optimem™. The magnetic nanoparticles were eluted by removing the column from the magnet and adding 100 µl of Optimem™. The resulting brownish solution contained DNA tethered magnetic nanoparticles.

5.2.3. Lipid coating of DNA tethered magnetic nanoparticles

The DNA tethered magnetic nanoparticles were coated with Lipofectamine™ 2000 as per the manufactures instructions for DNA. The DNA tethered magnetic nanoparticles were treated as DNA for lipid coating. Briefly, the eluted magnetic nanoparticles were diluted in the appropriate amount of Optimem™ (50 μl for one well in a 24 well plate) and incubated for 5 minutes at room temperature. An appropriate amount of Lipofectamine™ 2000 (2 μl for one well in a 24 well plate) was diluted in a separate tube and incubated at room temperature for 5 minutes. After 5 minutes, the two tubes were mixed gently and combined. This mixture was allowed to stand for 20 minutes before added to the cell culture.

5.3. RESULTS

5.3.1. Biotin labeling of DNA fragments

Biotin labeled PCR primers were used to generate CMV-EGFP-pA containing DNA fragments (1.5kb) with 5' biotin labeled (**Figure 5.3** Lane A), 3' biotin labeled (**Figure 5.3** Lane B), and unlabeled (**Figure 5.3** Lane C). These fragments contain all of the information needed to express pEGFP-C1 from within the nucleus and will be conjugated to magnetic nanoparticles for transfection.
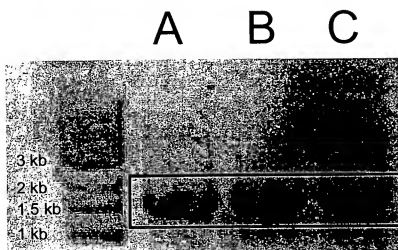
Figure 5.3. Biotin labeling of DNA fragments.
Agarose gel containing PCR fragments (1.5 kb) with
5' biotin labeled (Lane A), 3' biotin labeled (Lane B),
and unlabeled (Lane C).

5.3.2. Conjugation of DNA to magnetic nanoparticles

Streptavidin coated magnetic nanoparticles were incubated with each of the DNA fragments and analyzed by agarose gel electrophoresis (**Figure 5.4**). Lanes A, C, and E contained only the PCR product. Lanes B, D and F contained magnetic nanoparticles incubated with the PCR fragments. Only the DNA in Lanes A to D contained biotin tags. While DNA in lanes E and F contained no biotin tag and were therefore used as a negative control and also as a DNA only contamination control. The black squares indicate where high molecular weight. The dark staining seen in Lanes B and D indicates that the DNA was able to bind to magnetic nanoparticles and was now trapped at the top of the gel due to its large size. This gel also shows that there is a significant amount of unbound DNA present. Because of this, the magnetic nanoparticles need to be purified from the contaminating free DNA fragments as described in the next section. Lane F. shows that without a biotin tag, there is no DNA attached to the particles.

	A	B	C	D	E	F
Nanoparticles:	-	+	-	+	-	+
Biotin tag:	5'	5'	3'	3'	-	-

Nanoparticles

EGFP DNA
fragment
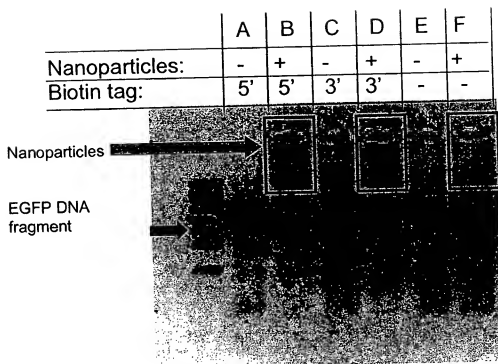
Figure 5.4. Conjugation of DNA to magnetic nanoparticles. Agarose gel
of DNA and nanoparticles. Lanes A, C, and E contain only the PCR product.
Lanes B, D and F contain nanoparticles incubated with the PCR fragments.
Lanes A to D contain biotin tags. Lanes E and F contain no biotin tag. Black
squares indicate where high molecular weight.

5.3.3. Removal of free DNA from magnetic nanoparticle/DNA solutions

In these experiments, the mixtures of DNA and magnetic nanoparticles were washed 4x to remove unbound DNA using a magnetic column. It was found that the magnetic properties of these particles enabled the rapid purification of the magnetic nanoparticles from the DNA solution. These samples were then run on an agarose gel (**Figure 5.5**). Lanes A. to C. represent only DNA fragments. Lanes D. to F. contain the magnetic nanoparticle/DNA mixture. After washing, a portion of the magnetic nanoparticles were run onto this gel (Lanes G. to I.). If carefully examined, (lower figure) dark staining can be seen only in lanes G. and H. near the loading well. This suggests that the free DNA has been removed and only the DNA tethered magnetic nanoparticles remain in suspension.

	A.	B.	C.	D.	E.	F.	G.	H.	I.
Nanoparticles:	-	-	-	+	+	+	+	+	+
DNA:	+	+	+	+	+	+	+	+	+
Biotin tag:	5'	3'	-	5'	3'	-	5'	3'	-
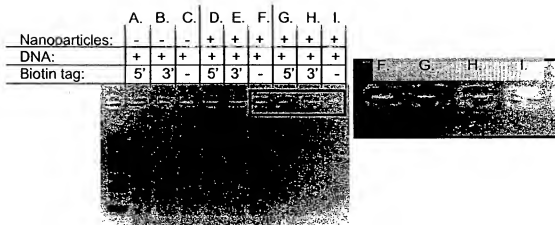
Figure 5.5. Purification of DNA tethered magnetic nanoparticles. Lanes A to C represent only DNA fragments. Lanes D to F contain the nanoparticle/DNA mixture. After washing, a portion of the nanoparticle mixtures were also run on this gel (Lanes G to I). The right panel is a magnified image of the box around Lanes F to I.

EXPRESSION LEVELS OF CELLS TRANSFECTED WITH DNA TETHERED MAGNETIC NANOPARTICLES

After washing, the DNA tethered magnetic nanoparticles were mixed with Lipofectamine™ 2000 in order to enhance transfection into cells. This complex was then delivered to cells cultured in chamber slides, incubated for 48 hours, fixed, permeablized, and finally counterstained with DAPI. Slides were subsequently photographed under fluorescence using a Nikon CoolPix digital camera. The images obtained were then analyzed with an in house slide based cytometry software program and the resulting data presented in **Figure 5.6**. Note that all of the values were normalized to the samples treated with the EGFP fragment transfected with Lipofectamine™ 2000. The intact pEGFP-C1 plasmid was found to express EGFP protein at ~2x the level of that seen from the EGFP fragment without a biotin tag. Overall, the expression levels of Lipofectamine coated DNA fragments was similar to that from Lipofectamine coated nanoparticles tethered to DNA. Finally, the non-biotinylated DNA exposed magnetic nanoparticles did not show any appreciable expression of EGFP. To date these are the only cells tested with these magnetic nanoparticles, but because the results were similar to that with DNA alone we expect that the same trend will occur with other cell types.
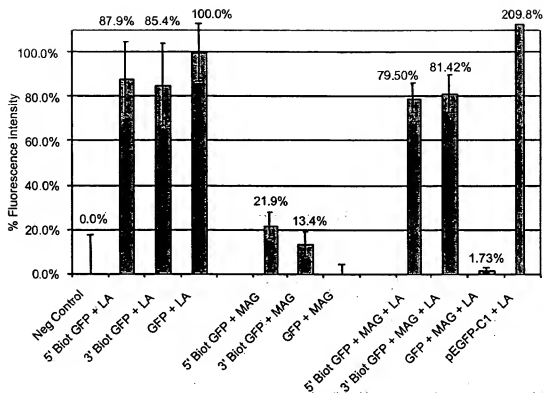
Figure 5.6. Expression levels of GFP from DNA tethered magnetic nanoparticles. In vitro gene expression levels are shown as the % of Lipofectamine transfected EGFP DNA (GFP+LA). Biotin tagged DNA was also transfected into cells (Biot GFP). Cells transfected with DNA bound nanoparticles are labeled BIOT+MAG. All samples were incubated with (LA) or without Lipofectamine 2000. DNA was added to an excess of magnetic nanoparticles in an attempt to achieve an equimolar ratio between groups.

5.3.4. *In vitro* gene expression with DNA tethered magnetic nanoparticles

Gene expression levels from cells exposed to EGFP tethered magnetic nanoparticles was determined by fluorescence microscopy and digital image analysis (**Figure 5.6**). Representative fluorescent images of the cells used for **Figure 5.6** are shown in **Figure 5.7**, Panel A. is an image of untreated cells. Panels B, C, and D. represent cells transfected with DNA fragments with 5', 3', and no biotin tags using Lipofectamine™ 2000. Panels E., F., and G. show cells exposed to DNA tethered to magnetic nanoparticles from 5', 3', and no (control for free DNA) biotin tags; these magnetic nanoparticles were also coated with Lipofectamine™ 2000.

These data showed that this system is capable of delivering genes to the nucleus of the cell and that the transfected DNA can be utilized. The tethered genes were able to be expressed in a time frame similar to that seen with DNA alone. These results were very encouraging and were the first to describe the use of small fragments of DNA in lieu of plasmid DNA. This capability is valuable because only PCR products are needed to transfect cells, rather than intact plasmids. This allows researchers to rapidly construct and test the expression of genes. There were no obvious differences between the DNA fragments and their magnetic nanoparticles tethered counterparts.

The expression levels of tethered EGFP genes were comparable to that seen with the DNA fragments alone.
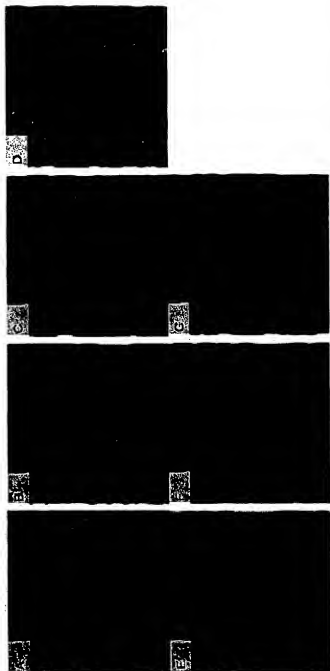
Figure 5.7. Expression of GFP from magnetic nanoparticles tethered to EGFP DNA. EGFP expression (green) and DNA (blue) are shown in these images. Untreated cells (Panel A), cells transfected with DNA fragments with 5', 3', and no biotin tags (Panels B, C, and D), and cells exposed to DNA tethered to MN from 5', 3', and no (control for free DNA) biotin tags Panels E, F, and G are shown here.

123

The results of these experiments show that the intact plasmid DNA was capable of the highest EGFP expression levels. The PCR product of the CMV promoter, EGFP gene, and a poly (A)-signal showed expression levels at about half of that seen with the intact plasmid (80% and 209%, respectively). These results were similar to that seen with the same DNA fragment but with either 5' or 3' biotin labels. Cells that expressed EGFP tethered to magnetic nanoparticles coated with Lipofectamine™ 2000 showed comparable levels of expression to those cells exposed to the untethered DNA fragments. Finally, cells exposed to magnetic nanoparticles tethered to EGFP without Lipofectamine™ 2000 coating had low EGFP expression levels.

5.3.5.   Recovery of DNA tethered magnetic nanoparticles

This section demonstrates that DNA tethered magnetic nanoparticles could be recovered from Huh7 cells. The incubation time was 72 hours post exposure to the magnetic nanoparticles. This is important because it shows that the DNA remains stable for at least 72 hours in physiological conditions. Cells were lysed and the magnetic nanoparticles were purified from the cell lysate with magnetic column separation. The magnetic nanoparticles were then eluted from the column and concentrated. The resulting solutions were then used as templates for PCR reactions. The resulting samples were then analyzed by agarose gel electrophoresis (**Figure 5.8**).

The results indicate that the 5' labeled DNA fragments were easily amplified by PCR indicating the DNA and the magnetic nanoparticles themselves remain stable in cell culture. Experiments with 3' labeled DNA fragments yielded few positive results and were therefore not utilized in further studies. The DNA fragments not containing any biotin labels were used as a negative control and as expected, did not yield any EGFP positive cells nor was any DNA amplified by PCR.
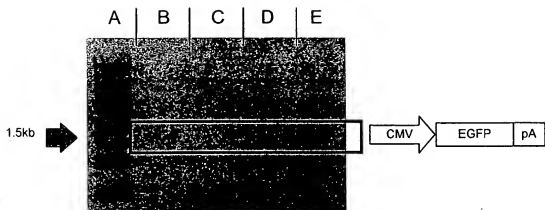
Figure 5.8. Recovery and PCR of DNA tethered to magnetic nanoparticles. Agarose gel showing the PCR products of DNA tethered magnetic nanoparticles isolated from within cells. Lane A. 1kb marker; B. 5' tethered; C. 3' tethered; D. no tether; and E. positive control.

126

5.3.6. Nanoparticle delivery of genes *in vivo*

Translation of a gene delivery technology from an *in vitro* model to *in vivo*, is notoriously difficult. To track the expression of EGFP *in vivo*, an *in vivo* rat imaging system was used 48 hours after hepatic injection with the EGFP encoding DNA labeled magnetic nanoparticles. Fluorescent tracking agents (EGFP) were employed instead of enzymatic reporters. These studies were designed to develop an *in vivo* assay to monitor biosensor activity in living animals. *In vivo* imaging was achieved with a mercury arc lamp for excitation wavelengths and the images were captured via a high resolution digital camera. It was found that the fluorescence levels noted were below the limits of detection for this system, hence 10 μm fluorescent beads were injected into the liver of rats to simulate a large number of transfected hepatocytes near the surface. This superficial injection of beads were immediately visible (**Figure 5.9** Panel B, upper arrow) with the *in vivo* imaging system (**Figure 5.9.** Panel A, before; Panel B, after). **Figure 5.9** shows the low fluorescence intensity observed with a cell tracking dye which was used to mark the site of injection (**Figure 5.9** Panel B, arrow).

Figure 5.9. Nanoparticle delivery of genes *in vivo*. Panel A. and B. Photograph of liver injected with nanoparticles tethered to EGFP encoding DNA and coated with lipid. Photo was taken with 488nm excitation on an in vivo imaging system. Green highlights are FITC label 20um polystyrene beads directly injected into the liver. Blue highlights are reflections of the excitation light.

While cells transfected with magnetic nanoparticles could not be detected in whole liver, **Figure 5.10** shows the presence of magnetic nanoparticle delivered EGFP in cryosections of rat liver. These three different sections show that one or more EGFP positive cells were found within this region. There have been cases in which other researchers have reported bright autofluorescence of the liver under these conditions that were confirmed by an emission scan. Therefore, until these sections are scanned with a multispectral confocal microscope we cannot rule out this possibility. There were several sections from the same region that contained one or more clusters of EGFP positive cells. Sections from a lobe of the liver not injected with magnetic nanoparticles were also examined and did not contain any EGFP positive cells. Furthermore, there were several clusters of EGFP positive cells surrounding the injection site, but overall the transfection efficiency was very low (<1%). This may be due to several reasons including: a very short incubation time and relatively small injection volume ~100ul. Additionally, there was difficulty finding the exact site of injection. This experiment yielded several valuable pieces of information. First, we found that the magnetic nanoparticles were able to deliver the EGFP encoding DNA to cells *in vivo*. Second, the number of transfected cells was too small, therefore a larger dose of the magnetic nanoparticles may be necessary to achieve measurable results. Lastly, a better method for finding the site of injection is necessary for more efficient analysis after injection. Finally, it is imperative for

the future of this technology that methods be developed to determine something similar to an MOI for these magnetic nanoparticles.

Figure 5.10. Magnetic nanoparticle delivery of genes *in vivo*. Fluorescent micrographs of 5 micron cryosectioned liver from rats injected intrahepatically with nanoparticles tethered to EGFP encoding DNA and coated with lipid. These sections were counterstained with DAPI. Green highlights indicate cells expressing GFP from nanoparticles.

5.4. DISCUSSION

The three main findings of these experiments were 1) magnetic nanoparticles coated with lipid can be used for effective gene transfer vectors; 2) days after gene transfer, the DNA tethered particles could be recovered and the entire gene amplified by PCR; 3) DNA tethered magnetic nanoparticles coated with Lipofectamine™ 2000 could transfer genes *in vivo* with very low efficiency. Cells incubated with these magnetic nanoparticles showed no visible signs of toxicity, even though the magnetic nanoparticles are made of iron. The ability to isolate these magnetic nanoparticles days after their introduction suggests that they are stable within the cellular matrix. This may be due, at least in part, to the conjugation of proteins to the core magnetic nanoparticles. These proteins could serve as a buffer zone inhibiting contact with fouling agents within the cellular milieu. So far, exposure up to several days has been explored. Future experiments will define the limits of this technology.

An EGFP encoding DNA fragment was successfully delivered with magnetic nanoparticles coated with lipid coating and expressed at levels ~40% with respect to the linear fragment alone **(Figure 5.6)**. DNA fragments with 5' or 3' biotin tags were attached to streptavidin coated magnetic nanoparticles. Free DNA fragments were successfully removed through washing the particles using a magnetic column. Cells exposed to uncoated

DNA tethered magnetic nanoparticles did not express detectable levels of EGFP. Cells exposed to DNA tethered magnetic nanoparticles coated with Lipofectamine™ 2000 expressed high levels of EGFP.

One important finding is that the uncoated DNA tethered magnetic nanoparticles were able to successfully transfect cells *in vitro*. Another interesting result is that cells treated with the DNA tethered magnetic nanoparticles coated with lipid had expression levels well within range of those transfected with only labeled DNA fragments and about half of that seen from the intact plasmid. These data show that we can effectively express gene products from DNA tethered to magnetic nanoparticles in either the 5' or 3' configuration. Finally, cells exposed to DNA fragments not labeled with biotin and incubated with streptavidin coated magnetic nanoparticles did not show any appreciable expression of EGFP, as expected. Therefore the expression we observed with the labeled DNA and magnetic nanoparticles was from the DNA tethered to magnetic nanoparticles.

Simple streptavidin coated magnetic particles can be used to deliver genes into cells and recover those same genes after expression studies. This technology can then be used for screening genetic libraries and determining the effects of bio-fouling of the magnetic nanoparticles themselves.

Additionally, this magnetic nanoparticles technology is being developed for use with the layer by layer paradigm.

In summary, multilayered magnetic nanoparticles were found to be an efficient platform to deliver and recover genes *in vitro*. These experiments showed that magnetic nanoparticles tethered DNA could express EGFP at a level similar to free DNA. Lipid coating these particles was a fast and efficient way to enhance the uptake and use of the particles both *in vitro* and *in vivo*.

CHAPTER 6.   BIOSENSOR DEVELOPMENT AND TESTING

6.1.   INTRODUCTION

The objective of this chapter is to design and test biosensors for 1) toxicity; 2) effectiveness; and 3) adaptability to other systems. These characteristics are critical for the biosensor to safely detect the presence of a pathogenic process and induce therapy. To this end, protease and promoter activated biosensors have been developed and explored.

Protease activity is necessary for a plethora of biological systems, such as viral replication and apoptosis (Martin and Green 1995; Rice and Hagedorn 2000). Knowledge of the status of a given protease has been critical for the elucidation of many normal and pathogenic processes in biological systems. During the last decade much effort has been made to provide researchers and clinicians with fast and effective protease assays. These efforts have chiefly focused on the development of instrument based assays that utilize cell free systems. Viral and apoptotic proteases have been the primary focus of many protease activity assays. A small number of cell based assays have also been described for use with a limited number of systems, for example hepatitis C and HIV (Lee et al. 2003; Lindsten et al. 2001; Mao et al. 2003). The majority of these systems are based on cloned viral proteases or replicons that are

difficult and time consuming to construct. These systems are difficult to generate and time consuming to develop. This chapter describes a novel cell based protease activity system that can be produced rapidly and easily adapted to multiple systems, including viral and non-viral systems.

One example of a protease based biosensor system is based on a EGFP fusion protein (Lindsten et al. 2001). This system specifically targets the HIV protease and is based on the ability of a protease precursor to auto-catalytically cleave and thereby become active (Lindsten et al. 2001). The activated protease is toxic to cells and is therefore difficult to study (Lindsten et al. 2001). Thus the addition of protease inhibitors results in the accumulation of the EGFP fusion protein. Cells that do not receive protease inhibitors succumb to the toxic effects of the activated protein and die (Lindsten et al. 2001). This HIV protease biosensor strategy can be used for screening protease inhibitors but could not easily be adapted for therapeutic use. This and similar protease biosensors were designed for screening, but not therapy. We feel that our biosensor is more versatile and ultimately more useful than other systems because ours can be used for both anti-viral screening and therapeutic purposes, whereas others can only be used for anti-viral agent screening (Lee et al. 2003; Lindsten et al. 2001; Mao et al. 2003).

In addition to the protease activated biosensors, this chapter will describe the characterization and utilization of promoter based biosensors for the detection of oxidative stress. This sensor is to be used to induce the expression of DNA repair enzymes during times of increased oxidative stress. The antioxidant response element was coupled to a EGFP reporter. Zhu and Fahl first adapted this promoter for use as an *in vitro* assay for cells experiencing oxidative stress (Zhu and Fahl 2000). Repeats of the were found to enhance the responsiveness of this construct (Zhu and Fahl 2000). The most sensitive of the constructs produced contained four repeats of the antioxidant response element followed by the EGFP gene and a poly A tail (Zhu and Fahl 2000). This construct was obtained from Dr. Zhu, Arizona Cancer Center, and put to use in our laboratory.

6.2. METHODS

6.2.1. Biosensor construction

The tetracycline activated transactivator (tTA) region of pTet-Off (Clontech, Inc., San Jose, CA) was amplified by PCR with the primers described in Chapter 2.03.1. The cleavage domain for the hepatitis C virus NS3/4A protease and localization signal were added to the tTA region through three consecutive PCR reactions using the previously described 5' primer and three 3' primers. The purpose of the localization signal was to keep the

biosensor in the same intracellular location as the hepatitis C virus NS3/4A protease, perinuclear. This PCR product was then purified (Qiagen, Inc., Valencia, CA) and cloned into a vector containing both CMV and T7 promoters, pCMV-Script (Stratagene, Inc., La Jolla, CA). The ligated constructs were then transformed into bacteria and plated on agar with kanamycin (Sigma-Aldrich Chemical, Inc., St. Louis, MO) as a selection marker. Individual colonies were then selected the following day, grown in LB broth (Sigma-Aldrich Chemical, Inc., St. Louis, MO) and the plasmids were isolated in each clone after 16 hours (Qiagen, Inc., Valencia, CA). The presence and direction of the biosensor gene was determined through PCR and restriction digestion.

6.2.2.   Intracellular localization and co-localization studies

Huh-7 or hepatitis C replicon cells were transiently transfected (Lipofectamine™ 2000, Invitrogen, Inc., Carlsbad, CA) with the biosensor or NS3/4A constructs with/without pBI-EGFP (Clontech, Inc., San Jose, CA) and subsequently incubated for 24, 48, or 72 hours. Huh-7 cells were derived from a human hepatoma (Nakabayashi et al. 1984). An in depth description of the hepatitis C replicon can be found in Ikeda et al. (Ikeda et al. 2002). The replicon is similar to the Bartenschlager replicon that utilizes a synthetic viral mRNA construct that is G418 selectable (Bartenschlager 2002;

Bartenschlager, Kaul, and Sparacio 2003; Lohmann et al. 1999; Pietschmann and Bartenschlager 2001; Vrolijk et al. 2003). The NS3/4A construct was constructed with a CMV promoter upstream and a poly A tail signal downstream of the hepatitis C virus NS3/4A gene. After incubation, cells were fixed with 4% paraformaldehyde for 10 minutes and permeablized with 0.25% Triton X-100 for a further 5 to 10 minutes. Fluorescent immunocytochemistry was used to detect the presence of the biosensor within the cell. Briefly, a primary polyclonal antibody (Clontech, Inc., San Jose, CA) raised in rabbit to the tTA protein was used to stain the cells to assay for biosensor at 1:100 dilution and the reaction visualized using fluorescent conjugated goat anti-rabbit secondary antibodies (Alexa Fluor 488, Molecular Probes, Inc., Eugene, OR). Hepatitis C NS3 was detected with a mouse monoclonal anti-NS3 antibody (Maine Biotechnology, Inc., Portland, ME) and then visualized with fluorescent goat-anti mouse conjugated secondary antibodies (Alexa Fluor 546 or 633, Molecular Probes, Inc., Eugene, OR). Counter staining was used to help determine the subcellular localization of the proteins. DAPI was used to detect DNA and a fluorescent phalloidin (Alexa Fluor® 546 phalloidin) was used to stain actin. All of the counterstaining dyes were purchased from Molecular Probes, Inc., Eugene, OR.

6.3. RESULTS

6.3.1. Protease activated biosensors

6.3.1.1. Development of protease activated biosensors

The protease activated biosensor is based on a tetracycline inactivated transactivator (tTA). This protein is an engineered transactivator composed of viral and bacterial genes that bind the tetracycline response element. Once bound, the transactivator constitutively induces the transcription of downstream genes. Tetracycline binds to the transactivator and inhibits the induction of transcription in a dose dependant manner. An overview of this system is illustrated in **Figure 6.1**.
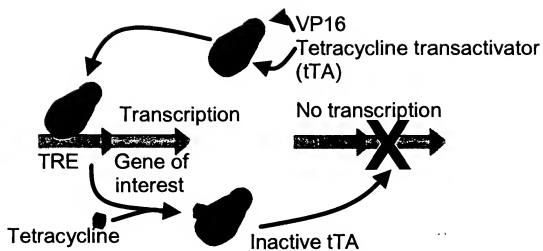
Figure 6.1. Overview of the tetracycline inactivated system. Th tetracycline inactivated transactivator (tTA) induces transcription of an gene down stream of the tetracycline response element (TRE), only i the absence of tetracycline. Tetracycline binds to the tTA and thereb inhibits transcription through inactivation of the tTA.

6.3.1.2. Anatomy of the protease activated biosensor

The protease activated biosensor is a triple fusion protein consisting of transactivator, cleavage, and localization domains that should target the protein to the perinuclear region (**Figure 6.2**). The transactivator region functions to activate transcription when released from the localization signal that serves as an anchor near the endoplasmic reticulum. This anchored protein cannot initiate transcription in the nucleus due to its cytoplasmic localization. The cleavage domain separates the transactivator from the anchor region and is modeled to mimic the target site of a specific protease. If the appropriate protease is present and cleaves the substrate, the transactivator is released from the anchor domain end and is free to induce transcription in the nucleus.
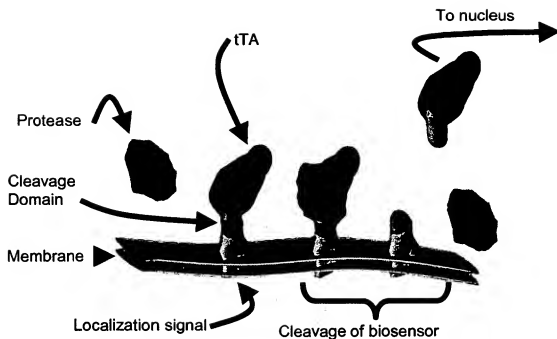
Figure 6.2. Overview of the protease biosensor. The biosensor protei
is a triple fusion protein containing a tetracycline inactivated transactivato
(tTA), a protease specific cleavage domain, and a localization signal. Th
activated protease cleaves the cleavage domain, releasing the tTA. Th
tTA then localizes to the nucleus and activates transcription of
predetermined gene.

6.3.1.3. Biosensor gene arrangement

The first biosensors constructed (**Figure 6.3**) served as templates to which modifications were made to generate other biosensors. This biosensor is a protein that can be cleaved by a specific protease and when cleaved, becomes able to activate the transcription of a specific gene. All biosensors contain the tetracycline inactivated transcription factor (tTA) as activator element. The activator domain is coupled to the localization signal (LS) consisting of the last 27 amino acids of the hepatitis C E2 glycoprotein (BS- 1 and BS- 3) or the first 30aa of the hepatitis C NS5A protein (BS-2). The localization signal derived from the E2 transmembrane domain was hypothesized to anchor the protein to intracellular membranes, whereas the NS5A derived signal localizes proteins to the membranes associated with the endoplasmic reticulum. The activator domain is separated from the LS by means of a cleavage domain (CD) consisting of an optimized hepatitis C NS5A/5B cleavage site DVVCC/SMSY, specific for the NS3/4A protease.

Sub-cellular target:
        Nucleus   ER   Membranes
Gene arrangement:

LS CD TA   LS CD TA   TA   CD LS
BS-1   BS-2   BS-3
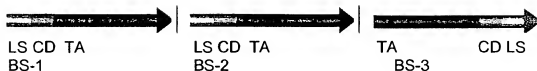
Figure 6.3. Schematic representation of biosensor constructs. Gene structure of three biosensor fusion proteins. All of these biosensors contain a protease cleavage domain (CD, medium gray) and a tetracycline inactivated transcription factor (tTA, black). Each construct also contains a localization signal (LS, light gray). BS-1 and BS-3 contain a portion of the Flavivirus E2 glycoprotein sequence thought to be responsible for membrane anchoring as the LS. The LS in BS-2 is composed of a 30aa sequence shown to localize near the endoplasmic reticulum.

6.3.1.4. Gene arrangement and construction of protease activated biosensors

The biosensors (BS-1, BS-2, and BS-3) are composed of sequences from the tetracycline inactivated transactivator; a short cleavage domain (~9 amino acids); and a localization domain (either the C terminal region of the hepatitis C E2 glycoprotein or the N terminus of the hepatitis C NS5A protein) (**Figure 6.3**). Transcription of these genes is driven by either a T7 or CMV promoter (**Figure 6.4**). The gene arrangements of the three biosensors are shown in **Figures 6.3 and 6.4** The biosensor genes were verified by restriction digest and subsequent agarose gel electrophoresis (**Figure 6.5 left panel**). A plasmid containing the hepatitis C NS3/4A protease was also constructed and verified by PCR and subsequent gel electrophoresis (**Figure 6.5 right panel.**). A construct containing only the transactivator and a cleavage domain was assembled to test the ability of the transactivator to initiate expression of a reporter protein. These experiments were conducted to confirm that the addition of a partial cleavage domain would not render the transactivator inoperative. The results indicated that the transactivator protein was able to induce the expression of a EGFP reporter (**Figure 6.6**).
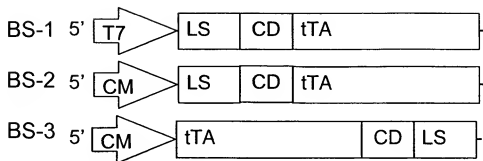
Figure 6.4. Biosensor constructs. Gene structure of three biosensor fusion proteins. All of these biosensors contain the hepatitis C NS5A/B cleavage domain (CD) and a tetracycline inactivated transcription factor (tTA). Each construct also contains a localization signal (LS). BS-1 and BS-3 contain a portion of the hepatitis C E2 glycoprotein sequence thought to be responsible for membrane anchoring as the LS. The LS in BS-2 is composed of the first 90 nucleotides of the hepatitis C NS5A gene that has been shown to localize near the endoplasmic reticulum.
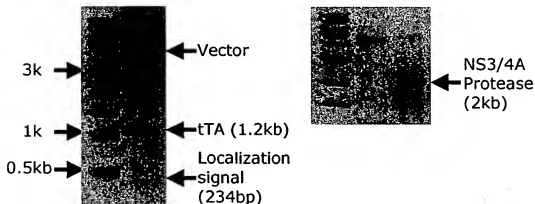
Figure 6.5. Construction of the biosensor and protease genes. Restriction digest (EcoRI & BamHI) of the BS-1 biosensor gene containing plasmid rendered vector, tTA, and localization signal fragments (left panel). PCR of a plasmid containing the hepatitis C NS3/4A protease using NS3/4A specific primers yielded a ~2kb fragment (right panel). Both panels are ethidium bromide stained agarose gels.

Figure 6.6. Transcriptional activation from the tTA with a partial cleavage domain. An EGFP containing reporter gene was co-transfected with construct containing the tTA with a partial cleavage domain into T7 polymerase expressing Huh-7 cells. Resulting green fluorescence can be seen in the right panel.

6.3.1.5. Intracellular localization of three protease activated biosensors

Plasmids expressing BS-1, BS-2, or BS-3 were transfected in to BT7H cells and immunofluorescence confocal microscopy was used to determine the exact intra cellular localization of the three biosensors 24h post transfection (**Figure 6.7**). Nuclei were stained using DAPI while tTA specific antibodies labeled with anti-rabbit FITC secondary antibodies where used to localize the tTA part of the biosensor. The three BS proteins were found to localize in the nucleus, perinuclear, and cytoplasm, respectively (**Figure 6.7**). Because the goals for this biosensor were specifically to target hepatitis C replication machinery, further experiments focused on BS-2 and BS-3. This is because the viral proteases are localized outside of the nucleus.

Figure 6.7. Intracellular localization of BS-1, BS-2, and BS-3 in BT7H cells. Confocal images from BT7H cells transfected with BS-1 (Panel A), BS-2 (Panel B), or BS-3 (Panel C) were stained for biosensor (red) and the DNA counterstained with DAPI (blue).

The BS-2 and BS-3 proteins, were associated with small vesicular structures (**Figure 6.7, Panels B and C.**). BS-2 and BS-3 were not found within the nucleus in the absence of the NS3 protease. Both BS-2 and -3 showed intracellular localization patterns that were similar to that of previously reported *Flavivirus* proteins, including hepatitis C and West Nile NS3/4A. Therefore, BS-2 and BS-3 were selected for further studies. Importantly, the biosensor proteins were found to be localized in two distinct cytoplasmic regions, which were peri-nuclear or evenly distributed throughout the cytoplasm (**Figure 6.7**).

6.3.1.6.   Cytotoxicity of the biosensor proteins

TUNEL analysis was used to determine how toxic the biosensors were to cells. Only BS-2 and BS-3 were tested, because hepatitis C replication occurs in the cytoplasm and excludes the nucleus. BS-2 induces apoptosis in ~28% of cells **Figure 6.8**). The overall transfection efficiency in Huh-7 cells is normally 30-40%. Therefore, BS-2 appears to induce apoptosis in a substantial proportion of the transfected cells. BS-3 only induces apoptosis in ~5% of cells, making this biosensor the least toxic. Control levels of apoptosis in Huh-7 cells typically remain below 1%. Visual inspection of the cells showed clear toxicity in cells transfected with BS-2, but not with BS-3.
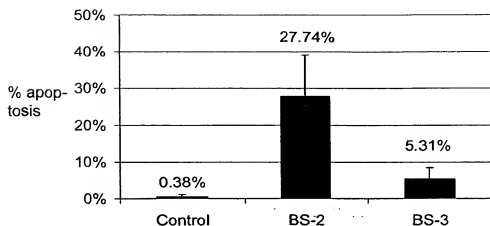
Figure 6.8. Induction of apoptosis by biosensor proteins. TUNEL analysis was used to determine the induction of apoptosis by either control (Panel A), ER localizing BS-2 (Panel B), or membrane localizing BS-3 (Panel C).

6.3.1.7. Intracellular localization of BS-2 and BS-3 in the presence of the hepatitis C NS3/4A protease

To determine if the BS proteins co-localized with their target, hepatitis C NS3 protease, the expressed BS-2 and BS-3 proteins were examined via confocal microscopy. Both BS-2 and -3 appeared to co-localize with hepatitis C virus NS3 as shown by dual immunofluorescence staining for biosensor and NS3 proteins (**Figure 6.9 Panels B and C**). These proteins were differentiated by specific antibodies and spectrally distinct fluorescent secondary antibodies. After observing over 100 biosensor positive cells from three experiments, there were two distinct types of biosensor intracellular staining. In approximately 20% of the biosensor positive cells, biosensor staining appears to be excluded from what appears to be the nuclear compartment (**Figure 6.9 Panels B and C**). Biosensor staining in the remaining cells was found throughout the cell, including the nucleus (**Figure 6.9 Panels E and F**). The intracellular localization of tTA was examined as a surrogate for tTA released from the biosensor proteins by cleavage from the anchor region by NS3 (**Figure 6.9, Panel D**). The tTA expressed from pTet-Off (Clontech, Inc., San Jose, CA) showed a sub-cellular distribution similar to observed in several of the BS- 2 and –3 transfected cells (**Figure 6.9, Panels E and F**).
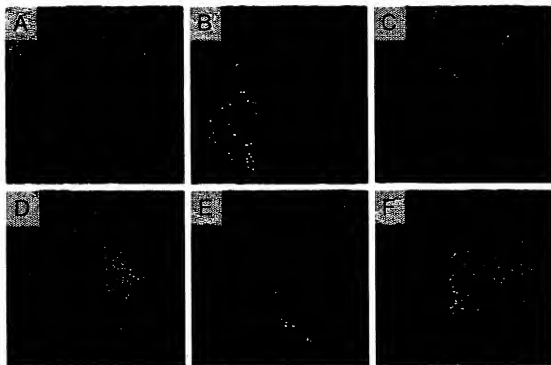
Figure 6.9. Intracellular localization of BS-2 or BS–3 and flavivirus NS3. Protease containing Huh7 cells were transfected with nothing (A), BS-2 (B and E), BS-3 (C and F), and pTet-Off (D). Panels B and C show what appears be inactivated BS proteins that seem to localize within the cytoplasm. Panels D, E, and F show cells with tTA, BS-2, or BS-3 throughout the entire cell, which indicates activated BS proteins. The cells shown in Panel D were transfected with only the transactivator portion of the BS protein and therefore serve as a positive control for the activated BS protein from either BS construct. Panels D, E, and F were found to have BS throughout the z axis, as opposed to Panels B and C that were found to have large regions without protease or BS proteins. Because previous experiments described the localization of the BS proteins to the nucleus, all cells were counterstained with a fluorescent phallotoxin (actin stain, blue) to visualize the localization of the BS proteins (green) with respect to the entire cell. The NS3 protease was also stained and is shown in red.

6.3.1.8. Activity of BS-2 and BS-3 in the presence of hepatitis C NS3/4A

To assess the ability of the hepatitis C NS3 protease to cleave the biosensor cleavage domain and allow the transactivator region of the biosensor to migrate to the nucleus, we transfected BS-2 and -3 into Huh7 cells stably infected with subgenomic hepatitis C replicon (Ikeda et al. 2002). Cells were transfected with a biosensor expressing plasmid and a reporter plasmid containing either EGFP (pBI-EGFP), a blasticidin resistance protein (pTRE-Blast), or a luciferase reporter, (pTRE-Luc) (all from Clontech, Inc.). These reporter genes will only be expressed under conditions where the hepatitis C NS3 protease cleaves off the LS from the tTA domain of the biosensor and the tTA is free to activate the inducible promoter upstream of the reporter gene. Experiments to determine if the biosensor only induces reporter gene expression in the presence of the hepatitis C replicon were designed to include Huh-7 cells with or without the hepatitis C replicon. Additionally, pTet-Off was transfected with pBI-EGFP or pTRE-Blast served as a positive control in all experiments. The resulting cells were analyzed by fluorescence microscopy and flow cytometry (**Figure 6.10**).

Flow cytometric analysis supported the fluorescence microscopy observations described above (**Figure 6.10**). Briefly, both Huh-7 hepatitis C

replicon positive and negative cells were transfected with BS-2 or BS-3 and pBI-EGFP. pBI-EGFP alone and with pTet-Off were transfected as controls. There was little detectable expression of EGFP from either BS-2 or -3 co-transfected with pBI-EGFP within replicon negative Huh-7 cells (**Figure 6.10**). BS-2 was much less sensitive to the hepatitis C replicon than BS-3, only showing low levels of EGFP expression after 48 hours. BS-3 was obviously positive after only 24 hours in replicon positive cells (**Figure 6.10**). 48 hours after transfecting replicon positive cells with pBS-3, there were ~57% as many EGFP positive cells, with respect to the positive control minus background fluorescence. Therefore, BS-3 is the most responsive sensor protein to the hepatitis C subgenomic replicon.

Figure 6.11 shows fluorescence microscopy photos representative of those observations. None of the Huh-7 cells, without the hepatitis C replicon, contained detectable levels of EGFP at neither 24 nor 48 hrs PT (**Figure 6.11, Panels A and B**). BS-2 transfected cells showed a low level of EGFP activation after 48 hours, however, there was no visible EGFP expression after 24 hours (**Figure 6.11 Panel C**). Transfection of the BS-3 expressing plasmid showed a more intense, and a more rapid, response in the replicon positive cells (**Figure 6.11 Panels E and F**). Similar results were found in preliminary experiments using luciferase or blasticidin reporters (Data not shown).
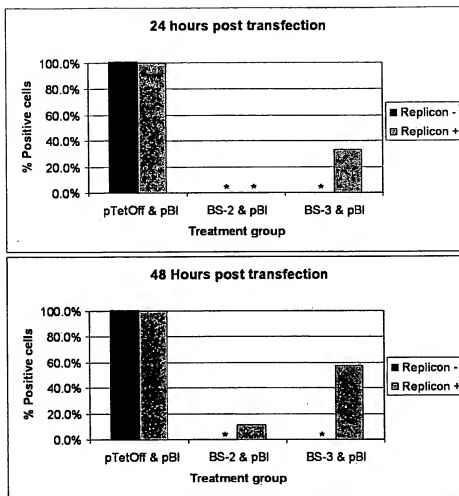
Figure 6.10. Hepatitis C replicon activated biosensor flow cytometry data. Values were calculated as the percent of GFP positive cells normalized to the pTet-Off/pBI values. Huh7 cells are protease/replicon negative and Huh7-RG cells are protease/replicon positive. * indicates 0%.
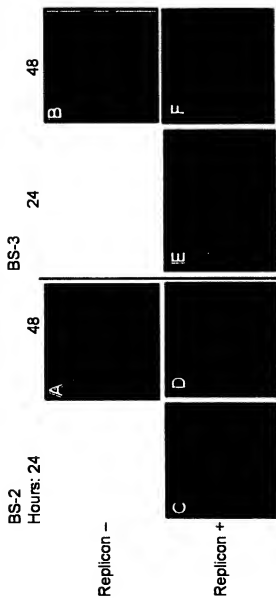
Figure 6.11. Activation of biosensors in HCV replicon containing Huh-7 cells. Huh7 cells (A and B) or Huh-7 cells containing a HCV subgenomic replicon [6] (C-F) were transfected with BS-HCV-2 (C and D) and -3 (E and F), and pBI-EGFP. EGFP expression was visualized after 24 and 48 hours post transfection by fluorescent microscopy. After 48 hours, the cells were fixed, permeabilized, and the nuclei counter stained with DAPI.

158

6.3.2. Oxidative stress induced biosensor

Recent work in the area of oxidative stress has yielded some anti-oxidant response element based sensors that are capable of initiating gene expression only in the presence of oxidative stress inducing chemicals. An overview of this system is depicted in **Figure 6.12.** The reactive oxygen species (ROS) induced biosensor is a promoter based system that relies on the cellular machinery for the detection of ROS. The cell detects ROS and activates transcription factors which bind to specific promoter regions. Transcription downstream of these response elements is then activated. The construct used was constructed by Zhu and Fahl, 2000. This construct is composed of a number of antioxidant response element (ARE) repeats followed by a minimal thymidine kinase promoter, ahead of a EGFP reporter gene. The sensitivity of the biosensor is dramatically affected by the number of ARE repeats, with four repeats giving optimal sensitivity (Zhu and Fahl, 2000). The activity of this biosensor can be seen in T24 cells through the addition of 100 µM tert-butylhydroquinone, an inducer of ROS (**Figure 6.13**) (Sigma-Aldrich Chemical, Inc., St. Louis, MO). T24 cells are a human cell line derived from a transitional cell carcinoma that constitutively expresses CD95 on the surface (Mizutani et al. 1997) (American Type Culture Collection, Manassas, VA).

A stable T24 cell line sensitive to 50-100 µM tert-butylhydroquinone was created and tested with UVB (up to 1 hour exposure). These cell lines were developed in an attempt to increase the sensitivity to UVB exposure. 24 hours after the UVB exposure, there were no EGFP positive cells (data not shown). 30 clones were created and tested for sensitivity to tert-butylhydroquinone, a reactive oxygen species inducing agent. These experiments resulted in a single sensitive clone named T24-AG (T24 is the cell line and AG stands for antioxidant response element followed by EGFP). The T24 cell line was chosen for these studies as these cells are resistant to CD95 mediated apoptosis. This choice was based on the fact that the CD95 protein was targeted by the earliest nanoparticles. CD95 is one of the first extracellular markers to appear in irradiated cells. Additional studies were done to assess the ability of this biosensor to detect ROS induction through UVB exposure, but these studies yielded no positive cells.
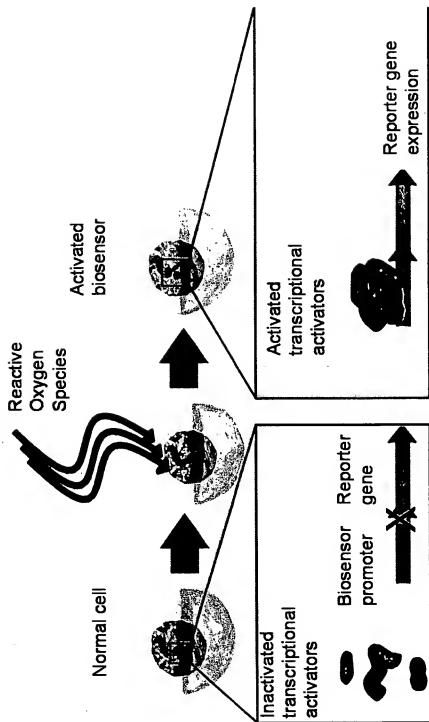
Figure 6.12. Overview of the Reactive Oxygen Species Biosensor. Cells containing this biosensor and a reporter remain silent, until the cell is exposed to reactive oxygen species. Once exposed, the biosensor is activated and the reporter gene product is expressed.
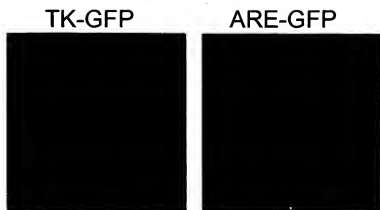
TK-GFP **ARE-GFP**

Figure 6.13. ROS Activated Biosensor. The ROS sensor (ARE-GFP) and negative control vestor (TK-GFP) were transfected into T24 cells. After 24 hours incubation, the cells were exposed to a ROS inducing agent (tert-butyl hydroquinone). 24 hours after ROS induction, the cells were photographed and evaluated for EGFP expression.

6.4. DISCUSSION

6.4.1. Protease activated biosensors

All biosensors contain the tetracycline inactivated transcription factor (tTA) as the activator element. The activator domain is coupled to a localization signal (LS) consisting of the last 27aa of the hepatitis C E2 glycoprotein (BS-1 and BS-3) or the first 30aa of the hepatitis C NS5A protein, BS-2. The activator domain is separated from the LS by means of a cleavage domain (CD) consisting of an optimized hepatitis C NS5A/5B cleavage site DVVCC/SMSY (Zhang et al. 1997).

hepatitis C proteins have previously been reported to be associated with lipid laden vesicles, sometimes described as being associated with small vesicular structures (Rice and Hagedorn 2000). Similarly, BS- 2 was localized in a perinuclear pattern that is similar to hepatitis C structural and non-structural proteins. BS- 2 showed a punctuate distribution reminiscent of the endoplasmic reticulum. Staining for BS-3 revealed an association with small vesicular structures throughout the cytoplasm, while distinct from the nuclear compartment. BS-3 appeared to have a disseminated staining pattern, distinctly different from the reticular pattern of BS -2.

These and the previously described data suggest that the inactivated form of the biosensor is excluded from the nuclear compartment, but the presence of hepatitis C NS3 can cleave off the LS thus allowing the protein to enter the nucleus. All of the hepatitis C replicon cells examined had NS3, but the relative amounts appeared to vary. One explanation for the two types of staining observed may be that the more NS3 and biosensor present in the cell, the more biosensor can be cleaved, thus leading to an increased amount of biosensor in the nuclear compartment. This could be the result of the variations in replicon expression that is thought to occur during different phases of the cell cycle.

6.4.2. Oxidative stress induced biosensor

In order to ameliorate the carcinogenic effects of long term exposure to radiation, we have proposed to deliver DNA repair enzymes to white blood cells. One important problem with this approach is that long term administration of these enzymes would be needed to counteract the long term exposure to radiation during space travel.

One alternate approach would be to administer the DNA repair genes to the cells that may need those enhanced DNA repair enzymes. In fact the penultimate system may be one which is administered once and then only

expresses those therapeutic genes only when needed. As a result, the system would cease to express the DNA repair enzymes in the absence of radiation. To this end, we have begun to develop such a system. In this model there is a biosensor element (either DNA or protein sequences) that activates translation of a therapeutic gene only in the presence of an environmental insult, which in this case is radiation damage.

These studies show that a stable cell line can be derived without any apparent toxicity while maintaining biosensor stability and sensitivity. Thus this approach may be suitable for use *in vivo*. The absence of biosensor activity post UV exposure could be due to the length of exposure time and the amount of UV exposure actually reaching the cells. Because of the great body of literature detailing UV induced oxidative stress (Wenk et al. 2001), it is likely that experimental conditions need to be further optimized. Alternately, other response elements could be used in this model to achieve the same goal.

CHAPTER 7.   GENE THERAPY

7.1.   *INTRODUCTION*

The third and final goal of this dissertation was to develop novel gene therapies to treat either hepatitis C virus infection or radiation induced DNA damage. These therapies should be capable of being activated by the biosensors described in Chapter 6. Therefore, our strategy was to generate therapeutic products through biosensor induced gene expression. This allows for many different expression systems to be tested. For the purpose of this dissertation, the therapeutic gene would be activated as part of the Tet-off system that the biosensors were based on. The tetracycline response element would trigger the transcription of the therapeutic gene only in the presence of the pathologic process at work.

Two main therapies were developed for these purposes. The first, was developed for the treatment of hepatitis C virus infection. This gene therapy approach was based on a targeted ribozyme developed by Kuwabara et al. (Kuwabara et al. 2001). Ribozymes are catalytic, single stranded fragments of RNA that can bind to a complimentary strand of RNA and cleave the complimentary strand at a specific site. Ribozymes can be thought of a targeted molecular scissors that can deactivate targeted RNA strands through cleavage. Kuwabura et al. improved the ribozyme based approach through splicing a tRNA sequence to the 5' end of the ribozyme sequence (Kuwabara

et al. 2001). This caused the tRNA-ribozyme RNA to be actively exported from the nucleus to the cytoplasm where it can be used to cleave the IRES region of hepatitis C genome (**Figure 7.1**). They also added a tRNA promoter so that the transcription product would have defined ends and be expressed at a high level.

We further refined this system to meet our own specifications. For the biosensor to activate the expression of the ribozyme, the promoter must be the tetracycline response element. Unfortunately RNA polymerase II is responsible for the transcription of any gene downstream of this promoter and this polymerase caps the 5' ends of all transcription products. Therefore, through a collaboration with Dr. Rijnbrand at UTMB, self cleaving hammerhead ribozymes were developed for use on the 5' and 3' ends of the tRNA-ribozyme construct (**Figure 7.1**). These flanking ribozymes should self cleave once expressed and result in a tRNA-ribozyme construct with defined ends (**Figure 7.1 and 7.3**). The purpose of the defined ends and tRNA regions of this construct are nuclear export. The stem loop region of the tRNA is responsible for its active transport out of the nucleus. Coincidentally, the target of this ribozyme based system is one of the stem loops found in the hepatitis C virus genome (**Figure 7.2,** red arrow). The specific target of the ribozyme can be found at position 195 of the hepatitis C genome (**Figure 7.2**) (Lee et al. 2000). The 5' non-translated region of the viral mRNA genome forms the

internal ribosome entry site (IRES) and primarily promotes translation of the viral genome (**Figure 1.7**). The 5' non-translated region including the part encoding the IRES is also thought to contribute to viral replication. By cleaving the IRES at this particular point, it is thought that there should be a dramatic decrease in IRES mediated activity and in hepatitis C virus replication.
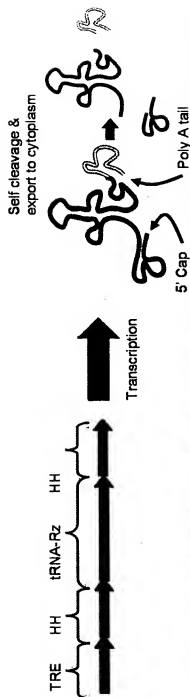
Figure 7.1. tRNA-ribozyme expression and self cleavage. This diagram depicts the transcription (left of the black arrow) of the tRNA-ribozyme cassette and its subsequent cleavage (right of the black arrow). The self cleaving hammerhead ribozymes are shown as light (5') and dark (3') segments, whereas the tRNA-ribozyme itself is shown as a red stem loop segment. The Hepatitis C IRES specific ribozyme is shown as the last hairpin loop on the right side of the tRNA-ribozyme segment.
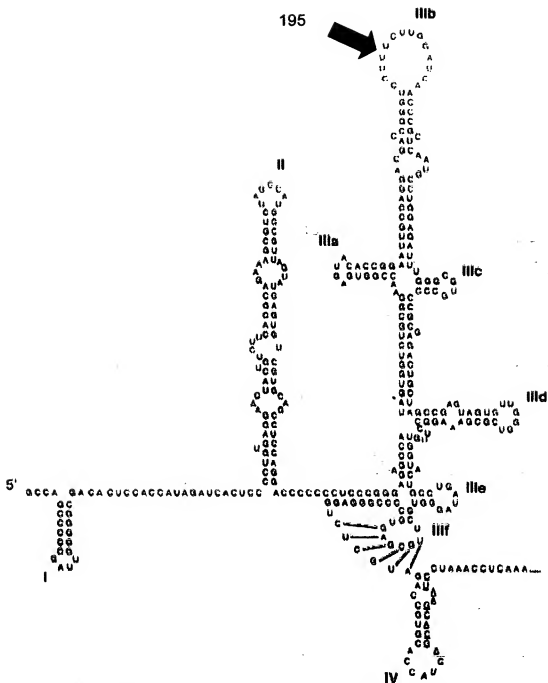
Figure 7.2. Hepatitis C virus internal ribosome entry site. The 5' end of the hepatitis C virus genome is composed of several stem loop structures. At the top of stem loop IIIb is the ribosome target (195, red arrow). (Adapted from Rijnbrand et al. 2001).
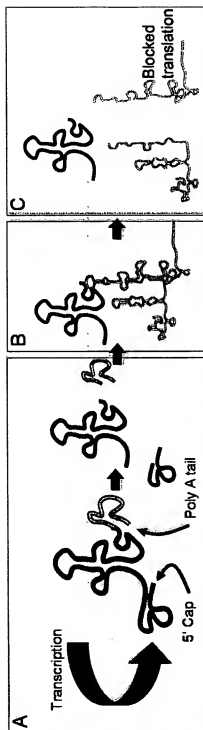
Figure 7.3. tRNA-ribozyme expression and IRES cleavage. Once transcribed, the tRNA-ribozyme undergoes self cleavage (Panel A). The resulting tRNA-ribozyme is then actively transported to the cytoplasm where it encounters the Hepatitis C genome. The ribozyme then binds to the IIIb region of the IRES (Panel B). The IRES is then cleaved by the ribozyme and the translation of the viral genome blocked (Panel C).

7.2. RESULTS

The entire cassette **(Figure 7.4)** was generated through several overlapping PCR reactions **(Figure 7.5)**. This was done very efficiently because the sequence of the entire construct was around 280 bases long. The actual sequence is shown in **Figure 7.4.** Each PCR cycle was followed by gel electrophoresis. The appropriate band was then cut out and purified. The resulting DNA was quantified and used as a template for the next reaction. Finally, the complete construct was obtained and cloned into a vector (pTRE2, Clontech, Palo Alto, CA) that contained the tetracycline response element.

tRNA

AccguugGUUUCCGUAGUGUAGUGGUUAUCACGUUCGCCU

AACACGCGAAGGUCCCCGGUUCGAAACCGGGCacuacaaaaac

caacuuuUCCAAGACUGAUGAGGCCGUUAGGCGAAAGGACCC

Rz
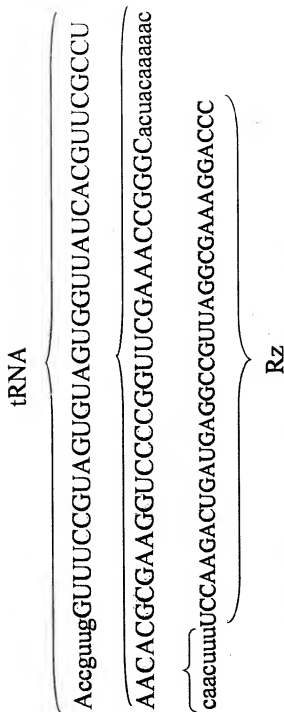
Figure 7.4. Genetic sequence of the tRNA-ribozyme. The red sequences indicate the tRNA region and the black sequences denote the ribozyme portion of the construct.

173
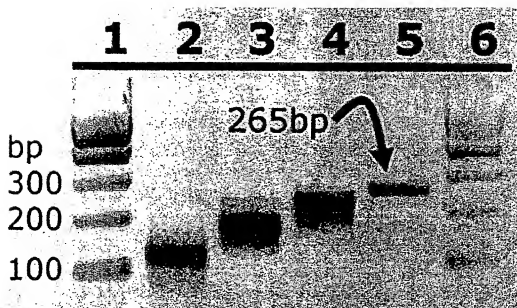
Figure 7.5. Construction of the tRNA-ribozyme cassette. The left panel shows the primer design. These primers were then used in subsequent PCR reactions. The products of these reactions are shown in the panel to the left. The left lane is a 100 base DNA ladder.

Very few studies were undertaken with this construct due to the lack of a model system to test the ribozyme. One of the pilot studies done with this construct was an experiment with a hepatitis C replicon positive cell line (Ikeda et al. 2002). These cells were transfected with BS-3, pBi-EGFP (an EGFP reporter capable of being induced by the TA), and pTRE2-Rz (the ribozyme construct) and allowed to incubate for 96 hours. Immunocytochemistry was used to probe for the presence of NS3 and the TA portion of the biosensor (**Figures 7.6 to 7.8**). The replicon in these cells was driven with an EMCV IRES and neomycin resistance by the hepatitis C virus IRES. Therefore, if the ribozyme did cleave the hepatitis C IRES, the replicon mRNA would be compromised. This could leave the replicon genome unprotected at the 5' end and facilitate the degradation of the genome.

Figure 7.6. Hepatitis C NS3 activated biosensor/ribozyme. These confocal micrographs show hepatitis C replicon cells transfected with BS-3 and pTRE2-Rz. The cells were stained with DAPI (blue), anti-TA (specific for the biosensor, green), anti-phalloidin (cytoskeleton, yellow), and anti-NS3 (red). This set of images shows a typical field, where there is visible NS3 staining in every cell. Each panel shows individual colors and the bottom right panel is a composite image. This negative result shows no decrease in protease levels.
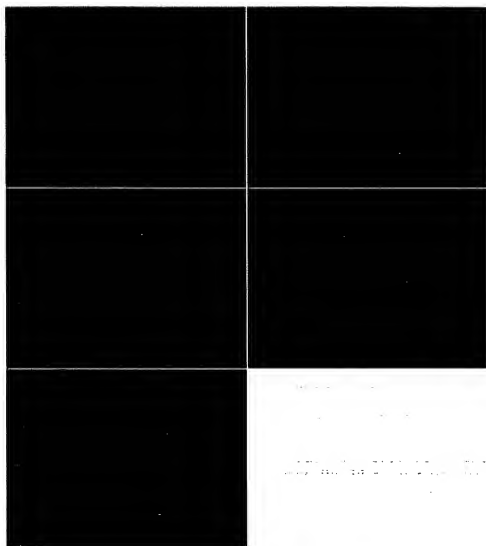
Figure 7.7. Hepatitis C NS3 activated biosensor/ribozyme.
These confocal micrographs show hepatitis C replicon cells transfected with BS-3 and pTRE2-Rz. The cells were stained with DAPI (blue), anti-TA (specific for the biosensor, green), anti-phalloidin (cytoskeleton, yellow), and anti-NS3 (red). This set of images shows two cells, one without the biosensor and one with the biosensor. The cell with the biosensor has visibly less NS3 staining. The bottom panel is a composite image. This image shows a decrease in protease levels in a cell with the biosensor.

Figure 7.8. Hepatitis C NS3 activated biosensor/ribozyme. Thes confocal micrographs show hepatitis C replicon cells transfected with BS- and pTRE2-Rz. The cells were stained with DAPI (blue), anti-TA (specific fo the biosensor, green), anti-phalloidin (cytoskeleton, yellow), and anti-NS (red). This set of images shows several cells, one with the biosensor. The cel with the biosensor has visibly less NS3 staining. The bottom panel is composite image. This image shows a decrease in protease levels in a cel with the biosensor.

The results seen in **Figure 7.6** are typical with respect to the levels of NS3 staining seen throughout the cells (red punctuate staining). **Figures 7.7 and 7.8** show a different staining pattern. In these cells, it appears that there is visibly less NS3 staining in only biosensor positive cells (green staining). This suggests that the ribozyme may be cleaving the hepatitis C IRES in these few cells. Of all of the biosensor positive cells (~100 cells examined), this type of staining was seen ~5% of the time. Therefore only a small proportion of the biosensor positive cells examined demonstrated a decrease of NS3 staining with respect to the neighboring cells.

7.3. DISCUSSION

There were two major findings in this chapter. First, with the tRNA-ribozyme construct completed, it seems reasonable to assume that future ribozyme construction should be relatively simple and quick. Because of their small size a series of the same or different ribozymes could be constructed to eliminate specific RNA fragments. We used an optimized hepatitis C virus specific ribozyme developed in the late 1990's (Lee et al. 2000). This greatly decreased the amount of time necessary to construct the ribozyme described in this chapter. Future experiments with this construct will include a hepatitis C IRES driven fluorescent protein. This model system will provide the necessary

components to further optimize the activity of this gene therapy strategy.

Note:

  The targeted DNA repair gene therapy was developed by the Lloyd laboratory, at UTMB. These experiments were carried out by the Lloyd lab and are only touched upon here to be comprehensive. The goal of these experiments was to develop a targeted DNA repair enzyme that was more efficient than those currently found in humans. To this end a series of bacterial DNA repair enzymes were fitted with eukaryotic targeting sequences. In this way, bacterial DNA repair enzymes were targeted to the nucleus and mitochondria. Later studies demonstrated that these enzymes were capable of repairing DNA damage induced by UV radiation in human cell lines. These enzymes were also more efficient than their human counterparts.

CHAPTER 8. DISCUSSION

8.1. NANOMEDICINE OVERVIEW: A COLLABORATIVE EFFORT

Nanoparticle based treatment holds great promise as a multi-step approach to treating disease. By using functionally interlaced layers of a nanoparticle, we are developing a treatment platform technology which can be tailored to specific requirements. Nanoparticle functionality can be thought of as being organized from the exterior to the core. The function of the outermost layer is generally considered to be targeting and cell entry. Multiple inner layers can be composed of biological, chemical, or synthetic materials that perform different tasks based on what layer is exposed. In this dissertation, a biosensor was developed to monitor levels of a foreign protease or reactive oxygen species. This and the accompanying reporter or gene therapy constructs will be prime candidates for inner nanoparticle layers.

Developing a multilayered nanoparticle that does all of the formerly mentioned tasks in a prescribed order is a complex project that requires a widely multidisciplinary team. The development of these technologies was carried out as a collaborative effort between five laboratories. Nanoparticle construction was carried out by two labs headed by Drs. Kotov and Lvov. The semiconductor based nanocrystals were developed by Dr. Kotov at Oklahoma State University, although he recently moved to the University of Michigan,

Ann Arbor, MI. The layer by layer nanoparticles were developed by Dr. Lvov at Louisiana Tech University. These investigators were involved in nanoparticle development and layering technologies. *In vivo* and *in vitro* imaging was done in collaboration with the biomedical engineering group at UTMB headed by Dr. Motamedi. Targeted gene therapy for DNA damage was developed at UTMB by Dr. Lloyd. The multiple technologies developed by these four laboratories was then tested and further enhanced by the Lloyd laboratory. Additionally, biosensor and magnetic nanoparticle development was carried out exclusively in the Leary laboratory.

8.2. *PROJECT RATIONAL AND MAJOR FINDINGS*

Nanomedicine can be distilled into three discrete elements: delivery (nanoparticles), sensor (biosensor), and an affecter (gene therapy). All three parts have to work together in order for this strategy to be useful in the clinic. These technologies were developed separately in order to reduce inherent complexity of the system. This dissertation describes the development of these technologies. The development of a nanoparticle delivery system is the first logical step, however, in practice each of the three components of the nanomedicine system were developed in parallel.

8.2.1. Nanoparticle development

The nanoparticle development evolved into several different technologies. The nanoparticle development was broken into three elements: the outer coating, inner payload, and core. Initial experiments to develop an outer coating used polystyrene beads that were between 300 and 1000 nm. These experiments were initially used to test the feasibility of an antibody mediated targeting. In order to use antibody mediated targeting, one has to find an antigen on the surface of the targeted population; an antibody that can correctly identify and bind to that antigen; and finally, that antigen would have to be internalized upon antibody binding. Antibody coated particles were easily able to attach to the desired cells (**Chapter 2.**). These criteria, along with the cost and concentration limitations lead us to look in other directions for a outer coating for the nanoparticles to direct targeting/internalization. To this end two more strategies were tested to the criteria for these targeting/internalizing moieties were that they had to be:

1. inexpensive;

2. available in large quantities;

3. non-toxic;

4. target relevant cell populations while inducing internalization when bound to the surface of the cell.

8.2.2. Nanoparticle coatings

Viruses are a model example of nanoparticle based gene delivery agents. Viral mediated gene delivery is quite efficient and has evolved to its host for many years, in some cases millennia. Therefore, it was postulated that by attaching the viral structural proteins on the outer surface of the nanoparticle, thus minimizing the tissue specificity. Viral proteins are routinely generated by recombinant protein expression in bacteria or insect cells. Using molecular mimicry to target the same cells as the virus of choice could prove to be a very accurate way to target possibly infected cells. This approach, however, has several obvious drawbacks, including the cost of membrane spanning protein preparations and the orientation of protein attachment on the nanoparticle. This is a problem with hepatitis C virus due to the lack of a cell culture system. Although, this approach is biologically attractive, it would require a large investment to successfully develop and is technically complicated. Finally, the toxicity of these proteins or even viral protein fragments is unknown. Using viral proteins could not only induce an immune response, but also has the potential to cause intracellular toxicity.

8.2.2.1. Layer by layer nanoparticle targeting

A layered nanoparticle coating strategy that utilizes a chemical agent agrees well with the previously mentioned criteria. Just such a strategy was

developed especially for the early stages of nanoparticle development, when large quantities of the coating agent were used to develop and test the targeting and delivery system. Because hepatitis C targets primarily liver cells, these cells were investigated for endocytotic receptors. Liver cells are widely known to endocytose sugars through the asioglycoprotein receptor (Chowdhury et al. 1993). This well documented pathway is also known for its ability to facilitate the internalization of relatively large complexes. This lead to the development of sugar coated layer by layer nanoparticles which were used for targeted gene delivery. This strategy is inexpensive and the coatings are commercially available in large quantities. Using sugars like galactosamine are also nontoxic in low doses. While several different sugar based outer coatings were considered for use, none achieved transfection efficiencies rivaling liposome mediated gene delivery. This was hypothesized to be partially due to the physical characteristics of the layered nanoparticle.

8.2.3. Semiconductor nanocrystals

Nanocrystals offer several unique advantages over traditional nanoparticles and lipid mediated gene delivery tools. Nanocrystals have spectral properties that are especially convenient for *in vitro* use (Chan et al. 2002; Dubertret et al. 2002; Jaiswal et al. 2003). These nanocrystals fluoresce very brightly and do not photobleach like traditional dyes or fluorescent

proteins. Nanocrystals are also small enough (<6 nm) to enter the cell without endocytotic signals. Additionally, a multitude of biological moieties can be bioconjugated to the surface of nanocrystals. Even with large, biologically active molecules conjugated to the surface of these nanocrystals, they remain under 20 nm in diameter. With these characteristics in mind, streptavidin was bioconjugated to the surface of these particles to give this system the flexibility needed for development and testing. The streptavidin-biotin bridge allows for bioconjugation of single or even multiple targeting, internalization, and therapeutic molecules. The components that are used to generate these nanocrystals are relatively inexpensive and commercially available, but there is considerable expertise needed for their synthesis. The toxicity of semiconductor nanocrystals is currently being explored by many laboratories and is discussed in detail during the next section.

8.2.3.1. Nanocrystal toxicity

The spectral characteristics of these particles would facilitate the development of targeting, sub-targeting, and cell entry strategies. Toxicity of the nanocrystals is a major concern as the core of these particles is composed of toxic elements. Throughout these experiments the nanocrystals have been shown to cause problems with membrane permeability, as demonstrated with the trypan blue dye exclusion assay. One reason for this may be the poisoning

of the transporter for trypan blue export. The cells do not appear to undergo necrosis or apoptosis. In fact, the cells appear to tolerate the nanocrystals quite well, allowing for multi-day studies. One concern brought to light by these observations was that incompletely coated nanocrystals may slowly release the toxic core elements into the cells/media. Although no data has been published, these particles do not appear to dissolve in water. This can be alleviated by using a different core particle that allows for purification and/or does not contain a toxic core particle.

8.2.4. Magnetic nanoparticles

The magnetic nanoparticles were tested in this dissertation as they are relatively inexpensive, commercially available with a variety of well defined and controlled coatings and sizes, well documented in vivo use as contrast agents, and can be readily purified with magnetic columns. These characteristics make magnetic nanoparticles relatively easy to modify for use in these nanomedicine experiments. Magnetic nanoparticles with streptavidin conjugated to the outer surface were purchased and adapted for gene delivery. Streptavidin was chosen as the linking agent for the inherent ease of use and wide variety of biotin labeled molecules available. Although the streptavidin-biotin method of conjugation is not as elegant as the layer by layer adsorption approach, this system is assured to allow the quick and permanent

attachment of molecules to the magnetic nanoparticles. These characteristics allowed for the development of a novel gene delivery tool that has many different uses, including gene delivery/recovery, and library screening. In order to deliver genes into cells with these magnetic nanoparticles we utilized PCR fragments containing all of the elements necessary for expression in eukaryotic cells. The process of constructing a batch of these particles takes less than an hour, making them ideal for development purposes. These particles were commercially available with streptavidin already bioconjugated and a diameter of 50 nm. The intended use of this particle was to isolate biotin labeled DNA or protein. Therefore, this product came with the buffers optimized for either DNA or protein binding. Some of the disadvantages to this approach are that the DNA is exposed on the surface and that there was no targeting specificity. Both of these issues could be overcome by developing a more complex coating strategy that both protected the DNA and targeted the magnetic nanoparticle.

8.2.4.1. Magnetic nanoparticle transfection

The magnetic nanoparticles were initially tested for DNA binding and were found to bind a large enough proportion of the DNA to be seen in gel electrophoresis experiments (>50 ng) using ethidium bromide to fluorescently label the DNA. These particles were then coated with lipid and exposed to

cells. Magnetic nanoparticles should not cluster during the DNA layer deposition, as there is only one biotin label per DNA fragment. The ability to wash the particles during their construction with the aid of magnetic columns and optimized buffer solutions played a role in the relatively good transfection efficiencies achieved with these particles. The binding conditions necessary for efficient DNA binding to magnetic particles has already been optimized, therefore there were more magnetic nanoparticles with attached DNA than would be possible if these conditions were suboptimal. In future studies, the amount of DNA bound to these nanoparticles could be quantified by incorporating a restriction site near the biotin tag. This restriction site could then be cleaved and the amount of DNA once bound to a volume of nanoparticles quantified. This would yield valuable information that could be used to better compare transfection efficiencies. Additionally the quantity of DNA attached to the magnetic nanoparticles could be determined by examining the ethidium bromide staining during gel electrophoresis.

8.2.4.2. Magnetic nanoparticle recovery from transfected cells

An unexpected benefit was discovered while using the magnetic nanoparticles for gene delivery was that the particles and their tethered genes could be extracted from living cells expressing the delivered genes. The novel concept of gene delivery and expression analysis followed by tethered gene

extraction and purification was explored in some detail and found to be relatively easy to implement. Even at the single cell level, specific DNA was capable of being recovered in 6 out of 10 cells. Although the system works ~60% of the time, there was no identifiable PCR fragment 40% of the time. This may be due to many causes. The first point at which the system could fail is during construction. Although we saw no transfections from the negative control, DNA with no biotin labeling, there could be some loosely attached DNA /streptavidin that could dissociate later in the experiment. Although the DNA should be tightly bound, the intracellular milieu could digest either the DNA or the protein necessary for DNA tethering. In this scenario, cellular enzymes could cleave the DNA from the nanoparticle in such a way that the promoter and gene are left intact, thus allowing the reporter gene to be expressed without being tethered to the nanoparticle. This could be an issue if genetic integration could not be tolerated, such as *in vivo* treatment. Another possibility could be that the number of particles-DNA present in the cell was sufficient for gene expression, but not recovery. Only the brightest cells were isolated for gene recovery to preclude this potential problem. Despite these pitfalls, this system appeared to be very robust and proved to be useful for a number of studies.

8.2.4.3. Library screening with magnetic nanoparticles

One application for this technology is high throughput screening. A library containing protease activated biosensors with different cleavage domains could be constructed and tethered to the magnetic nanoparticles. This library could be screened in cell culture and the successful candidates extracted by fluorescence activated cell sorting, through the use of a fluorescent reporter protein. In this scenario the magnetic nanoparticle would be a platform from which specific biosensors would be developed. Using this paradigm, biosensors for unknown proteases or pathogens could rapidly be developed through the use of this library.

8.2.5. Protease activated biosensors

The rapid development of protease activated biosensors through the use of magnetic nanoparticles is just the first of many steps towards a successful nanomedicine strategy. The goal of biosensor development is to give the cell the ability to detect and active anti-pathogenic genes when necessary. Equally important is the ability to switch off those genes in the absence of the pathogen. This ability to turn on and off useful genes is a simple concept, however this is far beyond any therapies available today. Current drug and gene therapies are controlled by the dosage and not the level of pathogen present. With a biosensor present, the pathogen or pathogen induced activity

dictates how much of the therapeutic gene is necessary for its own termination. The promise of biosensors is to detect pathogenic processes and subsequently alter therapeutic dosages in real time, which is not possible in today's clinical setting. The concept of the biosensor has been shown to function correctly, even though the biosensors described herein do not perform at 100% efficiency. In fact, several different types of biosensors have been developed through this effort.

8.2.5.1. Protease activated biosensor subcellular targeting

The biosensor protein has to be kept inactive in the absence of the protease and this translates to making the protein or very bulky to induce a constant state of steric hindrance so the protein can not bind to the targeted promoter sequence. An alternate strategy was that the biosensor could be targeted to specific membranes thereby anchoring the protein to extra-nuclear structures. One of the original strategies was to use the viral protein localization signals to target the biosensor to the correct subcellular region. The hepatitis C E2 envelope protein is known to co-localize with the replication complex that harbored the targeted NS3/4A protease (Rice and Hagedorn 2000). Therefore, the transmembrane region of the hepatitis C virus E2 glycoprotein was used as the anchor domain. Studies with this peptide sequence coupled to the TA showed a retention of the TA to the endoplasmic

reticulum or to cytoplasmic membranes depending on the biosensor configuration. The biosensor would localize to what appeared to be the endoplasmic reticulum if the membrane anchor was attached to the N terminus of the TA (BS-2). Whereas the biosensor with the membrane anchor cloned onto the C terminus of the TA protein (BS-2) localized to membranes throughout the cytoplasm (Chapter 6.). Toxicity studies showed that with the E2 transmembrane region cloned onto the N terminal region, the biosensor induced apoptosis in a large proportion of the cells. The alternate version of the biosensor (BS-3) was found to be much less toxic and was also capable of NS3/4A cleavage.

8.2.5.2. Protease activated biosensor cleavage domains

Two biosensors were tested with cells containing the hepatitis C virus NS3/4A protease. The results indicated that the least leaky biosensor was BS-2. BS-3 showed positive cells earlier, was less toxic, and was found to be leakier. Overall the results from these studies were encouraging and lead to the development of BS-3 biosensors targeted to different cellular and viral proteases, such as the West Nile and Dengue virus proteases and the caspases. The relative decrease in the activity of the BS-2 biosensor was due in part to the toxicity. Another problem with this biosensor could have been that its limited coverage of the cytoplasm led to less biosensor interacting with

the protease, with respect to BS-3. Overall, both biosensors were able to detect the presence of the targeted protease thus proving the concept of a protease activated biosensor is possible and setting the stage for the development of second generation biosensors with less background, better responsiveness, and decreased toxicity.

8.2.6. Antioxidant response system based biosensors

Researchers have been developing promoter based biosensors for many years (Blanchard et al. 1993; Blasberg 2003; Uzan, Prandini, and Berthier 1995). This is because so many cellular activities are mitigated at the promoter level. Many of these studies have focused on determining the activities of specific promoters during times of cellular stress induced by pathogenic processes (Blanchard et al. 1993; Blasberg 2003; Uzan, Prandini, and Berthier 1995). Cloning a reporter gene downstream of the promoter of interest is one way of determining the activity under experimental conditions. This has been done with a plethora of promoters (Blanchard et al. 1993; Blasberg 2003; Uzan, Prandini, and Berthier 1995). One which was chosen for these experiments was based on the antioxidant response element. This particular sequence of DNA is targeted by a group of proteins that are activated as part of a cellular response to reactive oxygen species (Zhu et al. 2001; Zhu and Fahl 2000, 2001). Once activated, these proteins bind to the

antioxidant response element, also known as the electrophile response element, and trigger the transcription of any downstream genes (Zhu et al. 2001; Zhu and Fahl 2000, 2001). Researchers from the Arizona Cancer Institute cloned this promoter upstream from the EGFP gene (Zhu and Fahl 2000). Although this construct was able to report the presence of induced oxidative damage, the researchers found that repeated response element sequences in parallel enhanced the reporter activity. This construct was used during this dissertation as a surrogate for a radiation activated biosensor.

The hypothesis for these experiments was that the radiation encountered by astronauts during deep space travel would be modeled *in vitro* with UV light. This model could then be used to evaluate the DNA repair enzymes developed by the Lloyd lab (Lloyd et al. unpublished data). If the biosensor detected the oxidative stress generated by the UV light exposure, then the DNA repair enzymes could be cloned downstream of the promoter sequence. The results from these experiments show that this biosensor can be used to detect reactive oxygen species and could be further adapted for use in the radiation model system. In conclusion, the antioxidant response element based biosensor is functional and has many different potential applications when implemented within the framework of nanomedicine.

8.2.7. Gene therapy

Modern gene therapy has, to date, focused on the delivery of genes delivered through naked DNA/RNA, liposomes, or viral mediated delivery (Brenner 1995; Cavazzana-Calvo et al. 2000; Check 2002; Cristiano et al. 1993; Kaiser 2003; Kennedy and Steiner 1993; Kotin 1994; Pfeifer and Verma 2001). Gene therapy can be used to add a gene or inactivate an existing gene. The nanomedicine paradigm is capable of a more sophisticated Boolean type of therapy. This system can only be effective if there is a therapeutic gene to be activated. Gene ablation is the chosen therapy for pathogenic viruses.

8.2.7.1.   Targeted ribozymes

A targeted ribozyme was developed for the treatment of hepatitis C virus infection. This pair of molecular scissors was targeted to the 5' region of the hepatitis C genome known as the internal ribosome entry site (IRES). The IRES regulates viral gene expression and plays a role in viral replication. Previous studies have optimized the ribozyme sequences necessary for cleavage of the IRES. The targeted ribozyme described within this dissertation has three distinct parts. First there are two self cleaving ribozyme sequences flanking the ribozyme cassette. The purpose of these flanking sequences is to generate defined RNA ends. This function is critical for efficient intracellular trafficking, target RNA binding, and cleavage. Next there is a tRNA$_{val}$ between

the 5' self cleaving hammerhead ribozyme and the IRES specific ribozyme. This region contains a signaling stem loop domain that causes the ribozyme to be exported from the nucleus. The rational behind this segment is that the hepatitis C virus replicates in the cytoplasm, excluding the nucleus. The ribozyme itself is transcribed within the nucleus and would stay there if not for the nuclear export signal of the tRNA segment. Therefore, the tRNA serves to target the ribozyme to the cytoplasm, where the tRNA normally functions.

The literature reports that the addition of the tRNA to the ribozyme does not significantly inhibit the activity of that ribozyme (Kuwabara et al. 2001). Although the experiments for this section of the dissertation are at the early stages, there are some encouraging results. Studies with a hepatitis C replicon showed that some biosensor positive cells containing the hepatitis C specific ribozyme reporter had virtually no NS3 protease compared to the neighboring cells. Whereas, cells with no ribozyme promoter had high levels of NS3 present and there was very little difference in the NS3 levels between cells. These results are encouraging and have prompted the construction of a IRES driven EGFP construct that will be used to quantify the effectiveness of the ribozyme.

8.3. NANOMEDICINE CHALLENGES

Although the concept of creating a synthetic virus was the one of the driving forces behind the development of this nanoparticle based system. One of the results of this paradigm was adhering synthetic peptide fragments derived from viral envelope sequences to the surface of nanoparticles in an effort to help create a "synthetic virus". This particular methodology was explored early in this dissertation and largely abandoned. The initial work that was done in this area focused on the generation of a gene that contained part of the hepatitis C virus E2 envelope protein thought to be displayed on the outer surface of the virus, fused to a gene that could be used to isolate the recombinant protein after expression. Several approaches were explored both to clone the gene fusions (several purification methods were considered) and express the construct (mammalian, bacterial, and insect cell culture). Although there was a sincere effort to carry out this plan, there was not enough time, money, or energy to follow through with this plan. The entire effort was a tedious and technically challenging project in itself. In the final analysis, the concept of putting viral derived proteins on the surface of nanoparticles to mimic the virus has potential, but the realization of that goal is fraught with problems. There were three main issues that stopped us from pursuing this strategy: first, the cost of getting the system going and achieving a reasonable level of quality control was overwhelming; second, producing and purifying gram quantities of this protein were only reasonable with the bacterial system,

which could not properly glycosylate the viral proteins; lastly, there is a reasonable risk of inducing an immune response when treating animals with this type of coated nanoparticle.

Another targeting strategy explored at the beginning of this project was antibody labeled nanoparticles. We initially used antibodies to target nanoparticles to cells of interest for many reasons discussed in **Chapters 1 and 2**. While this methodology is popular for targeting a multitude of agents (ie fluorochromes, drugs, enzymes, etc.), there are some significant drawbacks to this approach. One of the most obvious of these is cost and quantities available. These issues immediately come into play during the earliest meetings between the Leary and nanoparticle construction laboratories. Joining the worlds of chemistry and biology was difficult and antibody labeling of nanoparticles was among the first of the challenges facing this technology. The problems facing chemists synthesizing nanoparticles on a daily basis appear to be the opposite to that facing biologists. The chemistry necessary to generate layered nanoparticles, thin films, and nanocrystals is based on having a great excess of starting materials. This is contrasted by the field of biology which uses relatively minute amounts of chemicals to treat living cells, tissues, and animals. In essence, chemists routinely deal with grams and a milligram is a large quantity to a molecular biologist. This single issue took many different forms and as such required many hours of effort on both sides

to resolve. In the end, grams of antibody could not be used to coat nanoparticles, and when considering scaled up models, this was not a feasible long term approach. Therefore, only the earliest experiments utilized antibodies. An additional consideration that was not immediately apparent was the presence of Fc receptors on white blood cells. The presence of this receptor on a cell could lead to binding any nanoparticle labeled with an antibody containing the correct Fc portion. This additional consideration also helped lead us to the conclusion that antibodies are more of a liability than a solution. This is not intended to condemn antibody targeted nanoparticle research, but in our case the cost greatly outweighed the benefit.

These nanomaterial challenges were not limited to the outer layer of the nanoparticles by any means. Generating a particle that could transfect cells with a reporter gene was one of the first goals of this project. Due to the inherent difficulties of this task, the targeting and gene delivery methods were carried out in parallel until the gene delivery strategy was successful enough to accommodate some level of targeting. In fact, each of the nanoparticles explored in this dissertation were very difficult to adapt to the task of delivering genes. The layered approach had its own set of unique difficulties. These issues began with the selection of a core particle. Dr. Lvov's group supplied use with three different core particles to choose from. Those particular particles were chosen based on their experience with those specific

nanomaterials. The chemistry necessary for the construction of these particles was difficult and therefore using a familiar nanoparticle core facilitated the charged layer deposition necessary for particle construction. Unfortunately, all three particles showed signs of toxicity. This was further complicated by the fact that the particles could not be counted by any known means, other than by weighing large quantities or by AFM/electron microscopy. The inability to enumerate these nanoparticles made experiments very difficult to execute and interpret. In fact, there were no nanoparticles used in this dissertation that could be counted by any reasonable means. This lead to experimental design based on volumes of nanoparticles in place of concentrations. Although this drew much criticism, there have been very few suggestions on how to address this problem. However, since this work has matured, some strategies are currently being adapted from virology to address the issue of nanoparticle quantitation biological systems.

The spectral and fluorescent properties of the semiconductor based nanocrystals made them easier to work with in one respect but their tendency to cluster and fall out of solution made time a critical issue. Initial experiments with CdTe nanocrystals showed that these early preparations were not stable at physiological pH. This presented a serious issue that was quickly addressed by Kotov laboratory. The following nanocrystal preparations were composed of CdSe and external layers were also added to enhance stability under

biological conditions. These efforts resulted in a relatively stable nanocrystal coated with streptavidin. Unfortunately, these particles were subject to clustering and falling out of solution over time. The CdSe nanocrystal bioconjugation to streptavidin method was painstakingly optimized. Although this nanocrystal optimization helped us to define a better bioconjugation protocol, further work needs to be done to prevent the formation of the large aggregates. This is now the primary challenge for this technology and the focus of current research.

8.4. NANOMEDICINE LIMITATIONS

Nanomedicine is designed to add molecular functionality to the cell in order to combat disease. This platform technology can be tailored to many different circumstances. There are a multitude of infection based diseases to which nanomedicine could be applied. There are however many other pathogenic processes that nanomedicine could not be applied to, in fact, with today's technology, there are many pathogenic processes that would be very difficult if not impossible to by treated be cellular re-programming.

One important limitation of the nanomedicine process is the time it takes to detect and react to the pathogenic stimulus. Although the detection of the pathogenic process can be considered real time, the cell still has to build

the biological components to fight the pathogenic process. This could take up to several hours to complete. This may not be enough time to save the cell from irreparable damage, but may be faster than scheduling an appointment with a physician.

8.5.   NANOPARTICLE JOURNEYS

Time is also an issue when considering nanoparticle mediated delivery. We have seen that the expression of nanoparticle delivered genes can be up to 48 hours later than liposome delivered genes (unpublished observation). This delay in gene expression was most notable in both layer by layer and magnetic nanoparticles. This delay in gene expression is most likely due to the "uncoating" of the layer by layer constructed nanoparticles. In the case of the magnetic nanoparticles, the delay in expression could be due to increased time necessary for the nanoparticle to arrive in the nucleus. The transport of the magnetic nanoparticle to the nucleus may be facilitated by the breakdown of the nuclear membrane during cell division. Therefore only the fraction of those cells undergoing mitosis would be capable of expressing nanoparticle tethered genes at a particular point in time. This would then limit the usefulness of this system, such that additional strategies would have to be developed to overcome this problem. The other cells may just be harboring nanoparticles tethered to genes within compartments outside of the nucleus.

8.6. TOXICITY ISSUES

Toxicity of the nanoparticle components is a critical issue that has to be dealt with carefully. Even FDA approved materials can be toxic to cells in culture and presumably *in vivo*. The problems encountered while purifying the nanoparticles can lead to increased toxicity once put into cell culture. The semiconductor based nanocrystals are a prime example of potential toxicity (McKenzie, Arthur, and Beckett 2002; Vinceti et al. 2001). These particles appear to be harmless to cells *in vitro* when properly coated, but could be harmful if even traces of the semiconductor materials are present when delivered into cells. This is why the purification of the correctly constructed nanoparticles is paramount to the reduction of nanoparticle toxicity. Additionally, the last layer prior to reaching the core particle could contain an excretion molecule as an attempt to get rid of the nanoparticles. In conclusion, correctly constructed nanoparticles are no substitute for using non-toxic components for nanoparticles, because eventually the layers may break down exposing the cell to the nanoparticle components.

8.7. TARGETING EFFICIENCY

Correctly targeting cell populations is another critical step in nanomedicine. Nanoparticle targeting is a difficult task. Much attention is

currently being placed worldwide on this important topic (Benns and Kim 2000; Douglas, Davis, and Illum 1987). The nanomedicine system is unique as we have at least two targeting steps, nanoparticles and biosensing. This allows for broader and less specific nanoparticle targeting due to the intracellular activation by the pathogenic process carried out by the biosensor. These nanoparticles also have the ability to be targeted using Boolean logic, i.e. AND, OR, etc. By using multiple nanoparticles with these functions, one could effectively target rare cells in a fashion similar to rare cell analysis, but in a living animal (Leary 1994). This can be accomplished by placing multiple targeting agents on nanoparticles and using additional nanoparticles that inhibit the biosensor and gene therapy expression. Very accurate nanoparticle targeting to cells can be achieved simply by using combinations of positive and negative targeting molecules nanoparticles (Leary 1994).

Some of the major limitations of biosensors and therapeutic gene products also include targeting, in addition to toxicity, efficiency, and the precision with which they operate. Developing a biosensor or gene therapy strategy that both accurately and precisely detects a pathogenic process is a difficult task. The biosensor or gene therapy also has to be non-toxic. The first biosensors produced during this dissertation were especially toxic, while others with the same genetic materials were not. Therefore, thorough toxicity

testing is of great importance and can be a significant limitation of this technology.

8.8. FUTURE STUDIES

The overall goal of this research is to produce an integrated working system that can be tailored to a range of pathogenic processes. The fist stage of this project is to develop working models for each of the three components, nanoparticle delivery, biosensing, and gene therapy. The results from this dissertation show some working nanoparticle delivery prototypes, biosensors, and novel gene therapies.

8.8.1. Integration

The next step for this field of research is to begin to integrate the different tools with each other. Each step of integration is significant in its own right and will be difficult. This necessity becomes readily apparent when one considers that only a fraction of cells are capable of being transfected by nanoparticles (~40% at best) and the hepatitis C virus biosensor appears to be functional in a fraction of cells (~30%). This results in very few cells with a completely functional system. The selection of cell lines for these studies is crucial. During this dissertation, the chief cell line of interest was the human hepatoma cell line Huh-7. These cells are difficult to transfect with any

method, including electroporation and lipid mediated transfection protocols. Therefore, they may be a poor choice for integration studies. Cell lines which are more susceptible to transfection by common protocols like liposome based techniques would likely give more encouraging results. Like most therapies in development, there are probably going to be a multitude of problems when converting the system for use *in vivo*. This will likely be the most difficult although rewarding part of this project. The human body is a very complex organization there for the introduction of a new biological system, no matter how beneficial, will not be easy. Although cell culture systems give a clue as to how the nanomedicine system will work, only *in vivo* work will make this effort worth while.

8.8.2. Molecular programming

Another evolution of this technology is the addition of multiple layers of programming on individual nanoparticles. The ability to deposit multiple layers of molecular instructions on a single particle is a powerful tool. In combination with protective layers that can be triggered to reveal the next coating gives the researcher the ability to program the cell with decision tree like logic. This could be carried out by utilizing cleavable layers specifically targeted to different subcellular compartments. These instructions cannot only be used to express genes or detect the cellular status, but also to retarget the

nanoparticle from one subcellular locale to another using subcellular localization signals. Such a nanoparticle could also be programmed to be secreted upon a given signal (such as the SEAP secretion signal), thereby targeting other cells. This nanometer sized particle has the ability to become a functioning tool capable of very complex operations including cellular programming and retargeting on a molecular level.

8.9. CONCLUSIONS

Nanomedicine is a novel paradigm that attempts to augment the cell's ability to fight pathogenic processes. This method of treatment has several characteristics that make it potentially more effective and safer than current therapies. Currently, clinicians see patients that are grossly ill and generally treat the symptoms of the disease until the ailment resolves. Some illnesses, such as cancer, require surgery or worse yet radiation or chemotherapy. These are not individual cell specific therapies, but in most cases the physician treats the entire patient, thereby attempting to kill the cancer cells faster than the normal cells. The goal of nanomedicine is therefore to give individual cells the ability to treat themselves through molecular programming. This genetic software can then provide the effected cells with the information to build the hardware, i.e. ribozymes/DNA repair enzymes, necessary to maintain normal cellular function.

This dissertation describes the development the basic molecular software needed to prove the feasibility of the nanomedicine paradigm. The individual components needed for a nanomedicine based therapy are a targeted delivery system, pathological sensor, and finally a therapeutic response. These three components have been developed and shown to work *in vitro* within this dissertation. Although these technologies are at their earliest stage, these data represent the starting point for second generation nanomedicine tools. The overall purpose of this dissertation was to conceive, build, and test the feasibility of each individual component of this system. These goals were reached and the tools developed herein will continue to be refined and integrated in a working nanomedicine based system.

REFERENCES

Allander, T., X. Forns, S. U. Emerson, R. H. Purcell, and J. Bukh. 2000. Hepatitis C virus envelope protein e2 binds to cd81 of tamarins. *Virology* 277, no. 2: 358-67.

Barrera, J. M., M. Bruguera, M. G. Ercilla, C. Gil, R. Celis, M. P. Gil, M. del Valle Onorato, J. Rodes, and A. Ordinas. 1995. Persistent hepatitis C viremia after acute self-limiting posttransfusion hepatitis C. *Hepatology* 21, no. 3: 639-44.

Bartenschlager, R. 2002. In vitro models for hepatitis C. *Virus Res* 82, no. 1-2: 25-32.

Bartenschlager, R., A. Kaul, and S. Sparacio. 2003. Replication of the hepatitis C virus in cell culture. *Antiviral Res* 60, no. 2: 91-102.

Beard, M. R., L. Cohen, S. M. Lemon, and A. Martin. 2001. Characterization of recombinant hepatitis a virus genomes containing exogenous sequences at the 2a/2b junction. *J Virol* 75, no. 3: 1414-26.

Benns, J. M. and S. W. Kim. 2000. Tailoring new gene delivery designs for specific targets. *J Drug Target* 8, no. 1: 1-12.

Bizollon, T., C. Ducerf, C. Trepo, and D. Mutimer. 1999. Hepatitis C virus recurrence after liver transplantation. *Gut* 44, no. 4: 575-8.

Blanchard, K. L., J. Fandrey, M. A. Goldberg, and H. F. Bunn. 1993. Regulation of the erythropoietin gene. *Stem Cells* 11 Suppl 1: 1-7.

Blasberg, R. G. 2003. Molecular imaging and cancer. *Mol Cancer Ther* 2, no. 3: 335-43.

Bonnemain, B. 1998. Superparamagnetic agents in magnetic resonance imaging: Physicochemical characteristics and clinical applications. A review. *J Drug Target* 6, no. 3: 167-74.

Boyle, M. D., W. A. Wallner, G. O. von Mering, K. J. Reis, and M. J. Lawman. 1985. Interaction of bacterial fc receptors with goat immunoglobulins. *Mol Immunol* 22, no. 9: 1115-21.

Brenner, M. K. 1995. Human somatic gene therapy: Progress and problems. *J Intern Med* 237, no. 3: 229-39.

Cavazzana-Calvo, M., S. Hacein-Bey, G. de Saint Basile, F. Gross, E. Yvon, P. Nusbaum, F. Selz, C. Hue, S. Certain, J. L. Casanova, P. Bousso, F. L. Deist, and A. Fischer. 2000. Gene therapy of human severe combined immunodeficiency (scid)-x1 disease. *Science* 288, no. 5466: 669-72.

Chan, W. C., D. J. Maxwell, X. Gao, R. E. Bailey, M. Han, and S. Nie. 2002. Luminescent quantum dots for multiplexed biological detection and imaging. *Curr Opin Biotechnol* 13, no. 1: 40-6.

Check, E. 2002. A tragic setback. *Nature* 420, no. 6912: 116-8.

Chowdhury, N. R., C. H. Wu, G. Y. Wu, P. C. Yemeni, V. R. Bommineni, and J. R. Chowdhury. 1993. Fate of DNA targeted to the liver by

asialoglycoprotein receptor-mediated endocytosis in vivo. Prolonged persistence in cytoplasmic vesicles after partial hepatectomy. *J Biol Chem* 268, no. 15: 11265-71.

Cornberg, M., H. Wedemeyer, and M. P. Manns. 2002. Treatment of chronic hepatitis C with pegylated interferon and ribavirin. *Curr Gastroenterol Rep* 4, no. 1: 23-30.

Cripe, L. D. and S. Hinton. 2000. Acute myeloid leukemia in adults. *Curr Treat Options Oncol* 1, no. 1: 9-17.

Cristiano, R. J., L. C. Smith, M. A. Kay, B. R. Brinkley, and S. L. Woo. 1993. Hepatic gene therapy: Efficient gene delivery and expression in primary hepatocytes utilizing a conjugated adenovirus-DNA complex. *Proc Natl Acad Sci U S A* 90, no. 24: 11548-52.

Cristiano, R. J., L. C. Smith, and S. L. Woo. 1993. Hepatic gene therapy: Adenovirus enhancement of receptor-mediated gene delivery and expression in primary hepatocytes. *Proc Natl Acad Sci U S A* 90, no. 6: 2122-6.

Cucinotta, F. A., W. Schimmerling, J. W. Wilson, L. E. Peterson, G. D. Badhwar, P. B. Saganti, and J. F. Dicello. 2001. Space radiation cancer risks and uncertainties for mars missions. *Radiat Res* 156, no. 5 Pt 2: 682-8.

Dautry-Varsat, A. 1986. Receptor-mediated endocytosis: The intracellular journey of transferrin and its receptor. *Biochimie* 68, no. 3: 375-81.

De Smedt, S. C., J. Demeester, and W. E. Hennink. 2000. Cationic polymer based gene delivery systems. *Pharm Res* 17, no. 2: 113-26.

Douglas, S. J., S. S. Davis, and L. Illum. 1987. Nanoparticles in drug delivery. *Crit Rev Ther Drug Carrier Syst* 3, no. 3: 233-61.

Dubertret, B., P. Skourides, D. J. Norris, V. Noireaux, A. H. Brivanlou, and A. Libchaber. 2002. In vivo imaging of quantum dots encapsulated in phospholipid micelles. *Science* 298, no. 5599: 1759-62.

Emery, D. W. and G. Stamatoyannopoulos. 1999. Stem cell gene therapy for the beta-chain hemoglobinopathies. Problems and progress. *Ann N Y Acad Sci* 872: 94-107; discussion 107-8.

Feray, C., L. Caccamo, G. J. Alexander, B. Ducot, J. Gugenheim, T. Casanovas, C. Loinaz, M. Gigou, P. Burra, L. Barkholt, R. Esteban, T. Bizollon, J. Lerut, A. Minello-Franza, P. H. Bernard, K. Nachbaur, D. Botta-Fridlund, H. Bismuth, S. W. Schalm, and D. Samuel. 1999. European collaborative study on factors influencing outcome after liver transplantation for hepatitis C. European concerted action on viral hepatitis (eurohep) group. *Gastroenterology* 117, no. 3: 619-25.

Fischer, A. 2001. Gene therapy: Some results, many problems to solve. *Cell Mol Biol (Noisy-le-grand)* 47, no. 8: 1269-75.

Flint, M., J. M. Thomas, C. M. Maidens, C. Shotton, S. Levy, W. S. Barclay, and J. A. McKeating. 1999. Functional analysis of cell surface-expressed hepatitis C virus e2 glycoprotein. *J Virol* 73, no. 8: 6782-90.

Flotte, T. R. 1993. Prospects for virus-based gene therapy for cystic fibrosis. *J Bioenerg Biomembr* 25, no. 1: 37-42.

Flotte, T. R. and B. J. Carter. 1995. Adeno-associated virus vectors for gene therapy. *Gene Ther* 2, no. 6: 357-62.

Forns, X., T. Allander, P. Rohwer-Nutter, and J. Bukh. 2000. Characterization of modified hepatitis C virus e2 proteins expressed on the cell surface. *Virology* 274, no. 1: 75-85.

Fraser, N. W. 1994. Herpes simplex virus-1 latency and its implications for gene therapy of the nervous system. *Gene Ther* 1 Suppl 1: S51.

Geller, A. I., K. Keyomarsi, J. Bryan, and A. B. Pardee. 1990. An efficient deletion mutant packaging system for defective herpes simplex virus vectors: Potential applications to human gene therapy and neuronal physiology. *Proc Natl Acad Sci U S A* 87, no. 22: 8950-4.

Ghobrial, R. M., D. G. Farmer, A. Baquerizo, S. Colquhoun, H. R. Rosen, H. Yersiz, J. F. Markmann, K. E. Drazan, C. Holt, D. Imagawa, L. I. Goldstein, P. Martin, and R. W. Busuttil. 1999. Orthotopic liver transplantation for hepatitis C: Outcome, effect of immunosuppression, and causes of retransplantation during an 8-year single-center experience. *Ann Surg* 229, no. 6: 824-31; discussion 831-3.

Ghosh, S. S., M. Takahashi, N. R. Thummala, B. Parashar, N. R. Chowdhury, and J. R. Chowdhury. 2000. Liver-directed gene therapy: Promises, problems and prospects at the turn of the century. *J Hepatol* 32, no. 1 Suppl: 238-52.

Gutfreund, K. S. and V. G. Bain. 2000. Chronic viral hepatitis C: Management update. *Cmaj* 162, no. 6: 827-33.

Hacein-Bey-Abina, S., C. von Kalle, M. Schmidt, F. Le Deist, N. Wulffraat, E. McIntyre, I. Radford, J. L. Villeval, C. C. Fraser, M. Cavazzana-Calvo, and A. Fischer. 2003. A serious adverse event after successful gene therapy for x-linked severe combined immunodeficiency. *N Engl J Med* 348, no. 3: 255-6.

Heng, G., L. Yongjun, Z. Yuehong, L. Changwei, Y. Jing, S. Cunxian, W. Pengyan, Z. Sanmei, W. Zongli, and S. Mingpeng. 2002. Nanoparticle as a new gene transferring vector in specific expression gene. *Chin Med Sci J* 17, no. 4: 220-4.

Herrmann, F. 1995. Cancer gene therapy: Principles, problems, and perspectives. *J Mol Med* 73, no. 4: 157-63.

Hino, K., S. Sainokami, K. Shimoda, H. Niwa, and S. Iino. 1994. Clinical course of acute hepatitis C and changes in hcv markers. *Dig Dis Sci* 39, no. 1: 19-27.

Ikeda, M., M. Yi, K. Li, and S. M. Lemon. 2002. Selectable subgenomic and genome-length dicistronic rnas derived from an infectious molecular clone of the hcv-n strain of hepatitis C virus replicate efficiently in cultured huh7 cells. *J Virol* 76, no. 6: 2997-3006.

Jaiswal, J. K., H. Mattoussi, J. M. Mauro, and S. M. Simon. 2003. Long-term multiple color imaging of live cells using quantum dot bioconjugates. *Nat Biotechnol* 21, no. 1: 47-51.

Kaiser, J. 2003. Gene therapy. Seeking the cause of induced leukemias in x-scid trial. *Science* 299, no. 5606: 495.

Kay, M. A., Q. Li, T. J. Liu, F. Leland, C. Toman, M. Finegold, and S. L. Woo. 1992. Hepatic gene therapy: Persistent expression of human alpha 1-antitrypsin in mice after direct gene delivery in vivo. *Hum Gene Ther* 3, no. 6: 641-7.

Kennedy, P. G., and I. Steiner. 1993. The use of herpes simplex virus vectors for gene therapy in neurological diseases. *Q J Med* 86, no. 11: 697-702.

Kotin, R. M. 1994. Prospects for the use of adeno-associated virus as a vector for human gene therapy. *Hum Gene Ther* 5, no. 7: 793-801.

Kuwabara, T., M. Warashina, S. Koseki, M. Sano, J. Ohkawa, K. Nakayama, and K. Taira. 2001. Significantly higher activity of a cytoplasmic hammerhead ribozyme than a corresponding nuclear counterpart: Engineered trnas with an extended 3' end can be exported efficiently and specifically to the cytoplasm in mammalian cells. *Nucleic Acids Res* 29, no. 13: 2780-8.

Latchman, D. S. 1994. Herpes simplex virus vectors for gene therapy. *Mol Biotechnol* 2, no. 2: 179-95.

Leary, J. F. 1994. Strategies for rare cell detection and isolation. *Methods Cell Biol* 42 Pt B: 331-58.

Lee, J. C., Y. F. Shih, S. P. Hsu, T. Y. Chang, L. H. Chen, and J. T. Hsu. 2003. Development of a cell-based assay for monitoring specific hepatitis C virus ns3/4a protease activity in mammalian cells. *Anal Biochem* 316, no. 2: 162-70.

Lee, P. A., L. M. Blatt, K. S. Blanchard, K. S. Bouhana, P. A. Pavco, L. Bellon, and J. A. Sandberg. 2000. Pharmacokinetics and tissue distribution of a ribozyme directed against hepatitis C virus rna following subcutaneous or intravenous administration in mice. *Hepatology* 32, no. 3: 640-6.

Lindsten, K., T. Uhlikova, J. Konvalinka, M. G. Masucci, and N. P. Dantuma. 2001. Cell-based fluorescence assay for human immunodeficiency virus type 1 protease activity. *Antimicrob Agents Chemother* 45, no. 9: 2616-22.

Lohmann, V., F. Korner, J. Koch, U. Herian, L. Theilmann, and R. Bartenschlager. 1999. Replication of subgenomic hepatitis C virus rnas in a hepatoma cell line. *Science* 285, no. 5424: 110-3.

Lvov, Y., A. A. Antipov, A. Mamedov, H. Mohwald, and G. B. Sukhorukov.
2001. Urease encapsulation in nanoorganized microshells. *Nano Letters* 1, no. 3: 125-128.

Lvov, Y. and F. Caruso. 2001. Biocolloids with ordered urease multilayer shells as enzymatic reactors. *Anal Chem* 73, no. 17: 4212-7.

Mamedov, A. A., A. Belov, M. Giersig, N. N. Mamedova, and N. A. Kotov. 2001. Nanorainbows: Graded semiconductor films from quantum dots. *J Am Chem Soc* 123, no. 31: 7738-9.

Mao, H. X., S. Y. Lan, Y. W. Hu, L. Xiang, and Z. H. Yuan. 2003. Establishment of a cell-based assay system for hepatitis C virus serine protease and its primary applications. *World J Gastroenterol* 9, no. 11: 2474-9.

Marshall, E. 1999. Gene therapy death prompts review of adenovirus vector. *Science* 286, no. 5448: 2244-5.

Martin, S. J. and D. R. Green. 1995. Protease activation during apoptosis: Death by a thousand cuts? *Cell* 82, no. 3: 349-52.

Maruyama, A., T. Ishihara, J. S. Kim, S. W. Kim, and T. Akaike. 1997. Nanoparticle DNA carrier with poly(l-lysine) grafted polysaccharide copolymer and poly(d,l-lactic acid). *Bioconjug Chem* 8, no. 5: 735-42.

McKenzie, R. C., J. R. Arthur, and G. J. Beckett. 2002. Selenium and the regulation of cell signaling, growth, and survival: Molecular and mechanistic aspects. *Antioxid Redox Signal* 4, no. 2: 339-51.

Mitchell, D. G. 1997. Mr imaging contrast agents--what's in a name? *J Magn Reson Imaging* 7, no. 1: 1-4.

Miyagishi, M., T. Kuwabara, and K. Taira. 2001. Transport of intracellularly active ribozymes to the cytoplasm. *Cancer Chemother Pharmacol* 48 Suppl 1: S96-101.

Mizutani, Y., Y. Okada, O. Yoshida, M. Fukumoto, and B. Bonavida. 1997. Doxorubicin sensitizes human bladder carcinoma cells to fas-mediated cytotoxicity. *Cancer* 79, no. 6: 1180-9.

Morgan, E. H. and E. Baker. 1988. Role of transferrin receptors and endocytosis in iron uptake by hepatic and erythroid cells. *Ann N Y Acad Sci* 526: 65-82.

Nakabayashi, H., K. Taketa, T. Yamane, M. Miyazaki, K. Miyano, and J. Sato. 1984. Phenotypical stability of a human hepatoma cell line, huh-7, in long-term culture with chemically defined medium. *Gann* 75, no. 2: 151-8.

Neutra, M. R., A. Ciechanover, L. S. Owen, and H. F. Lodish. 1985. Intracellular transport of transferrin- and asialoorosomucoid-colloidal gold conjugates to lysosomes after receptor-mediated endocytosis. *J Histochem Cytochem* 33, no. 11: 1134-44.

Nishikawa, M., S. Takemura, F. Yamashita, Y. Takakura, D. K. Meijer, M. Hashida, and P. J. Swart. 2000. Pharmacokinetics and in vivo gene

transfer of plasmid DNA complexed with mannosylated poly(l-lysine) in mice. *J Drug Target* 8, no. 1: 29-38.

Ohnishi, T., A. Takahashi, and K. Ohnishi. 2001. Biological effects of space radiation. *Biol Sci Space* 15 Suppl: S203-10.

Paunesku, T., T. Rajh, G. Wiederrecht, J. Maser, S. Vogt, N. Stojicevic, M. Protic, B. Lai, J. Oryhon, M. Thurnauer, and G. Woloschak. 2003. Biology of tio2-oligonucleotide nanocomposites. *Nat Mater* 2, no. 5: 343-6.

Petersein, J., S. Saini, and R. Weissleder. 1996. Liver. Ii: Iron oxide-based reticuloendothelial contrast agents for mr imaging. Clinical review. *Magn Reson Imaging Clin N Am* 4, no. 1: 53-60.

Pfeifer, A. and I. M. Verma. 2001. Gene therapy: Promises and problems. *Annu Rev Genomics Hum Genet* 2: 177-211.

Pietschmann, T. and R. Bartenschlager. 2001. The hepatitis C virus replicon system and its application to molecular studies. *Curr Opin Drug Discov Devel* 4, no. 5: 657-64.

Pileri, P., Y. Uematsu, S. Campagnoli, G. Galli, F. Falugi, R. Petracca, A. J. Weiner, M. Houghton, D. Rosa, G. Grandi, and S. Abrignani. 1998. Binding of hepatitis C virus to cd81. *Science* 282, no. 5390: 938-41.

Poynard, T., V. Leroy, M. Cohard, T. Thevenot, P. Mathurin, P. Opolon, and J. P. Zarski. 1996. Meta-analysis of interferon randomized trials in the treatment of viral hepatitis C: Effects of dose and duration. *Hepatology* 24, no. 4: 778-89.

Prabha, S., W. Z. Zhou, J. Panyam, and V. Labhasetwar. 2002. Size-dependency of nanoparticle-mediated gene transfection: Studies with fractionated nanoparticles. *Int J Pharm* 244, no. 1-2: 105-15.

Qian, Z. M., H. Li, H. Sun, and K. Ho. 2002. Targeted drug delivery via the transferrin receptor-mediated endocytosis pathway. *Pharmacol Rev* 54, no. 4: 561-87.

Reynolds, A. R., S. Moein Moghimi, and K. Hodivala-Dilke. 2003. Nanoparticle-mediated gene delivery to tumour neovasculature. *Trends Mol Med* 9, no. 1: 2-4.

Rice, C. M. and C. H. Hagedorn, eds. 2000. *The hepatitis C viruses.* Current topics in microbiology and immunology ; 242. Berlin ; London: Springer.

Rijnbrand, R., P. J. Bredenbeek, P. C. Haasnoot, J. S. Kieft, W. J. Spaan, and S. M. Lemon. 2001. The influence of downstream protein-coding sequence on internal ribosome entry on hepatitis C virus and other flavivirus rnas. *Rna* 7, no. 4: 585-97.

Rogach, A. L., D. Nagesha, J. W. Ostrander, M. Giersig, and N. A. Kotov. 2000. "raisin bun"-type composite spheres of silica and semiconductor nanocrystals. *Chem Mater* 12: 2676-2685.

Romano, G., P. P. Claudio, H. E. Kaiser, and A. Giordano. 1998. Recent advances, prospects and problems in designing new strategies for oligonucleotide and gene delivery in therapy. *In Vivo* 12, no. 1: 59-67.

Sandberg, J. A., C. D. Sproul, K. S. Blanchard, L. Bellon, D. Sweedler, J. A. Powell, F. A. Caputo, D. J. Kornbrust, V. P. Parker, T. J. Parry, and L. M. Blatt. 2000. Acute toxicology and pharmacokinetic assessment of a ribozyme (angiozyme) targeting vascular endothelial growth factor receptor mrna in the cynomolgus monkey. *Antisense Nucleic Acid Drug Dev* 10, no. 3: 153-62.

Scherer, F., M. Anton, U. Schillinger, J. Henke, C. Bergemann, A. Kruger, B. Gansbacher, and C. Plank. 2002. Magnetofection: Enhancing and targeting gene delivery by magnetic force in vitro and in vivo. *Gene Ther* 9, no. 2: 102-9.

Schwartz, A. L. 1984. The hepatic asialoglycoprotein receptor. *CRC Crit Rev Biochem* 16, no. 3: 207-33.

Sjoquist, J., B. Meloun, and H. Hjelm. 1972. Protein a isolated from staphylococcus aureus after digestion with lysostaphin. *Eur J Biochem* 29, no. 3: 572-8.

Stewart, M., R. P. Baker, R. Bayliss, L. Clayton, R. P. Grant, T. Littlewood, and Y. Matsuura. 2001. Molecular mechanism of translocation through nuclear pore complexes during nuclear protein import. *FEBS Lett* 498, no. 2-3: 145-9.

Stockert, R. J. 1995. The asialoglycoprotein receptor: Relationships between structure, function, and expression. *Physiol Rev* 75, no. 3: 591-609.

Strauss, M. 1994. Liver-directed gene therapy: Prospects and problems. *Gene Ther* 1, no. 3: 156-64.

Sullenger, B. A. and E. Gilboa. 2002. Emerging clinical applications of rna. *Nature* 418, no. 6894: 252-8.

Teradaira, R., V. Kolb-Bachofen, J. Schlepper-Schafer, and H. Kolb. 1983. Galactose-particle receptor on liver macrophages. Quantitation of particle uptake. *Biochim Biophys Acta* 759, no. 3: 306-10.

Thomas, C. E., A. Ehrhardt, and M. A. Kay. 2003. Progress and problems with the use of viral vectors for gene therapy. *Nat Rev Genet* 4, no. 5: 346-58.

Thurnher, M., E. Wagner, H. Clausen, K. Mechtler, S. Rusconi, A. Dinter, M. L. Birnstiel, E. G. Berger, and M. Cotten. 1994. Carbohydrate receptor-mediated gene transfer to human t leukaemic cells. *Glycobiology* 4, no. 4: 429-35.

Tiefenauer, L. X., G. Kuhne, and R. Y. Andres. 1993. Antibody-magnetite nanoparticles: In vitro characterization of a potential tumor-specific contrast agent for magnetic resonance imaging. *Bioconjug Chem* 4, no. 5: 347-52.

Uzan, G., M. H. Prandini, and R. Berthier. 1995. Regulation of gene transcription during the differentiation of megakaryocytes. *Thromb Haemost* 74, no. 1: 210-2.

Vinceti, M., E. T. Wei, C. Malagoli, M. Bergomi, and G. Vivoli. 2001. Adverse health effects of selenium in humans. *Rev Environ Health* 16, no. 4: 233-51.

Violante, M. R. 1990. Potential of microparticles for diagnostic tracer imaging. *Acta Radiol Suppl* 374: 153-6.

Vrolijk, J. M., A. Kaul, B. E. Hansen, V. Lohmann, B. L. Haagmans, S. W. Schalm, and R. Bartenschlager. 2003. A replicon-based bioassay for the measurement of interferons in patients with chronic hepatitis C. *J Virol Methods* 110, no. 2: 201-9.

Wagner, E., K. Zatloukal, M. Cotten, H. Kirlappos, K. Mechtler, D. T. Curiel, and M. L. Birnstiel. 1992. Coupling of adenovirus to transferrin-polylysine/DNA complexes greatly enhances receptor-mediated gene delivery and expression of transfected genes. *Proc Natl Acad Sci U S A* 89, no. 13: 6099-103.

Wang, Y. X., S. M. Hussain, and G. P. Krestin. 2001. Superparamagnetic iron oxide contrast agents: Physicochemical characteristics and applications in mr imaging. *Eur Radiol* 11, no. 11: 2319-31.

Weigel, P. H. 1993. Endocytosis and function of the hepatic asialoglycoprotein receptor. *Subcell Biochem* 19: 125-61.

Wenk, J., P. Brenneisen, C. Meewes, M. Wlaschek, T. Peters, R. Blaudschun, W. Ma, L. Kuhr, L. Schneider, and K. Scharffetter-Kochanek. 2001. Uv-induced oxidative stress and photoaging. *Curr Probl Dermatol* 29: 83-94.

Wu, G. Y. and C. H. Wu. 1991. Delivery systems for gene therapy. *Biotherapy* 3, no. 1: 87-95.

Wu, X., H. Liu, J. Liu, K. N. Haley, J. A. Treadway, J. P. Larson, N. Ge, F. Peale, and M. P. Bruchez. 2003. Immunofluorescent labeling of cancer marker her2 and other cellular targets with semiconductor quantum dots. *Nat Biotechnol* 21, no. 1: 41-6.

Wunschmann, S., J. D. Medh, D. Klinzmann, W. N. Schmidt, and J. T. Stapleton. 2000. Characterization of hepatitis C virus (hcv) and hcv e2 interactions with cd81 and the low-density lipoprotein receptor. *J Virol* 74, no. 21: 10055-62.

Zauner, W., N. A. Farrow, and A. M. Haines. 2001. In vitro uptake of polystyrene microspheres: Effect of particle size, cell line and cell density. *J Control Release* 71, no. 1: 39-51.

Zhang, R., J. Durkin, W. T. Windsor, C. McNemar, L. Ramanathan, and H. V. Le. 1997. Probing the substrate specificity of hepatitis C virus ns3 serine protease by using synthetic peptides. *J Virol* 71, no. 8: 6208-13.

Zhu, M., W. G. Chapman, M. J. Oberley, W. W. Wasserman, and W. E. Fahl. 2001. Polymorphic electrophile response elements in the mouse glutathione s-transferase gsta1 gene that confer increased induction. *Cancer Lett* 164, no. 2: 113-8.

Zhu, M. and W. E. Fahl. 2000. Development of a green fluorescent protein microplate assay for the screening of chemopreventive agents. *Anal Biochem* 287, no. 2: 210-7.

Zhu, M., and Fahl, W. E. 2001. Functional characterization of transcription regulators that interact with the electrophile response element. *Biochem Biophys Res Commun* 289, no. 1: 212-9.

2. **TITLE**: Nanoparticles, Molecular Biosensors, and Multispectral Confocal Microscopy

AUTHORS: Tarl W. Prow, Nicholas A. Kotov, Yuri M. Lvov, Rene Rijnbrand, James F. Leary.

Nanoparticles, Molecular Biosensors, and Multispectral Confocal Microscopy

Tarl W. Prow, Department of Pathology, University of Texas Medical Branch, Galveston, Texas, USA.

Nicholas A. Kotov, Department of Chemical Engineering, University of Michigan, Michigan, USA

Yuri M. Lvov, Institute for Micromanufacturing, Louisiana Tech University, Ruston, Louisiana, USA

Rene Rijnbrand, Department of Microbiology and Immunology, University of Texas Medical Branch, Galveston, Texas, USA.

James F. Leary, Department of Internal Medicine, University of Texas Medical Branch, Galveston, Texas, USA.

Summary

    Complex, multilayered nanoparticles hold great promise for more sophisticated drug/gene delivery systems to single cells. Outermost layers can include cell targeting and cell-entry facilitating molecules. The next layer can include intracellular targeting molecules for precise delivery of the nanoparticle complex inside the cell of interest. Molecular biosensors can be used to confirm the presence of expected molecules (for example signs of infection, ROS activation in radiation damage, etc.) prior to delivery of counter-measure molecules such as drugs or gene therapy. They can also be used as a feedback control mechanism to control the proper amount of drug/gene delivery for each cell. Importantly, the full nanoparticle system can be used to prevent any cells from encountering the drug unless that cell is specifically targeted. Thus, if a cell is initially non-specifically targeted, a secondary check for other molecular targets which must also be present inside the target cell of interest can be used to catch initial targeting mistakes and prevent subsequent delivery of treatment molecules to the wrong cells. The precise intracellular location of nanoparticles within specific regions of a cell can be confirmed by 3D multispectral confocal microscopy. These single cell molecular morphology measurements can be extended from individual cells, to other cells in a tissue in tissue monolayers or tissue sections.

Introduction

    Existing gene delivery systems have a variety of limitations (De Smedt, Demeester et al. 2000). These systems are designed to eliminate an infection by transferring a therapeutic gene to host cells, however, they have been are largely unsuccessful since only low doses of genetic material can reach the specific cell types that are infected. Increased side effects also include the treatment of non-infected cells with high levels of genes and the host cells reacting to the carrier molecules associated with their delivery. To date, the available gene delivery systems reported have been those that contain retroviral vectors, are liposome based, or are systems in which

naked DNA, RNA and modified RNA have been injected directly into the blood stream, all of which produce many undesirable side effects which can compromise the treatment of patients. Retroviral vectors have potential dangerous side effects which include incorporation of the virus into the hosts immune system and hence, have been less successful than originally hoped (De Smedt, Demeester et al. 2000). Liposome based gene transfer has relatively low transfection rates, are difficult to produce in a specific size range, can be unstable in the blood stream, and are difficult to target to specific tissues (De Smedt, Demeester et al. 2000). Injection of naked DNA, RNA, and modified RNA directly into the blood stream leads to clearance of the injected nucleic acids with minimal beneficial outcome (Sandberg, Sproul et al. 2000). As such, there is currently a need for a gene delivery system which has minimal side effects but high affectivity and efficiency. One such system could be that of the self-assembled nanoparticles coated with targeting biomolecules (Lvov and Caruso 2001).

Nanoparticle complexes, while still in their infancy as a new bionanotechnology, hold great promise for more sophisticated and targeted and controlled drug/gene delivery to specific cells. Merely delivering the drug/gene to a cell surface by conventional targeting does not insure that it is delivered to the site of required action within the cell. The nanosystems can contain intracellular targeted molecules that re-direct the nanomedical system to the correct intracellular location for specific molecular and biochemical actions. The interior of a cell is approximately a billion times larger than the volume of an individual nanoparticle. Prior studies using confocal microscopy can insure that the drug/gene is targeted to the correct location within single cells.

Molecular biosensors can confirm the correct targeting, sense the environment to provide an initial control of drug/gene delivery, and then shut off this delivery when the desired response inside a single cell is reached. These secondary checks for correct targeted and control of drug/gene delivery can be used to help minimize "bystander" effects now common as "side effects" in conventional drug administrations.

Two major biological models were chosen as vehicles for development during this project: 1) the Hepatitis C virus (HCV) infection of single cells, and 2) cellular radiation damage to single cells accumulated during long term/deep space missions by astronauts. In the case of the HCV infection model, one expression product of these constructs, the biosensor, is targeted to the same sub-cellular location as the HCV translation machinery and monitors for the presence of the HCV. Only when detected, would the expression of an anti-HCV gene product be triggered. For the DNA repair component of this project, the aim was to develop a gene therapy technique which would provide increased *in vivo* protection against radiation damage to the blood and bone marrow of astronauts who experience long term/deep space missions. The primary goal was to develop an *in vivo* intra-cellular DNA repair system for radiation damaged cells in astronauts before they progress to radiation induced leukemia. This system would therefore use a promoter based sensor which could detect the presence of reactive oxygen species (ROS). When ROS is present, the sensor would trigger the transcription of foreign DNA repair enzymes, which may be more efficient and effective than our innate DNA repair system.

The approaches described in this paper are advantageous for the following reasons: (1) these techniques have the ability to deliver genes with targeted particles that cannot replicate and are biodegradable; (2) the therapeutic gene generated can be silenced at any time by the addition of tetracycline; (3) the amount and duration of the gene therapy developed can be controlled without having to treat the individual with extremely high non -physiological doses of harmful drugs, as is currently being done with ribavirin/interferon therapies and chemotherapy for cancer; (4) the gene therapy products are only specifically expressed when the pathogen or radiation

damage is present in the cell; (5) the anti-HCV treatment is genuinely specific for HCV, thereby minimizing side effects.

Nanoparticles capable of delivering DNA payloads were developed from different core components. Biosensor platform technology was developed in a way that facilitates the rapid development of biosensors for other applications. *In vitro* experiments were designed to test the feasibility of a protease activated biosensor.

Materials and Methods:

Overview of Methods

This work is part of a general program for development of nanomedical systems for both diagnostics and therapeutics. Multilayered nanoparticle systems are usually, but not always, built on a nanoparticle core of polystyrene, silica, gold or other material. Drug or genes, molecular biosensors, and extracellular (as well as intracellular) targeting molecules can be added to the nanoparticles to construct a "nanomedical system".

Nanoparticles

The details of nanomaterials science are beyond the scope of this paper. But briefly, multilayered nanoparticle systems are usually, but not always, built on a nanoparticle core of polystyrene, silica, gold or other material. These nanoparticles are self-assembled atom-by-atom or molecular layer-by-layer (LBL). Additional layers can be added containing drugs or genes to deliver, molecular biosensors, and targeting molecules (including both extracellular and intracellular). Two types of nanoparticles were used in this work - nanocrystals and nanocapsules. Nanocrystals, self-assembled atom-by-atom and made of semiconductor materials such as CdTe from the laboratory of Dr. Kotov, were used to provide very small (7-10 nm diameter) nanoparticle delivery systems. They also have advantages in terms of brightness of fluorescence and absence of photobleaching during confocal microscopic analyses. Nanocapsules, typically self-assembled layer-by-layer using alternately charged polymers from the laboratory of Dr. Lvov, are typically much larger – on the order of 100 nm in diameter. These nanocapsules can be with or without solid cores and have a larger capacity for holding drugs or genes in their interior. The polymers can also be made from biodegradable polymers, some of which already have FDA approval for in-vivo human use. Layer by layer nanoparticles are formed around a core particle (Lvov, Antipov et al. 2001; Lvov and Caruso 2001). The layers are held together by the charge of the individual molecules, thus they are composed of alternating positive and negative charged species (Lvov, Antipov et al. 2001; Lvov and Caruso 2001). One benefit of using this type of particle is that once constructed, the particle core can be suspended and then made porous by changing solvents without damaging the layers. Incubating these porous nanocapsules with dissolved chemicals, one can load the nanocapsules through diffusion. Once loaded, the nanocapsules can be made non-porous by changing the solvent, thereby encapsulating the chemical of choice. Through this technique one can encapsulate fluorescent dyes and possibly other molecules (Lvov, Antipov et al. 2001; Lvov and Caruso 2001). Reporter genes may also be used as an interior layer because of the inherently negative charge of DNA. Additional layers of targeting molecules may then be added to help direct the particle to the correct cell types (Lvov, Antipov et al. 2001; Lvov and Caruso 2001).

Molecular biosensors

A number of molecular biosensor strategies were tried. For detection of reactive oxygen species in chemically or radiation-damaged cells, an ROS molecular biosensor constructed based on previously reported sequences (Zhu and Fahl, 2000). This paper briefly describes the characterization and utilization of promoter based biosensors for the detection of oxidative stress. The ROS biosensor is being used to identify and help induce the expression of DNA repair enzymes during times of increased oxidative stress. The antioxidant response element was coupled to an EGFP (enhanced green fluorescent protein) reporter. Zhu and Fahl first adapted this promoter for use as an *in vitro* assay for cells experiencing oxidative stress. The most sensitive of the constructs produced contained four repeats of the antioxidant response element followed by the EGFP gene and a poly A tail (Zhu and Fahl 2000). This construct was obtained from Dr. Zhu, Arizona Cancer Center, and put to use in our laboratory.

The protease activated biosensor is a triple fusion protein consisting of a transactivator, cleavage, and localization domains that should target the protein to the perinuclear region. The transactivator region functions to activate transcription when released from the localization signal that serves as an anchor near the endoplasmic reticulum. This anchored protein cannot initiate transcription because of the cytoplasmic localization, thus the transactivator is restrained such that it cannot move to the nucleus and bind to DNA. The cleavage domain separates the transactivator from the anchor region and is designed to the enzymatic activity of a specific protease. If the appropriate protease is present and cleaves the substrate, the transactivator released from the anchor domain end is then free to induce transcription within the nucleus.

Confocal microscopy

Multispectral confocal microscopy was used as a validation tool for both nanoparticle/ biosensor targeting and intracellular localization. Since multiple fluorescent colors were used to label biosensors, cell membranes, endoplasmic reticulum and nuclei, it became necessary to use a multispectral confocal microscope that could deal with the color optical overlaps. The method of spectral deconvolution was developed at JPL/Cal Tech (Pasadena, CA) and this patent (Bearman et al. 2002) was implemented in a new generation of multispectral confocal microscope (Model 510 META, Zeiss, Inc.). The basics of the method are shown in Figure 1. The "emission fingerprinting" algorithm (Bearman et al. 2002) works by fitting the spectral components over low or non-overlapping portions of the combined spectrum of a multicolor image. The components are appropriately weighted so that the combination of color components matches the overall spectrum from the image pixel-by-pixel in each image plane.
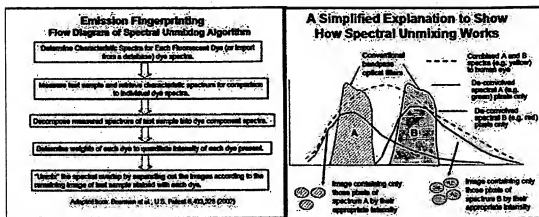
Figure 1: A schematic and illustration of the spectral unmixing algorithm implemented on the Zeiss 510 META multispectral confocal microscope used for this work.

Results:

Nanoparticle targeting:

Initial experiments were conducted to compare the behavior of conventional antibody staining and nanoparticle labeling. In Figure 2A, live human BJAB cells were labeled with FITC-labeled anti-CD95 IgG. In Figure 2B, live BJAB cells were labeled with unlabeled anti-CD95 IgG and then incubated with 500nm polystyrene-labeled nanoparticles containing a goat anti-mouse secondary antibody against IgG. The nanoparticle labeling system showed similar results to that of the conventional antibody labeling system.

To test the targeting accuracy and efficiency of the nanoparticle system, we first labeled non-targeted, CD95-negative, MOLT-4 cells with CMAC, a fluorescence tracking dye (Molecular Probes, Eugene, Oregon). A mixture of CD95 positive BJAB cells labeled with anti-CD95 antibody (non-fluorescent) and MOLT-4 cells was made. Green fluorescent nanoparticles (as described in Figure 1) were then added to the cell mixture. Figure 3A shows a 10X objective phase-fluorescence photomicrograph of the combined mixture of cells and nanoparticles. Figure 3B shows a 40X two color fluorescence only photomicrograph. While not all of the CMAC-negative BJAB cells were labeled at this ratio of nanoparticles and cells (Figure 3A), none of the CMAC-positive, CD95-negative MOLT-4 cells bound nanoparticles (Fig. 3B).

The MOLT4 cells were used as a negative control because they do not normally express CD95 on their surface whereas BJAB cells were used as a positive control because most, but not all, BJAB cells constitutively express CD95 on their surface. Only the BJAB (unstained) cells, that are CD95 positive, were bound to the green particles.

Biocompatibility of nanoparticles

While molecular membrane transport facilitating sequences were being developed, the biocompatibility of CdTe semiconductor material nanocrystals to living T24 human cells was

tested by direct microinjection of nanocrystals into living cells using a Narashige microinjection system mounted on to an inverted phase-fluorescence microscope (Nikon) as shown in Figure 4. Initial results showed considerable cytotoxicity in the absence of biocoatings being applied to the nanoparticle surface. This led to a search for appropriate biocoatings for the nanoparticles. Either galactosamine or Lipofectamin[e] reduced this cytotoxicity to controls.

Molecular Biosensor Design

The successful design and construction of a triple fusion protein molecular biosensor that detects its target on the basis of protease sensitivity to sequences of the target is shown in Figure 5. The overall biosensor construct must contain a subcellular domain localization sequence, a cleavable segment that is activated upon contact with the intracellular target sequences, and a gene which is then released to target to the nucleus to be produced under the action of promoter sequences. The data obtained by use of this construct is shown in Figure 6. Measurements were made of the intracellular localization of BS-1, BS-2, and BS-3 (three different sequences) targeted molecular biosensors in BT7H cells. Confocal images from BT7H cells transfected with BS-1 (Panel A), BS-2 (Panel B), or BS-3 (Panel C) were stained for biosensor (red) and the DNA counterstained with DAPI (blue). The results show successful targeting to the nucleus, to the endoplasmic reticulum, and to the plasma membrane.

Intracellular Localization of Molecular Biosensors

Three color multispectral confocal intracellular co-localization of molecular biosensors and NS3-specific flavivirus protein in Huh7 cells (Figure 6). Protease containing Huh7 cells were transfected with nothing (A), BS-2 (B and E), BS-3 (C and F), and pTet-Off (D). Panels B and C show what appears be inactivated BS proteins that seem to localize within the cytoplasm. Panels D, E, and F show cells with tTA, BS-2, or BS-3 throughout the entire cell, which indicates activated BS proteins. The cells shown in Panel D were transfected with only the transactivator portion of the BS protein and therefore serve as a positive control for the activated BS protein from either BS construct. Panels D, E, and F were found to have BS throughout the z axis, as opposed to Panels B and C that were found to have large regions without protease or BS proteins. Because previous experiments described the localization of the BS proteins to the nucleus, all cells were counterstained with a fluorescent phalloidin (actin stain, blue) to visualize the localization of the BS proteins (green) with respect to the entire cell. The NS3 protease was also stained and is shown in red.

In a second application area involving detection of oxidative stress and DNA damage cause by either chemical agents or radiation, a reactive oxygen species (ROS) biosensor was used. This promoter based biosensor (Fahl and Zhu, 2000) is composed of three elements: a series of response elements (EpRE), minimal thymidine kinase promoter (TK), and a reporter gene (GFP). Cells were transiently transfected at ~60% confluence with either ARE-GFP or TK-GFP. 24 hours later the cells were treated with tert-butylhydroquinone (tBHQ), an ROS inducing agent. The cells were examined every 12 hours post treatment. Weak GFP fluorescence was present at 48 hours after treatment, and stronger GFP fluorescence was observed after 60 hours and photographs were taken (Figure 8). A fraction of cells, expected at this concentration of tBHQ showed signs of oxidative stress.

Nanocrystals will likely be of great benefit to quantitative confocal microscopy because they do not photobleach over long periods of time as shown in Figure 9. Regions of the image were sampled over almost 10 minutes of time and the degree of photobleaching was quantitated. The nanocrystals actually become slightly brighter after initial excitation, and then remain fairly constant over a number of minutes. The degree of photobleaching obviously various with nanocrystal composition and methods of construction, but this is a general characteristic.

It is important to note that nanocrystals are actually smaller than many proteins, including Streptavidin (Figure 10). Uncoated CdTe nanocrystals were not only cytotoxic, but also failed to bind to, or be phagocytosed, by cells. Once they were bound by antibody, in this case anti-CD95, to receptors on the cell surface, the nanocrystals began to enter the cells over time. HIV tat protein greatly accelerated cell entry and targeted the nanocrystals to the nucleus. A six amino acid peptide of Arginine had a similar effect.

Once the behavior of targeted nanoparticles without any drug or gene delivery payload was explored, experiments were initiated to compare the efficiency of expression of plasmid transfected DNA sequences with those same sequences on nanoparticles. Figure 11 shows the delivery of two different plasmids with lipid coated nanoparticles. Human Huh-7 liver cells (Panels A. and B.) were transfected either with a 1:1 mixture of plasmids pEGFP-C1 and pdsRed2-C1 or exposed to 100nm layer-by-layer (LBL) assembled nanocapsules containing a single layer of DNA (1:1 mixture of pEGFP-C1 and pdsRed2-C1) (Panels C. and D.). Although the transfection efficiency was low, there were cells expressing both EGFP (green) and dsRed (red) protein. All cells were counterstained with DAPI (blue).

Discussion

The core particle, onto which the coats are layered, primarily determines the overall size of the object to be delivered into the cell. Cells are widely known to only allow particles within a particular size range, 30-200 nm, to pass the outer membrane (Zauner, Farrow et al. 2001). The nuclear membrane is even more tightly guarded, only allowing specific molecules to pass into the nuclear compartment (Stewart, Baker et al. 2001). Passing through these barriers is paramount for the success of nanomedicine. The size of the particle delivered is therefore critical for the success of nanoparticle mediated gene delivery.

Nanocrystals offer several unique advantages over traditional nanoparticles and lipid mediated gene delivery tools. The nanocrystals have spectral properties that are especially convenient for *in vitro* use (Chan, Maxwell et al. 2002; Dubertret, Skourides et al. 2002; Jaiswal, Mattoussi et al. 2003). These particles fluoresce very brightly and do not photobleach like traditional dyes or fluorescent proteins. These nanoparticles are also small enough (<6 nm) to enter the cell without endocytotic signals. Additionally, a multitude of biological moieties can be bioconjugated to the surface of these tiny crystals. Even with large, biologically active molecules conjugated to the surface of these particles, they remain under 20nm in diameter. With these characteristics in mind, streptavidin was bioconjugated to the surface of these particles to give this system the flexibility needed for development and testing. The streptavidin-biotin bridge gives the researcher the ability to bioconjugate single or even multiple targeting, internalization, and therapeutic molecules.

Size undoubtedly plays a role in the localization of these particles. Even with no cell entry or targeting molecules on board, the nanocrystals readily gain entry into the cellular milieu. In the end analysis, these particles distribute throughout the cell for multiple reasons that would be very difficult to define. Because of their small size, optical properties, and structural flexibility, one can conceive of using nanocrystals as research based gene delivery agents.

To utilize semiconductor based nanoparticles as gene delivery agents could be beneficial for *in vitro* use. The spectral characteristics of these particles would facilitate the development of targeting, sub-targeting, and cell entry strategies. Toxicity of the nanocrystals is a major concern because the core of these particles is composed of toxic elements. Throughout these experiments the nanocrystals have been shown to cause problems with membrane permeability, as demonstrated with the trypan blue dye exclusion assay. One reason for this may be the poisoning of the transporter for trypan blue export. The cells do not appear to undergo necrosis or apoptosis. In fact, the cells appear to tolerate the nanocrystals quite well, allowing for multi-day studies. One concern brought to light by these observations was that incompletely coated nanocrystals may slowly release the toxic core elements into the cells/media. This can be alleviated by using a different core particle that allows for purification and/or does not contain a toxic core particle.
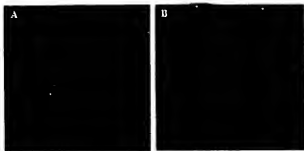
Figure 2: Nanoparticle targeting of CD95 positive cells. Live BJAB cells were labeled with anti-CD95 FITC (Panel A). BJAB cells labeled with anti-CD95 with no FITC and then exposed to FITC labeled polystyrene nanoparticles coated with secondary antibodies specific for the Fc portion of anti-human CD95antibodies (Panel B). Nuclei were counterstained with Hoechst 33342.

Figure 3: Nanoparticles were used to target CD95 positive cells in a 1:1 cell mixture of these cells and CD95 negative MOLT4 cells which were stained blue with a cell tracking dye (CMAC, Molecular Probes, Inc., Eugene, Oregon). As shown in both panels, none of the CD95 negative blue MOLT4 cells were targeted by the green particles. Only the BJAB (unstained) cells, that are CD95 positive, were bound to the green particles.
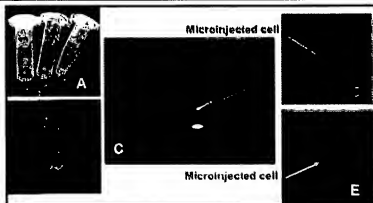
Figure 4: (A) CdTe nanocrystals in plastic tubes under room light, (B) the same nanocrystals under UV light. Tube contents (from left to right): Dry CdTe nanocrystals coated with BSA/Avidin, CdTe nanocrystals coated with BSA/Avidin in PBS (pH=7.4), SAA but diluted 1:10 in PBS. (C) CdTe nanocrystals loaded into micropipette prior to microinjection (D) CdTe nanocrystals coated with BSA/Avidin in PBS being microinjected into light field of T-24 cells (light field), (E) fluorescence image of T-24 cell microinjected with CdTe nanocrystals.
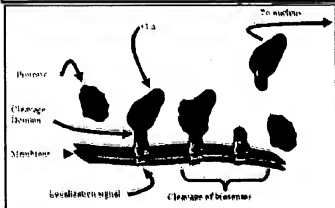
Figure 5: Overview of the protease biosensor. The biosensor protein is a triple fusion protein containing a tetracycline inactivated transactivator (tTA), a protease specific cleavage domain, and a localization signal. The activated protease cleaves the cleavage domain, releasing the tTA. The tTA then localizes to the nucleus and activates transcription of a predetermined gene.
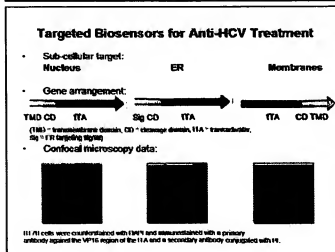
Figure 6: Intracellular localization of BS-1, BS-2, and BS-3 in BT7H cells. Confocal images from BT7H cells transfected with BS-1 (Panel A), BS-2 (Panel B), or BS-3 (Panel C) were stained for biosensor (red) and the DNA counterstained with DAPI (blue).
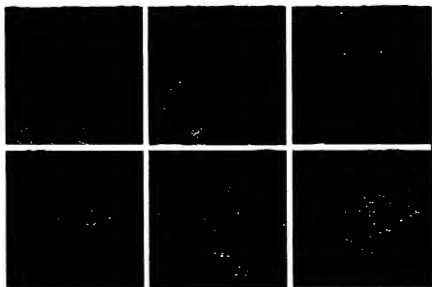
Figure 7: Three color multi-spectral confocal intracellular colocalization of molecular biosensors and NS3-specific flavivirus protein in Huh7 cells. Protease containing Huh7 cells were transfected with nothing (A), BS-2 (B and E), BS-3 (C and F), and pTet-Off (D). Panels B and C show what appears be inactivated BS proteins that seem to localize within the cytoplasm. Panels D, E, and F show cells with tTA, BS-2, or BS-3 throughout the entire cell, which indicates activated BS proteins.

ROS Activated Biosensor in Living Human Cells

Time (h):	0	24	60
Treatment:	Cells transfected with plasmid	Cells treated with 100mM tBHQ	Fluorescence photographed

ARE-GFP: (ROS Sensor) TK-GFP: (No Sensor)
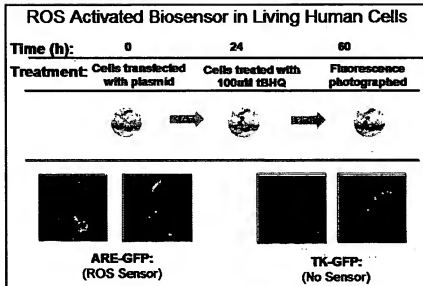
Figure 8: Reactive oxygen species biosensor. This promoter based biosensor (Fahl and Zhu, 2000) is composed of three elements: a series of response elements (EpRE), minimal thymidine kinase promoter (TK), and a reporter gene (GFP).
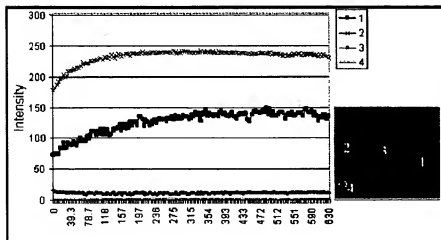
Figure 9: Nanocrystal photobleaching curves. Regions of the image were sampled over almost 10 minutes of time and the degree of photobleaching was quantitated. The nanocrystals actually become slightly brighter after initial excitation, and then remain fairly constant over a number of minutes.

Figure 10: Nanocrystal coated with nothing ("naked"), anti-CD95, HIV tat fragment, or a 6 x Arginine peptide were incubated with live cells and imaged by multispectral confocal microscopy. Hoechst 33342, an AT base pair specific dye that enters live cells, was added as a counterstain to delineate the nuclear boundary. These are composite images of fluorescence and Nomarski. Streptavidin coated nanocrystals were imaged by transmission microscopy (courtesy of Dr. Popov at UTMB).
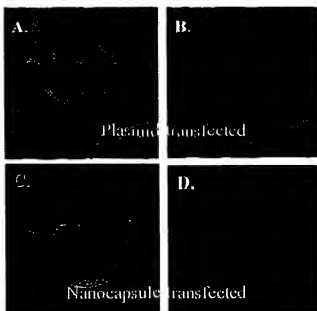
Figure 11: Delivery of 2 different plasmids with lipid coated LBL. Huh-7 cells (Panels A. and B.) were transfected with a 1:1 mixture of pEGFP-C1 and pdsRed2-C1 or exposed to ~100nm layer-by-layer (LB) assembled nanocapsules containing a single layer of DNA (1:1 mixture of pEGFP-C1 and pdsRed2-C1) (Panels C. and D.). Although the transfection efficiency was low, there were cells expressing both EGFP (green) and dsRed (red) protein. All cells were counterstained with DAPI (blue).

Acknowledgements

References

Bearman, G.H., Frasier, S.E., Lanford, R.D. (2002) System and method for monitoring cellular activity. U.S. Patent 6,403,328.

Chan, W. C., D. J. Maxwell, et al. (2002) Luminescent quantum dots for multiplexed biological detection and imaging. *Curr Opin Biotechnol* 13(1): 40-6.

De Smedt, S. C., J. Demeester, et al. (2000) Cationic polymer based gene delivery systems. *Pharm Res* 17(2): 113-26.

Dubertret, B., P. Skourides, et al. (2002) In vivo imaging of quantum dots encapsulated in phospholipid micelles. *Science* 298(5599): 1759-62.

Jaiswal, J. K., H. Mattoussi, et al. (2003) Long-term multiple color imaging of live cells using quantum dot bioconjugates. *Nat Biotechnol* 21(1): 47-51.

Lvov, Y., A. A. Antipov, et al. (2001) Urease Encapsulation in Nanoorganized Microshells. *Nano Letters* 1(3): 125-128.

Lvov, Y. and F. Caruso (2001) Biocolloids with ordered urease multilayer shells as enzymatic reactors. *Anal Chem* 73(17): 4212-7.

Prow, T. Nanomedicine: Targeted Nanoparticles for the Delivery of Biosensors and Therapeutic Genes. (2004) Ph.D. Thesis, University of Texas Medical Branch, Galveston, Texas USA

Sandberg, J. A., C. D. Sproul, et al. (2000) Acute toxicity and pharmacokinetic assessment of a ribozyme (ANGIOZYME) targeting vascular endothelial growth factor receptor mRNA in the cynomolgus monkey. *Antisense Nucleic Acid Drug Dev* 10(3): 153-62.

Stewart, M., R. P. Baker, et al. (2001) Molecular mechanism of translocation through nuclear pore complexes during nuclear protein import. *FEBS Lett* 498(2-3): 145-9.

Zauner, W., N. A. Farrow, et al. (2001) In vitro uptake of polystyrene microspheres: effect of particle size, cell line and cell density. *J Control Release* 71(1): 39-51.

Zhu, M. and W. E. Fahl (2000). Development of a green fluorescent protein microplate assay for the screening of chemopreventive agents. *Anal Biochem* 287(2): 210-7.

3.   **TITLE:** Nanomedicine – nanoparticles, molecular biosensors and targeted gene/drug delivery for combined single-cell diagnostics and therapeutics

AUTHORS: Tarl W. Prow, Jose H. Salazar, William A. Rose, Jacob N. Smith, Lisa N. Reece, Andrea A. Fontenot, Nan A. Wang, R. Stephen Lloyd, James F. Leary.

Nanomedicine – nanoparticles, molecular biosensors and targeted gene/drug delivery for combined single-cell diagnostics and therapeutics

Tarl W. Prow[1], Jose H. Salazar[1], William A. Rose[1], Jacob N. Smith[1], Lisa N. Reece[1], Andrea A. Fontenot[1], Nan A. Wang[1], R. Stephen Lloyd[2], James F. Leary[1]

Molecular Cytometry Unit; [1]Department of Internal Medicine, University of Texas Medical Branch, Galveston, TX 77555; [2]Center for Research on Occupational and Environmental Toxicology, Oregon Health Sciences Center, Portland, OR 97239

ABSTRACT

Next generation nanomedicine technologies are being developed to provide for continuous and linked molecular diagnostics and therapeutics. Research is being performed to develop "sentinel nanoparticles" which will seek out diseased (e.g. cancerous) cells, enter those living cells, and either perform repairs or induce those cells to die through apoptosis. These nanoparticles are envisioned as multifunctional "smart drug delivery systems".

The nanosystems are being developed as multilayered nanoparticles (nanocrystals, nanocapsules) containing cell targeting molecules, intracellular re-targeting molecules, molecular biosensor molecules, and drugs/enzymes/gene therapy. These "nanomedicine systems" are being constructed to be autonomous, much like present-day vaccines, but will have sophisticated targeting, sensing, and feedback control systems – much more sophisticated than conventional antibody-based therapies. The fundamental concept of nanomedicine is to not to just kill all aberrant cells by surgery, radiation therapy, or chemotherapy. Rather it is to fix cells, when appropriate, one cell-at-a-time, to preserve and re-build organ systems. When cells should not be fixed, such as in cases where an improperly repaired cell might give rise to cancer cells, the nanomedical therapy would be to induce apoptosis in those cells to eliminate them without the damaging bystander effects of the inflammatory immune response system reacting to necrotic cells or those which have died from trauma or injury.

The ultimate aim of nanomedicine is to combine diagnostics and therapeutics into "real-time medicine", using where possible in-vivo cytometry techniques for diagnostics and therapeutics. A number of individual components of these multi-component nanoparticles are already working in in-vitro and ex-vivo cell and tissue systems. Work has begun on construction of integrated nanomedical systems.

Keywords: nanomedicine; nanoparticles, molecular biosensors, drug delivery, gene therapy; flow cytometry; confocal microscopy; molecular diagnostics

1. INTRODUCTION

1.1 What is nanomedicine? Nanomedicine is a fundamentally different paradigm for medicine. It is "nano" not only because it uses nanometer scaled tools, but also because it employs a cell-by-cell regenerative and repair philosophy working at the single cell level rather than at the organ level. Medicine has progressed from primitive surgery to detailed microsurgery on small regions of organs. The next step is nanomedicine which performs "nanosurgery" inside living single cells to either repair those cells or to induce un-repairable cells to die by natural programmed cell death, avoiding the effects of a inflammatory response by the body's immune system which in many cases can be more severe than the original disease itself.

1.2 Some goals for nanomedicine: A goal of modern medicine is to provide earlier diagnostics so that diseases can be treated when they are most treatable. Dramatic results have been achieved in a number of diseases. However, diagnostics and therapeutics have not yet been combined in a continuous system to not only diagnose, but also to treat, at the earliest possible stage – perhaps before actual symptoms appear. The three conventional treatments for cancer are (1) surgical removal of the tumor, (2) radiation therapy, and (3) chemotherapy. Nanomedicine attempts to make smart decisions to either remove specific cells by induced apoptosis or repair them one cell-at-a-time. Single cell treatments will be based on molecular biosensor information that controls subsequent drug delivery to that single cell. Such a system would also need to be semi-autonomous, with pre-determined decisions points for when a diagnosed condition warrants treatment. Clinical decisions are usually much delayed by the negative potential side effects of that treatment, particularly if it turns out to be a misdiagnosis. If both the accuracy of treatment and the minimization of unfavorable side effects and bystander effects could be brought to acceptable levels, the consequences of faster autonomous treatments in continuous response to in-vivo molecular diagnostics with slightly higher probabilities of misdiagnosis could be tolerated. In this paper we discuss work still in the early stages of such a nanomedical system.

Conventional medicine is not readily available to much of humanity because it is labor-intensive. Medical labor is sophisticated and expensive. Nanomedicine will be much more preventive, combining very early diagnostics with initial therapeutics. In some ways it could resemble a smart, multifunctional vaccine. It might also be less expensive because it will minimize use of expense human experts for early diagnostics, and potentially could be mass produced and distributed.

1.3 Potential pitfalls of nanomedicine: We believe that it is important to discuss some of the potential pitfalls, as well as the promise, in nanomedical systems for future drug-gene delivery. We believe that the technology, while still in its infancy, has great promise to achieve those objectives. But a realistic examination of the tradeoffs must also be assessed. For example, some nanosystems very good for in-vitro work may have attributes that may preclude or limit their use in-vivo. Among these are the potentially long-term cytotoxic effects of some nanomaterials. The cytotoxicity of some nanomaterials in atom-by-atom or molecule-by-molecule nano self-assembly may prove to be very different from those same materials in elemental form. Also, cytotoxicity is a far more complex effect than simple cell killing, or even induction of apoptosis (programmed cell death). If the gene expression pattern is disturbed, those cells may not function, proliferate, or differentiate properly. There is currently very little "cytotoxicity" data for nanomaterials in biological systems.

Nonetheless, it should be kept in mind that one of the main barriers remaining in modern medicine is the effective and controlled delivery of drugs or genes to the targeted cells, with

minimal disturbance of non-targeted cells. The development of highly efficient and well-controlled delivery of drugs or genes to cells would represent a significant advance to modern medicine. That fact should be kept in mind in these still early days of nanomedical systems development. While there are risks in the new systems, there are many problems of the existing old systems, too readily accepted, because there have been no available alternatives. The proper development of nanomedicine will require the balancing of risks with opportunities.

1.4 Need for a nanoparticle gene delivery system: Existing gene delivery systems have a variety of limitations (De Smedt, Demeester, and Hennink 2000). Liposome based gene transfer methods have relatively low transfection rates, are difficult to produce in a specific size range, can be unstable in the blood stream, and are difficult to target to specific tissues (De Smedt, Demeester, and Hennink 2000). Injection of naked DNA, RNA, and modified RNA directly into the blood stream leads to clearance of the injected nucleic acids with minimal beneficial outcome (Sandberg et al. 2000). As such, there is currently a need for a gene delivery system which has minimal side effects but high affectivity and efficiency. One such system could be that of the self-assembled nanoparticles coated with targeting biomolecules (Lvov and Caruso 2001).

1.5 Application of nanomedicine to radiation damage in astronauts: In addition to describing the general concepts of nanomedicine, we show a particular application being developed for NASA as part of their nanomedicine for astronauts program. New paradigms of any technology, including nanomedicine, are often first developed for extreme environments and/or extreme circumstances. Longer voyage space exploration qualifies on both fronts. For example, on a manned roundtrip voyage to Mars and exploration on the surface of that planet, astronauts will encounter levels of radiation that are impossible to shield. There will also be no hospitals with either diagnostic or therapeutic treatments. The signal delays in Earth-Mars communications represents a major challenge to telemedicine, and largely precludes procedures requiring real-time Earth control. Any systems brought along must be small, low weight, intelligent, and autonomous. While there may be large radiation damage effects, the most likely scenario is a series of fractionated radiation doses, each of which is not necessarily a pivotal event, but whose accumulation can lead to further downstream events such as organ injury or cancer. The strategy of nanomedicine would be to try to repair the radiation damage on a continuous basis using DNA repair enzymes in nanoparticle systems targeted to cells likely to have experienced radiation as a counter-measure to more serious radiation injury at the organ level.

2. MATERIALS AND METHODS

In the early developmental stages of this project we have used a variety of experimental model systems which are very reproducible and testable, as described below. A basic strategy for a nanomedical system applied to the problem of repairing radiation damage in astronauts on a continuous basis is shown in the concept diagram of **Figure 1**.
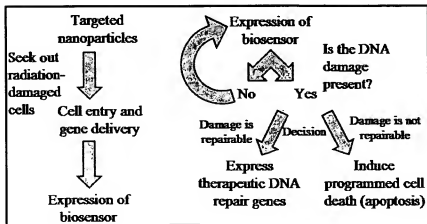

Figure 1: A nanomedicine concept applied to the problem of continuous repair of radiation damage in astronauts. A terrestrial application would be targeted repair of radiation-damaged normal tissue injured during radiation treatment of cancer patients.

2.1 Nanoparticles: There are two general categories of nanoparticles (with many variations) currently being used for applications in in-vitro and in-vivo nanomedicine: (1) nanoparticle cores with single or multilayered coatings, (2) hollow nanoparticle capsules without cores.

Nanoparticle cores materials vary greatly, the most common being made from gold, silica, or semiconductor materials. Some are made from magnetic materials which can be useful for recovery of gene products within cells (Prow et al., 2004a). Many are now commercially available. Most of these nanoparticles must be coated for two general purposes. First, some of them are not water-soluble. To exist and to function in an in-vivo aqueous environment, some of these hydrophobic materials must be marked with a layer of hydrophilic molecules. Second, some of these materials are cytotoxic to cells and tissues. Typically these are covered with lipophilic or other organic molecules to provide a barrier between the cell and the core nanoparticle materials.

Hollow nanocapsules without cores come in a variety of sizes and materials. The simplest ones consist of single or multiple layered liposomes, which are designed to fuse with the lipophilic molecules of a cell membrane and then to spill the contents of the liposome into the interior of the cell. More complex, layer-by-layer assembly nanocapsules are being made by some research groups. These nanocapsules are self-assembling by alternating charged layers of polymers and similar materials. In other work we have begun to develop nanosystems based on this concept (Prow et al., 2004b). These nanocapsules are potentially biodegradable and may be less cytotoxic to biological systems, although more detailed studies need to be conducted.

2.2 Nanoparticle targeting: Nanoparticle targeting can be accomplished in a variety of ways. But the two most common, as shown in this paper, are use of antibodies (e.g. anti-CD95 antibody) bound to the nanoparticle outer surface, or coating of the outer surface of the nanoparticles with molecules that are the ligands for cellular receptors (e.g. mannose to target nanoparticles to liver cells which have mannose receptors). While antibody targeting is very common for in-vitro applications, their use in-vivo can be problematical since some of these targeting antibodies can illicit an immune response from the human or animal. The mannose represents less of a problem in this regard because the body already recognizes mannose and does not tend to mount an immune response against it.

In the particular application of nanomedicine for astronauts we are using up-regulation and transport of the CD95 molecule to the radiation (or oxidative stress) damaged cell. Amounts of cell surface CD95 vary in roughly a dose dependent manner with radiation exposure (Sheard, 2001). So CD95 serves as the initial surrogate biomarker for radiation damage. We also have modeled radiation dosed cells with two cell lines, one of which expresses no CD95 (human MOLT-4 monocyte cell line) and another cell line (BJAB) which expresses high quantities of cell surface CD95. Once inside, the nanoparticle system performs a secondary check for oxidative stress which is highly correlated to radiation exposure using a biosensor sensitive to the presence of reactive oxygen species molecules. Since exact radiation exposure is difficult to control, we have used, in initial studies, a chemical which produces the same oxidative stress as radiation but in an easily dosed manner.

The other significant difference between in-vitro and in-vivo targeting is the great difference in specificity required. Cells are usually not rare in-vitro, while targeted cells are almost always rare in-vivo. Rare cell targeting presents considerable challenges in terms of specificity. Considering the number of possible interactions in-vivo, the specificity of the overall targeting system must, in most cases, be better than a million to one. No antibodies alone have this degree

of specificity. To solve this problem, Boolean combinations of antibodies must be chosen (for review, see Leary, 1994). The good news is that these levels of specificity can be reached with antibody combinations of two positive biomarkers and one negative biomarker. The correct repertoire of these three biomarkers (or cocktails of biomarkers as are frequently used for detection of rare stem cells)

2.3 Cell entry facilitation: Most people do not realize that targeting of nanoparticles to the cells of interest for nanomedicine represents only the first part of a long and complex journey. A nanoparticle is roughly one billionth the volume of a cell. So the interior of the cell represents another new universe to the nanoparticle. The nanoparticle and/or its contents must get successfully from the outside to the inside of a cell. How it enters the cell can control its subsequent fate. And simply dumping the drug or gene contents of the nanoparticle into the interior of the cell, while perhaps superior to dumping the drug or gene into the body for general circulation in the bloodstream, still does not guarantee that the drug or gene gets to the intracellular site where it can have therapeutic action. A further step of intracellular targeting is really required to be effective in this process. We have used three entry facilitation methods: (1) arginine-repeat peptides, (2) Lipofectamine^{TM} coatings to promote fusion of nanoparticles with the cell membrane, and (3) artificial tat-specific sequences, the entry and nuclear targeting molecule used by HIV-1.

2.4 Intracellular targeting: We have used a variety of specific amino acid localization sequences to deliver and anchor delivery of molecules to three intracellular regions of the cell: (1) the endoplasmic reticulum (ER), (2) the mitochondria, and (3) the nucleus. An important technology to visualize and study the proper localization of nanoparticles to their intracellular targets is confocal microscopy. Since to allow for improved detection of nanoparticles we used a Zeiss 510 META confocal microscope with multispectral imaging capabilities which correct for color overlaps on a pixel-by-pixel basis within each optical section. This spectral unmixing algorithm (Bearman et al., 2002), referred to as "emission fingerprinting" provides for improved color deconvolution compared to use of conventional optical bandpass filters as shown in **Figure**
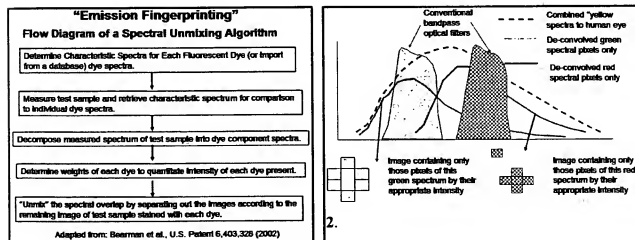
Figure 2: (A) The basic concept of emission fingerprinting is shown in schematic form. By knowing directly or indirectly, all of the spectral contributions of each dye or probe plus the autofluorescence spectrum of a cell, the colors can be "unmixed" on a pixel-by-pixel basis on each plane of a multi-plane confocal image. (B) The algorithm essentially fits the overall color curve using regions of each dye or component spectrum that are less contaminated with the overlap of other colors. The resulting emission fingerprinting technique can be superior to the use of conventional optical filters which still leave considerable optical overlap.

2.5 Molecular biosensing of the intracellular environment: Thus far we have explored both viral biosensors and reactive oxygen species (ROS) biosensors. This paper will describe use of ROS biosensors (Zhu and Fahl, 2000) coupled to an eGFP reporter gene which fluoresces green when activated. Many biosensors share certain characteristics as shown in **Figure 3**.

Targeting to initial region of interest	Cleavage domain sensitive to target molecule	Reporter molecule (e.g. GFP or luciferase)

For example, this biosensor can be designed to sense a target in the cell, then target to the nucleus to allow for transcription of a gene for therapy

TMD   CD   tTA

Figure 3: Many molecular biosensors used for diagnostics have targeting regions, a cleavage domain that is sensitive to enzymes or proteases, and a fluorescent reporter molecule.

2.6 Controlled drug-gene delivery: One of the ways we have tried to provide controlled drug/gene delivery to living single cells, is to attach the gene therapeutic to the biosensor. That way the therapeutic gene is only produced as long as the biosensor sees its target molecule. In this case we are developing a transient gene therapy for DNA repair of radiation-damaged DNA based on the biosensing of reactive oxygen species which has high correlation to radiation exposure.

An alternative treatment to repair is to accelerate the cell's natural "programmed cell death" or apoptosis. This is particularly important in the case of trying to repair radiation damaged cells in astronauts. If the cell is not repairable, we would prefer to have it die in a way that does not trigger inflammatory responses of the immune system which can, in many diseases and injuries, be of greater danger to the person than the disease or injury itself. In this application it is important to not allow cancerous cells to arise from mutations produced by radiation damage.

3. DATA/RESULTS

3.1 Comparison of molecular immunochemical and nanoparticle targeting: While the two processes are indeed quite different, fluorescent nanoparticle labeling can yield similar results to those of conventional fluorescent antibody labeling techniques as shown in **Figure 4**. In this case we used very large nanoparticles (approximately 500 nm diameter) in order to visualize the nanoparticle labeling pattern. Improved concordance of nanoparticle labeling with molecular labeling is obtained when nanoparticles are 100 nm or less diameters (data not shown, Prow thesis, 2004).
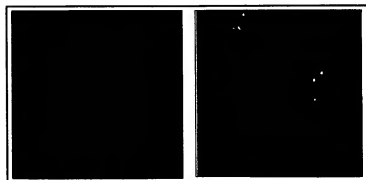

Figure 4: Nanoparticles with targeting molecules can label cells in a manner that gives similar results to conventional labeling with antibodies. However, as the nanoparticles get larger, they tend to bind in a "quantized" manner that leads to increasing discordance of results with increasing nanoparticle size.

3.2 Measures of nanoparticle targeting efficiency and accuracy: To study nanoparticle binding efficiency we performed phase contrast/fluorescence to allow viewing of cells that labeled or did not label with nanoparticles **(Figure 5A)**. Since this did not always allow for accurate identification of the specific cells of interest, we used tracking dye labeling of the larger contaminating cells, not of interest, to allow correct identification of all non-specific cell types in in-vitro experiments that allowed modeling of rare in-vivo targeting **(Figure 5B)**.
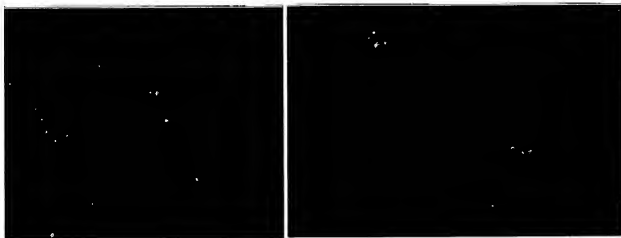
Figure 5: (A) BJAB and MOLT-4 cell mixtures were labeled with 500 nm diameter nanoparticles (small white spheres) and viewed by simultaneous phase contrast/fluorescence microscopy using a Nikon Optiphot microscope. (B) To improve assay accuracy we pre-labeled contaminating cell types (CD95 negative MOLT-4 cells) with CMAC (Molecular Probes, Inc.) a blue fluorescence tracking dye (shown in this grey scale image as diffuse grey). Nanoparticle (small white spheres in this grey level digital image) labeling showed highly specific labeling of the CD95-positive BJAB cells with undetectable labeling of CD95-negative MOLT-4 cells.

3.3 Targeted delivery of nanocrystals: Streptavidin labeled nanocrystals were targeted to cells labeled with biotinylated anti-CD95. The purpose of these experiments was to explore the entry mechanisms of semiconductor nanocrystal nanoparticles. "Naked" nanoparticles (with no biocoatings) did enter some cells non-specifically, showing that biocoatings were not only necessary to target nanoparticles to the cells of interest but also necessary to prevent non-specific uptake. Interestingly, Streptavidin coated nanocrystals when bound to the surface of cells labeled with biotinylated anti-CD 95 monoclonal antibodies, not only targeted those cells in a highly efficient manner, but also tended to internalize and track to the nuclei of those cells. HIV tat sequences proved highly efficient cell entry and nuclear localization molecules. Arginine rich amino acid repeat peptides did not prove useful for nuclear localization, at least in our hands.

3.4 Application of nanomedical strategies to repair of radiation-damaged cells: To test the feasibility of these approaches we conducted a series of in-vitro experiments. A antioxidants-sensitive biosensor (Zhu and Fahl, 2000) was attached to DNA repair enzymes previously designed and prepared in the lab of co-author RSL. When a cell undergoes oxidative stress it produces a series of molecules which will attach to the ARE biosensor which then can be used to drive the synthesis of special DNA repair enzymes MutY/Fpg designed by RSL **(Figure 7)**.
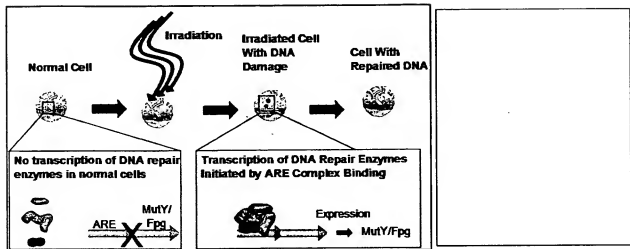
This ARE biosensor, attached to a green fluorescent protein reporter sequences (eGFP), was tested in cultures of T24 cells subjected to tert-butylhydroquinone (tBHQ), a chemical which produces oxidative stress in cells in a manner similar to UV radiation, but which is more easily dosed and controlled. The cell detects ROS and activates transcription factors which bind to specific promoter regions. Transcription downstream of these response elements is then activated. The construct used was constructed by Zhu and Fahl, 2000. This construct is composed of a number of antioxidant response element (ARE) repeats followed by a minimal thymidine kinase promoter, ahead of a EGFP reporter gene. The sensitivity of the biosensor is dramatically affected by the number of ARE repeats, with four repeats giving optimal sensitivity (Zhu and Fahl, 2000). The activity of this biosensor can be seen in T24 cells through the addition of 100 μM tert-butylhydroquinone, an inducer of ROS (Sigma-Aldrich Chemical, Inc., St. Louis, MO). T24 cells are a human cell line derived from a transitional cell carcinoma that constitutively expresses CD95 on the surface (Mizutani et al. 1997) (American Type Culture Collection, Manassas, VA). Cells showing signs of oxidative stress were detected as green fluorescent positive cells as shown in **Figure 8**.
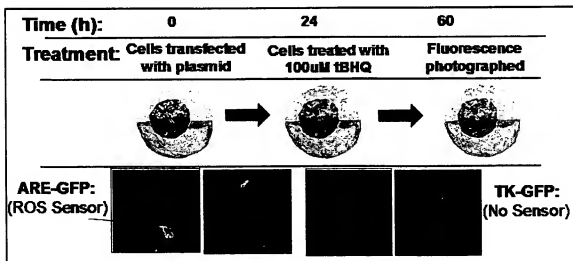
Figure 8: Cells were transiently transfected at ~60% confluence with either ARE-GFP or TK-GFP. 24 hours later the cells were treated with tert-butylhydroquinone (tBHQ), an ROS inducing agent, to simulate the ROS effects of radiation doses The cells were examined every 12 hours post treatment. Weak fluorescence (ARE-GFP) shown in white was present at hour 48 and photographs were taken at hour 60.

To test whether DNA repair enzymes could be introduced into cells damaged by actual UV radiation to accelerate normal DNA repair mechanisms by activating a second repair pathway, not normally expressed in human cells because one enzyme, a glycosylase is absent in normal human cells (**Figure 9**).
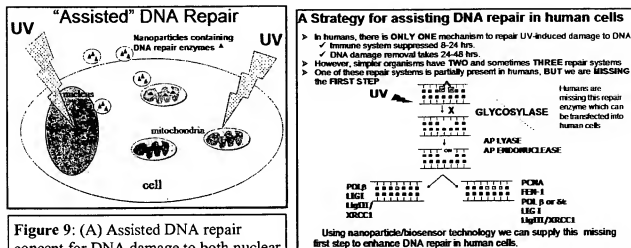
Figure 9: (A) Assisted DNA repair concept for DNA damage to both nuclear and mitochondrial DNA. (B) A specific strategy for assisting DNA repair of UV damage in human cells.

This normally absent repair mechanism was activated by transfection of a glycosylase containing gene sequence which also contained an eGFP reporter molecule. UV damage can occur in both nuclear and mitochondrial DNA. Since many molecules introduced into a cell frequently track non-specifically to the nucleus, we tested the ability of intracellular localization sequences to guide these repair molecules to the mitochondria. In the absence of localization sequences, the repair molecules did not appear to track to any specific region of the cell, as shown by the diffuse staining of **Figure 10A**. However when mitochondrial localization sequences were attached to the repair enzymes, they tracked to the mitochondria as shown by confocal microscopy (**Figures 10B** and **10C**). Either transient or stable gene therapy was demonstrated.

Figure 10: (A) T4 transfected DNA repair enzyme with no localization anchoring sequence (note diffuse fluorescence) with transient expression (Wt-T4-PDG-GFP in CHO-XPG. Transient expression. 100x objective)
(B) T4 transfected DNA repair enzyme with mitochondrial localization anchoring sequence, with transient expression (MLS35-T4-PDG-GFP in CHO XPG. 100x objective)
(C) T4 transfected DNA repair enzyme with mitochondrial localization anchoring sequence, with stable expression (MLS18-T4-PDG-GFP in hXPA. 100x objective)

In the present state of gene therapy concerns about patient safety, our efforts are concentrated on the production of potentially useful transient gene therapies using nanoparticle systems. To test the actual effectiveness of these DNA repair enzymes inside living cells, comet assays were performed in the laboratory of RSL. The "comet" assay (Tice, 2000) shows the attempt of cell trying to repair its DNA strand breaks as a comet-like tail. When successful in DNA repair, the comet tail is eliminated. **Figure 11** clearly shows that repairable human cells can be repaired in 6 hours by this assisted DNA repair transient gene therapy approach, as compared with a required repair time of more than 24 hours using the usual DNA repair pathway functioning in normal human cells. While far from proving efficacy in-vivo, these initial results show the promise of this approach.

Hxpa DNA repair-deficient human cells		NLSI DNA repairable-human cells	
No T4 treatment	T4 treated	No T4 treatment	T4 treated
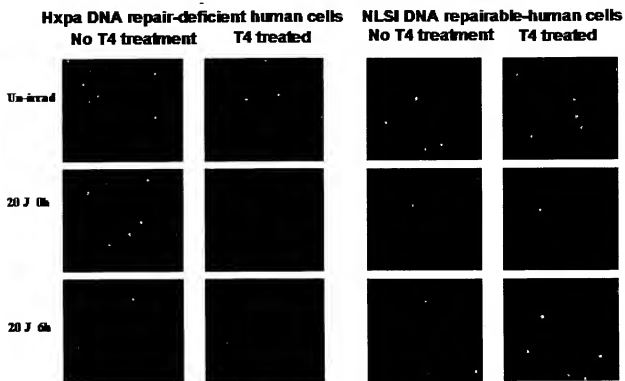
Figure 11: A comet assay shows that DNA damage is successfully repaired at an accelerated rate due to successfully activation of a second repair pathway in a transient gene therapy approach to repairing DNA damage as it occurs.

4. CONCLUSIONS

These results, while still very preliminary, reveal some of the promise of nanotechnology for the effective delivery of therapeutic genes to individual living cells. As such it presents important paradigm shifts in the delivery of medicine from a single choice of destruction of all affected cells to one of selective repair of cells whenever possible and desirable and safe destruction through apoptosis of un-repairable cells. It also shows how, in principle, autonomous nanoparticle systems can be constructed to provide continuous molecular diagnostics and therapeutics at the single cell level.

5. ACKNOWLEDGEMENTS

6. REFERENCES

Bearman, G.H., Frasier, S.E., Lanford, R.D. System and method for monitoring cellular activity. U.S. Patent 6,403,328. 2002.

De Smedt, S. C., J. Demeester, and W. E. Hennink. Cationic polymer based gene delivery systems. Pharm Res 17, no. 2: 113-126, 2000.

Leary, J. F. Strategies for rare cell detection and isolation. Methods Cell Biol 42 Pt B: 331-358, 1994.

Lvov, Y. and F. Caruso. Biocolloids with ordered urease multilayer shells as enzymatic reactors. Anal Chem 73, no. 17: 4212-4217, 2001.

Mamedov, A. A., A. Belov, M. Giersig, N. N. Mamedova, and N. A. Kotov. Nanorainbows: Graded semiconductor films from quantum dots. J Am Chem Soc 123, no. 31: 7738-7739, 2001.

Mizutani, Y., Y. Okada, O. Yoshida, M. Fukumoto, and B. Bonavida. Doxorubicin sensitizes human bladder carcinoma cells to fas-mediated cytotoxicity. Cancer 79, no. 6: 1180-1189, 1997.

Prow T.W., Rijnbrand, R., Wang, N., Salazar, J., Leary, J. F. Transient Gene Expression from DNA Tethered Magnetic Nanoparticles. Manuscript submitted for publication 2004a.

Prow T.W., Kotov, N.A., Lvov, Y.M., Rijnbrand, R, Leary, J.F. Nanoparticles, Molecular Biosensors, and Multispectral Confocal Microscopy. Journal of Molecular Histology (accepted) 2004b.

Prow, T.W. Nanomedicine: Targeted nanoparticles for the delivery of biosensors and therapeutic genes. Ph.D. thesis, University of Texas Medical Branch, Galveston, TX. 2004

Sandberg, J. A., C. D. Sproul, K. S. Blanchard, L. Bellon, D. Sweedler, J. A. Powell, F. A. Caputo, D. J. Kornbrust, V. P. Parker, T. J. Parry, and L. M. Blatt. 2000. Acute toxicology and pharmacokinetic assessment of a ribozyme (angiozyme) targeting vascular endothelial growth factor receptor mRNA in the cynomolgus monkey. Antisense Nucleic Acid Drug Dev 10, no. 3: 153-62.

Sheard, M.A. Ionizing radiation as a response-enhancing agent for CD95-mediated apoptosis. Int. J. Cancer 96: 213-220, 2001.

Tice RR, Agurell E, Anderson D, Burlinson B, Hartmann A, Kobayashi H, Miyamae Y, Rojas E, Ryu JC, Sasaki YF. Single cell gel/comet assay: guidelines for in vitro and in vivo genetic toxicology testing. Environ Mol Mutagen 35(3):206-221, 2000.

Zhu, M. and W. E. Fahl Development of a green fluorescent protein microplate assay for the screening of chemopreventive agents. Anal Biochem 287, no. 2: 210-217, 2000.

4. **TITLE:** Gene Delivery, Expression, and Recovery of DNA Tethered Nanoparticles

AUTHORS: Tarl Prow, Jose H. Salazar, Jacob N. Smith, William A. Rose, Nan Wang, Brent Bell, Massoud Motamedi, James Leary.

TITLE:
Gene Delivery, Expression, and Recovery of DNA Tethered Nanoparticles

AUTHORS:
Tarl Prow[1,2], Jose H. Salazar[2], Jacob N. Smith[2], William A. Rose[2], Nan Wang[2], Brent Bell[3], Massoud Motamedi[3], James Leary[*,1,2,3]

AFFILIATIONS:
[1]Department of Pathology, [2]Department of Infectious Diseases, [3]Biomedical Engineering Center, University of Texas Medical Branch, Galveston, TX 77555.

*To whom correspondence should be addressed. Tel: 409-747-1930; Email: jleary@utmb.edu

INTRODUCTION:

To date, the majority of nanoparticle research has been carried out by materials scientists, but recent trends have brought these tools into the hands of biologists. Nanoparticles have found two broad niches in biology, detection technologies and payload delivery (1,2). Since the late 1970s, nanoparticles have been used to deliver drugs (2,3). In fact, the majority of publications concerning biological applications of nanoparticles are focused on the delivery of chemotherapeutic agents with nanoparticles ranging from 2 to 3000nm. Nanoparticle mediated gene delivery has recently emerged as a promising tool for gene therapy strategies (4-6). One of the main problems with using nanoparticles for gene delivery is the construction, cost, and quality control of the nanoparticles themselves. These factors limit the usefulness of nanotechnology to laboratories that have chemists capable of nanoparticle synthesis or in collaboration with those chemists. This limits the usefulness of the technology, especially for small laboratories. To solve this problem there needs to be a commercially available nanoparticle that is readily available, easy to use, and flexible. To this end, we have adapted a magnetic nanoparticle system that is simple and quite flexible from a commercially available product intended for other uses.

To date, magnetic nanoparticles have been primarily applied to three fields: magnetic resonance imaging, molecular and cell separation technologies, and drug delivery (7-11). Many researchers use magnetic particles as contrast agents (12-16). Because these agents are used primarily in diagnostic in vivo imaging, many of the particle formulations are already approved for use in humans. The magnetic properties of these particles are quite favorable for layered construction of a non-viral based gene delivery vector. One of the most difficult challenges facing researchers constructing layered nanoparticles is the purification of the particles after each step. With magnetic particles, the purification is generally simple and utilizes off the shelf products. This is the first report describing DNA tethered magnetic nanoparticles for in vitro and in vivo gene delivery and subsequent recovery. The magnetic properties of nanoparticles have been used to enhance gene transfer for gene therapy applications (17-22). In this case the nanoparticles were used to concentrate the plasmid to a specific location and thereby increase the likelihood of transfection (22). This group used clusters of plasmid DNA and coated magnetic nanoparticles to target cells using the magnetic properties of the nanoparticle clusters (17).

Superparamagnetic nanoparticle cores coated with streptavidin were chosen for gene transfer and recovery because they were easily obtainable, simple to construct and could be purified from the layer components using magnetic columns. The core particles are composed of an iron oxide core coated with dextran and bioconjugated to streptavidin, with the complete particle measuring approximately 50nm in diameter. We have developed a simple procedure for DNA conjugation, purification, delivery to cells and recovery of these nanoparticles. These particles were found to have reasonably high expression, with respect to free DNA, when coated with Lipofectamine 2000© (Invitrogen, Inc.). It was found that intact nanoparticles could be recovered from populations

of positive and negative cells through purification and PCR analysis. These nanoparticles were also able to deliver genes in vivo.

MATERIALS AND METHODS:

Biotin labeled DNA fragment preparation

PCR amplification was used to create biotin labeled DNA fragments. Oligonucleotide primers were purchased from Integrated DNA Technologies, Inc. For initial studies, either the 5' or the 3' oligo was made with a single biotin tag. The sequences were based on the pEGFP-C1 (BD Clontech, Inc.) template: forward 5' - TAG TTA TTA ATA GTA ATC AAT TAC GGG GTC ATT AG - 3', reverse 5' - TAC ATT GAT GAG TTT GGA CAA ACC ACA ACT AGA AT - 3' (Integrated DNA Technologies, Inc.). Later studies used only 5' oligos labeled with biotin. These oligos were then used as PCR primers. A typical reaction would include 25 ul Red Taq, (Sigma Chemicals, Inc.), 1 ul 5' biotinylated primer, 1ul 3' primer, 1 ul template, to 50ul with water. The primers were at 200pM and the template at 50ng/ul. A typical reaction for DNA tethering to magnetic nanoparticles would include about 25 of these reactions. Typical PCR cycles would include ~35 cycles of denaturing temperature at 94°C for 30 seconds, annealing temperature at 65°C for 30 seconds and extension for 2 minutes at 72°C.

DNA tethered magnetic nanoparticle construction

Biotin labeled PCR products were tethered to streptavidin coated magnetic nanoparticles (Miltyni Biotech, Inc.). DNA tethered magnetic nanoparticles were constructed as per the manufactur's instructions. Briefly, the magnetic nanoparticles were incubated with the biotin labeled PCR fragments at the ratio prescribed by the manufacturer. The mixture was allowed to sit at room temperature for 30 minutes. During that time, the magnetic column was prepared by washing once with the 100ul of the included nucleic acid buffer and three times with 100ul Optimem (Gibco, Inc.). Once washed, the column was loaded with the DNA nanoparticle mixture. The column was then washed three times with 100ul Optimem. The nanoparticles were eluted by removing the column from the magnet and adding the 100ul of Optimem. The resulting brownish solution contained DNA tethered nanoparticles.

Lipid coating of DNA tethered magnetic nanoparticles

The DNA tethered nanoparticles were coated with Lipofectamine 2000 as per the manufactures instructions for DNA. The DNA tethered magnetic nanoparticles were treated as DNA for lipid coating. Briefly, the eluted particles were diluted in the appropriate amount of Optimem and incubated for 5 minutes at room temperature. An appropriate amount of Lipofectamine 2000 was diluted in a separate tube and incubated at room temperature for 5 minutes. After 5 minutes, the two tubes were mixed gently and combined. This mixture was allowed to stand for 20 minutes before added to the cell culture.

5

Confocal microscopy.

Cells were examined with a Zeiss 510 META confocal microscope. Excitation wavelengths included UV and/or 488nm depending on the fluorescent probes used. Appropriate emission wavelengths were determined and used for each fluorophore used. Cells were analyzed with either 20, 40, 63, or 100X objectives. A 20X objective was used for imaging large numbers of cells for analysis.

Image analysis

A standard wave-propagation algorithm was used to segment the images over a singular threshold. An upper and lower bound were chosen for sub-segmentation. Segments which fell below the lower area bound were removed. Segments which were above the upper bound were re-segmented with a higher threshold and reexamined. The threshold level was computed as the average of the intensity of the pixels within the segment minus the standard deviation of the intensity of the pixels bounded below by zero. Threshold levels are computed individually for each sub-segment. The output is a list of segments associated with a bitmap representing the segment, the total intensity, area and standard deviation of intensity for that segment (23).

Cell culture and transfections.

Cells were incubated at 37C in 5% CO_2. The Huh-7 cell line, derived from a human hepatoma, was cultured in DMEM supplemented with 10% FBS (Sigma, Inc.) and Penicillin/Streptomycin (Sigma, Inc.). Cells were transiently transfected with Lipofectamine2000 (Invitrogen, Inc.) according to the manufacture's instructions. Each experiment was done at least in triplicate and positive and negative controls were present in all experiments.

RESULTS:

Conjugation of DNA to magnetic nanoparticles

The initial construction of the DNA tethered nanoparticles began with the creation of biotin labeled DNA fragments containing the minimal genetic material to be constitutively expressed in mammalian cells. Biotin labeled PCR primers were used to generate CMV-EGFP-pA containing DNA fragments (1.5kb) with 5' biotin labeled, 3' biotin labeled, and unlabeled. These fragments contain all of the information needed to express pEGFP-C1 from within the nucleus and were conjugated to magnetic nanoparticles (magnetic nanoparticles) for transfection. Streptavidin coated magnetic nanoparticles were incubated with each of the DNA fragments and analyzed by agarose gel electrophoresis (**Figure 1.**). Lanes A., C., and E. contained only the PCR product. Lanes B., D. and F. contained magnetic nanoparticles incubated with the PCR fragments. Only the DNA in Lanes A. to D. contained biotin tags. DNA in lanes E. and F. contained no biotin tag and were therefore used as negative controls. The black squares indicate where high molecular weight or uncharged DNA runs. The dark staining seen in Lanes B. and D. indicates that the DNA was able to bind to magnetic nanoparticles and was now trapped at the top of the gel due to its large size. This gel also shows that there is a significant amount of unbound DNA present. Because of this, the magnetic nanoparticles need to be purified from the contaminating free DNA fragments as described in the next section.

Removal of Free DNA from Magnetic Nanoparticle/DNA Solutions

In these experiments, the mixtures of DNA and magnetic nanoparticles were washed 4x to remove unbound DNA using a magnetic column. It was found that the magnetic properties of these particles enabled the rapid purification of the magnetic nanoparticles from the DNA solution. These samples were then run on an agarose gel (**Figure 2.**). Lanes A. to C. represent only DNA fragments. Lanes D. to F. contain the magnetic nanoparticle/DNA mixture. After washing, a portion of the magnetic nanoparticles were run onto this gel (Lanes G. to I.). If carefully examined (lower figure) dark staining can be seen only in lanes G. and H. near the loading well. This suggests that the free DNA has been removed and only the DNA tethered magnetic nanoparticles remain in solution.

Expression Levels of Cells Transfected with DNA Tethered Magnetic Nanoparticles

After washing, the DNA tethered magnetic nanoparticles were mixed with Lipofectamine 2000 in order to enhance transfection into cells (24). This complex was then delivered to cells cultured in chamber slides, incubated for 48 hours, fixed, permeablized, and finally counterstrained with DAPI. Slides were subsequently photographed under fluorescence using a Nikon CoolPix 990 digital camera. The images obtained were then analyzed with an in house slide

based cytometry software program (written by JNS) and the resulting data presented in **Figure 3**. Note that all of the values were normalized to the samples treated with the un-labeled GFP fragment transfected with Lipofectamine 2000. The intact pEGFP-C1 plasmid was found to be ~2x the expression level as the un-labeled GFP fragment. Finally, the unlabeled DNA exposed magnetic nanoparticles as expected did not show any appreciable expression of GFP.

In Vitro Gene Expression with DNA Tethered Magnetic Nanoparticles

Figure 4. shows the fluorescent images of the cells used for Figure 4.27. Panel A. is an image of untreated cells. Panels B., C., and D. represent cells transfected with DNA fragments with 5', 3', and no biotin tags using Lipofectamine 2000. Panels E., F., and G. show cells exposed to DNA tethered to magnetic nanoparticles from 5', 3', and no (control for free DNA) biotin tags; these particles were also coated with Lipofectamine 2000. DNA tethered to magnetic nanoparticles showed similar levels of gene expression as those same free gene sequences directly transfected into these cells.

Recovery of DNA Tethered Magnetic Nanoparticles

These data demonstrate that DNA tethered nanoparticles could be recovered from in Huh-7 cells 72 hours post treatment. Cells were lysed and the magnetic nanoparticles were purified from the cell lysate with magnetic separation. The nanoparticles were then eluted from the column and concentrated. The resulting solutions were then used as templates for PCR reactions. The resulting Panels were then run on an agarose gel (**Figure 5.**). Tethering at the 5' end resulted in the greatest expression of the attached gene sequence and was easily recovered from populations of cells.

Nanoparticle Delivery of Genes in Vivo.

Translation of a gene delivery technology from an in vitro model to in vivo, is notoriously difficult. We report that we were able to transfect hepatocytes in vivo with DNA tethered magnetic nanoparticles. After intrahepatic injection, the animals were maintained for 72 hours prior to sacrifice. The livers were snap frozen, cryosectioned, and counterstained with DAPI. Many GFP positive cells were found within this region, but they occurred in small clusters of 1-10 cells per cluster. Furthermore, there were several clusters of GFP positive cells surrounding the injection site, but overall the transfection efficiency was very low (**Figure 6.**). This may be due to several reasons including: a short incubation time and relatively small injection volume ~100ul.

DISCUSSION:

The three main findings of these experiments were 1) magnetic nanoparticles can be used for effective gene transfer vectors; 2) days after gene transfer, the DNA tethered particles could be recovered and the entire gene amplified by PCR; 3) DNA tethered magnetic nanoparticles coated with Lipofectamine 2000 could transfer genes in vivo. Cells incubated with these particles showed no visible signs of toxicity (blebbing, apoptosis, etc.), even though the particles are made of iron. The ability to isolate these particles days after their introduction suggests that they are stable within the cellular matrix. This may be due, at least in part, to the conjugation of proteins to the core particle. These proteins could serve as a buffer zone inhibiting contact with fouling agents within the cellular milieu.

EGFP encoding DNA fragments that were transfected into cells showed about half of the fluorescence seen in cells transfected with the circular plasmid. DNA fragments with 5' or 3' biotin tags were attached to streptavidin coated magnetic nanoparticles. Free DNA fragments were successfully removed through washing the particles using a magnetic column. Cells exposed to uncoated DNA tethered nanoparticles did not express detectable levels of EGFP. Cells exposed to DNA tethered nanoparticles coated with Lipofectamine 2000 expressed high levels of EGFP. Only cells that expressed EGFP from DNA tethered nanoparticles were recovered with a magnetic column and detected by PCR.

One important finding is that the uncoated DNA tethered magnetic nanoparticles were able to successfully transfect cells *in vitro*. This result shows that the size range of these particles is, at least, close to optimal since they did not absolutely require the presence of lipofectamine for transfection. Another interesting result is that cells treated with the DNA tethered magnetic nanoparticles coated but also with lipid had expression levels well within range of those transfected with only labeled DNA fragments. These data show that we can effectively express gene products from DNA tethered to magnetic nanoparticles in either the 5' or 3' configuration. Finally, the unlabeled DNA exposed magnetic nanoparticles did not show any appreciable expression of GFP. Therefore the expression we observed with the labeled DNA and magnetic nanoparticles was from DNA tethered to magnetic nanoparticles. Tethering appears to greatly increase the expression of these genes by mechanisms not yet well understood.

Simple streptavidin coated magnetic particles can be used to deliver genes into cells and recover those same genes after expression studies. This technology can then be used for screening gene libraries and determining the effects of the intracellular environment on the nanoparticles themselves.

In summary, multilayered nanoparticles were found to be an efficient platform to deliver and recover genes in vitro. These experiments showed that nanoparticle tethered DNA could express GFP at a level similar to free DNA. Lipid coating these particles was a fast and efficient way to enhance the uptake and use of the particles both in vitro and in vivo.

REFERENCES:

1. Koropchak, J.A., Sadain, S., Yang, X., Magnusson, L.E., Heybroek, M., Anisimov, M. and Kaufman, S.L. (1999) Nanoparticle detection technology for chemical analysis. *Anal Chem*, **71**, 386A-394A.

2. Douglas, S.J., Davis, S.S. and Illum, L. (1987) Nanoparticles in drug delivery. *Crit Rev Ther Drug Carrier Syst*, **3**, 233-261.

3. Kreuter, J., Tauber, U. and Illi, V. (1979) Distribution and elimination of poly(methyl-2-14C-methacrylate) nanoparticle radioactivity after injection in rats and mice. *J Pharm Sci*, **68**, 1443-1447.

4. Panyam, J. and Labhasetwar, V. (2003) Biodegradable nanoparticles for drug and gene delivery to cells and tissue. *Adv Drug Deliv Rev*, **55**, 329-347.

5. Vijayanathan, V., Thomas, T. and Thomas, T.J. (2002) DNA nanoparticles and development of DNA delivery vehicles for gene therapy. *Biochemistry*, **41**, 14085-14094.

6. Benns, J.M. and Kim, S.W. (2000) Tailoring new gene delivery designs for specific targets. *J Drug Target*, **8**, 1-12.

7. Hogemann, D., Ntziachristos, V., Josephson, L. and Weissleder, R. (2002) High throughput magnetic resonance imaging for evaluating targeted nanoparticle probes. *Bioconjug Chem*, **13**, 116-121.

8. Lanza, G.M., Yu, X., Winter, P.M., Abendschein, D.R., Karukstis, K.K., Scott, M.J., Chinen, L.K., Fuhrhop, R.W., Scherrer, D.E. and Wickline, S.A. (2002) Targeted antiproliferative drug delivery to vascular smooth muscle cells with a magnetic resonance imaging nanoparticle contrast agent: implications for rational therapy of restenosis. *Circulation*, **106**, 2842-2847.

9. Sun, M.L. and Zhang, H. (2001) [The development of nanoparticles on DNA isolation and purification]. *Sheng Wu Gong Cheng Xue Bao*, **17**, 601-603.

10. Winter, P.M., Caruthers, S.D., Kassner, A., Harris, T.D., Chinen, L.K., Allen, J.S., Lacy, E.K., Zhang, H., Robertson, J.D., Wickline, S.A. *et al.* (2003) Molecular imaging of angiogenesis in nascent Vx-2 rabbit tumors using a novel alpha(nu)beta3-targeted nanoparticle and 1.5 tesla magnetic resonance imaging. *Cancer Res*, **63**, 5838-5843.

11. Albig, A. (2001) Isolation of mRNA binding proteins using the µMACS™ Streptavidin Kit. *MACS&more*, **5**, 6-7.

12. Violante, M.R. (1990) Potential of microparticles for diagnostic tracer imaging. *Acta Radiol Suppl*, **374**, 153-156.

13. Petersein, J., Saini, S. and Weissleder, R. (1996) Liver. II: Iron oxide-based reticuloendothelial contrast agents for MR imaging. Clinical review. *Magn Reson Imaging Clin N Am*, **4**, 53-60.

14. Mitchell, D.G. (1997) MR imaging contrast agents--what's in a name? *J Magn Reson Imaging*, **7**, 1-4.

15. Bonnemain, B. (1998) Superparamagnetic agents in magnetic resonance imaging: physicochemical characteristics and clinical applications. A review. *J Drug Target*, **6**, 167-174.

16. Wang, Y.X., Hussain, S.M. and Krestin, G.P. (2001) Superparamagnetic iron oxide contrast agents: physicochemical characteristics and applications in MR imaging. *Eur Radiol*, **11**, 2319-2331.

17. Plank, C., Schillinger, U., Scherer, F., Bergemann, C., Remy, J.S., Krotz, F., Anton, M., Lausier, J. and Rosenecker, J. (2003) The magnetofection method: using magnetic force to enhance gene delivery. *Biol Chem*, **384**, 737-747.

18. Krotz, F., Sohn, H.Y., Gloe, T., Plank, C. and Pohl, U. (2003) Magnetofection Potentiates Gene Delivery to Cultured Endothelial Cells. *J Vasc Res*, **40**, 425-434.

19. Plank, C., Anton, M., Rudolph, C., Rosenecker, J. and Krotz, F. (2003) Enhancing and targeting nucleic acid delivery by magnetic force. *Expert Opin Biol Ther*, **3**, 745-758.

20. Plank, C., Scherer, F., Schillinger, U., Bergemann, C. and Anton, M. (2003) Magnetofection: enhancing and targeting gene delivery with superparamagnetic nanoparticles and magnetic fields. *J Liposome Res*, **13**, 29-32.

21. Krotz, F., Wit, C., Sohn, H.Y., Zahler, S., Gloe, T., Pohl, U. and Plank, C. (2003) Magnetofection-A highly efficient tool for antisense oligonucleotide delivery in vitro and in vivo. *Mol Ther*, **7**, 700-710.

22. Scherer, F., Anton, M., Schillinger, U., Henke, J., Bergemann, C., Kruger, A., Gansbacher, B. and Plank, C. (2002) Magnetofection: enhancing and targeting gene delivery by magnetic force in vitro and in vivo. *Gene Ther*, **9**, 102-109.

23. Mullikin, J.C. (1993) In Press, D. U. (ed.), *Discrete and Continuous Methods for Three-Dimensional Image Analysis*, pp. 47-48.

24. Ohki, E.C., Tilkins, M.L., Ciccarone, V.C. and Price, P.J. (2001) Improving the transfection efficiency of post-mitotic neurons. *J Neurosci Methods*, **112**, 95-99.

FIGURE LEGENDS:

Figure 1. Conjugation of DNA to MN. Agarose gel of DNA and nanoparticles. Lanes A, C, and E contain only the PCR product. Lanes B, D and F contain nanoparticles incubated with the PCR fragments. Lanes A to D contain biotin tags. Lanes E and F contain no biotin tag. Black squares indicate where high molecular weight or uncharged DNA runs.

Figure 2. Purification of DNA tethered MN. Lanes A to C represent only DNA fragments. Lanes D to F contain the MN/DNA mixture. After washing, a portion of the MN mixtures were also run on this gel (Lanes G to I). The right panel is a magnified image of the box around Lanes F to I.

Figure 3. Expression levels of EGFP from DNA tethered MN. In vitro gene expression levels are shown as the % of Lipofectamine transfected EGFP DNA (EGFP+LA). Biotin tagged DNA was also transfected into cells (Biot EGFP). Cells transfected with DNA bound nanoparticles are labeled BIOT+MAG. All samples were incubated with (LA) or without Lipofectamine 2000.

Figure 4. Expression of EGFP from MN tethered to EGFP DNA. EGFP expression (green) and DNA (blue) are shown in these images. Untreated cells (Panel A), cells transfected with DNA fragments with 5', 3', and no biotin tags (Panels B, C, and D), and cells exposed to DNA tethered to MN from 5', 3', and no (control for free DNA) biotin tags Panels E, F, and G are shown here.

Figure 5. Recovery and PCR of DNA tethered to magnetic nanoparticles. Agarose gel showing the PCR products of DNA tethered magnetic nanoparticles isolated from within cells. Lane A. 1kb marker; B. 5' tethered; C. 3' tethered; D. no tether; and E. positive control.

Figure 6. Magnetic nanoparticle delivery of genes in vivo. Fluorescent micrographs of 5 micron cryosectioned liver from rats injected intrahepatically with nanoparticles tethered to EGFP encoding DNA and coated with lipid. These sections were counterstained with DAPI. Green highlights indicate cells expressing GFP from nanoparticles.

	A.	B.	C.	D.	E.	F.
Nanoparticles:	-	+	-	+	-	+
DNA only:	+		+		+	
Biotin tag:	5'	5'	3'	3'	-	-

Figure 1. Conjugation of DNA to MN. Agarose gel of DNA and nanoparticles. Lanes A, C, and E contain only the PCR product (2.). Lanes B, D and F contain nanoparticles incubated with the PCR fragments. Lanes A to D contain biotin tags. Lanes E and F contain no biotin tag. Black squares indicate where high molecular weight or uncharged DNA runs (1.).
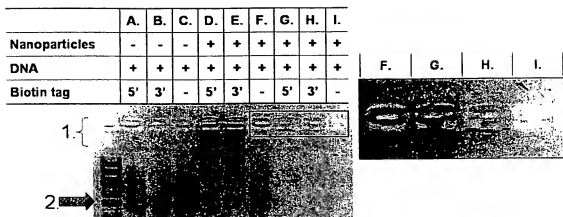
	A.	B.	C.	D.	E.	F.	G.	H.	I.
Nanoparticles	-	-	-	+	+	+	+	+	+
DNA	+	+	+	+	+	+	+	+	+
Biotin tag	5'	3'	-	5'	3'	-	5'	3'	-

Figure 2. Purification of DNA tethered MN. Lanes A to C represent only DNA fragments. Lanes D to F contain the MN/DNA mixture. After washing, a portion of the MN mixtures were also run on this gel (Lanes G to I). The right panel is a magnified image of the box around Lanes F to I.
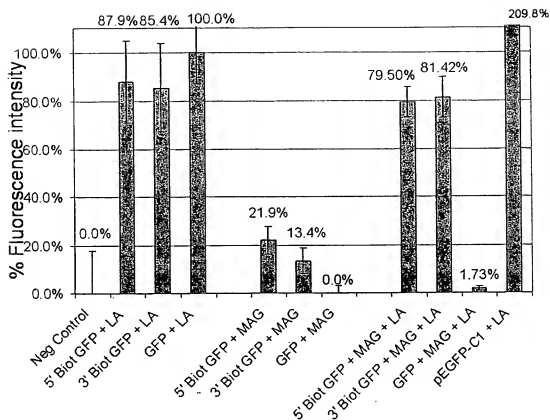
Figure 3. Expression levels of GFP from DNA tethered MN. In vitro gene expression levels are shown as the % of Lipofectamine transfected EGFP DNA (GFP+LA). Biotin tagged DNA was also transfected into cells (Biot GFP). Cells transfected with DNA bound nanoparticles are labeled BIOT+MAG. All samples were incubated with (LA) or without Lipofectamine 2000.

Figure 4. Expression of GFP from MN tethered to EGFP DNA. EGFP expression (green) and DNA (blue) are shown in these images. Untreated cells (Panel A), cells transfected with DNA fragments with 5', 3', and no biotin tags (Panels B, C, and D), and cells exposed to DNA tethered to MN from 5', 3', and no (control for free DNA) biotin tags (Panels E, F, and G are shown here.

Figure 5. Recovery and PCR of DNA tethered to magnetic nanoparticles. Agarose gel showing the PCR products of DNA tethered magnetic nanoparticles isolated from within cells. Lane A. 1kb marker; B. 5' tethered; C. 3' tethered; D. no tether; and E. positive control.

Figure 6. Magnetic nanoparticle delivery of genes in vivo. Fluorescent micrographs of 5 micron cryosectioned liver from rats injected intrahepatically with nanoparticles tethered to EGFP encoding DNA and coated with lipid. These sections were counterstained with DAPI. Green highlights indicate cells expressing GFP from nanoparticles.

Various basics of the invention have been explained herein. The various techniques and devices disclosed represent a portion of that which those skilled in the art would readily understand from the teachings of this application. Details for the implementation thereof can be added by those with ordinary skill in the art. Such details may be added to the disclosure in another application based on this provisional application and it is believed that the inclusion of such details does not add new subject matter to the application. The accompanying figures may contain additional information not specifically discussed in the text and such information may be described in a later application without adding new subject matter. Additionally, various combinations and permutations of all elements or applications can be created and presented. All can be done to optimize performance in a specific application.

The various steps described herein can be combined with other steps, can occur in a variety of sequences unless otherwise specifically limited, various steps can be interlineated with the stated steps, and the stated steps can be split into multiple steps. Unless the context requires otherwise, the word "comprise" or variations such as "comprises" or "comprising", should be understood to imply the inclusion of at least the stated element or step or group of elements or steps or equivalents thereof, and not the exclusion of any other element or step or group of elements or steps or equivalents thereof.

Further, any documents to which reference is made in the application for this patent as well as all references listed in any list of references filed with the application are hereby incorporated by reference. However, to the extent statements might be considered inconsistent with the patenting of this invention such statements are expressly not to be considered as made by the applicant(s).

Also, any directions such as "top," "bottom," "left," "right," "upper," "lower," and other directions and orientations are described herein for clarity in reference to the figures and are not to be limiting of an actual device, system, or process or implementation of the device, system, or process.

REFERENCES

Allander, T., X. Forns, S. U. Emerson, R. H. Purcell. and J. Bukh. 2000. Hepatitis C virus envelope protein e2 binds to cd81 of tamarins. *Virology* 277, no. 2: 358-67.

Barrera, J. M., M. Bruguera, M. G. Ercilla, C. Gil, R. Celis, M. P. Gil, M. del Valle Onorato, J. Rodes, and A. Ordinas. 1995. Persistent hepatitis C viremia after acute self-limiting posttransfusion hepatitis C. *Hepatology* 21, no. 3: 639-44.

Bartenschlager, R. 2002. In vitro models for hepatitis C. *Virus Res* 82, no. 1-2: 25-32.

Bartenschlager, R., A. Kaul, and S. Sparacio. 2003. Replication of the hepatitis C virus in cell culture. *Antiviral Res* 60, no. 2: 91-102.

Beard, M. R., L. Cohen, S. M. Lemon, and A. Martin. 2001. Characterization of recombinant hepatitis a virus genomes containing exogenous sequences at the 2a/2b junction. *J Virol* 75, no. 3: 1414-26.

Benns, J. M. and S. W. Kim. 2000. Tailoring new gene delivery designs for specific targets. *J Drug Target* 8, no. 1: 1-12.

Bizollon, T., C. Ducerf, C. Trepo, and D. Mutimer. 1999. Hepatitis C virus recurrence after liver transplantation. *Gut* 44, no. 4: 575-8.

Blanchard, K. L., J. Fandrey, M. A. Goldberg, and H. F. Bunn. 1993. Regulation of the erythropoietin gene. *Stem Cells* 11 Suppl 1: 1-7.

Blasberg, R. G. 2003. Molecular imaging and cancer. *Mol Cancer Ther* 2, no. 3: 335-43.

Bonnemain, B. 1998. Superparamagnetic agents in magnetic resonance imaging: Physicochemical characteristics and clinical applications. A review. *J Drug Target* 6, no. 3: 167-74.

Boyle, M. D., W. A. Wallner, G. O. von Mering, K. J. Reis, and M. J. Lawman. 1985. Interaction of bacterial fc receptors with goat immunoglobulins. *Mol Immunol* 22, no. 9: 1115-21.

Brenner, M. K. 1995. Human somatic gene therapy: Progress and problems. *J Intern Med* 237, no. 3: 229-39.

Cavazzana-Calvo, M., S. Hacein-Bey, G. de Saint Basile, F. Gross, E. Yvon, P. Nusbaum, F. Selz, C. Hue, S. Certain, J. L. Casanova, P. Bousso, F. L. Deist, and A. Fischer. 2000. Gene therapy of human severe combined immunodeficiency (scid)-x1 disease. *Science* 288, no. 5466: 669-72.

Chan, W. C., D. J. Maxwell, X. Gao, R. E. Bailey, M. Han, and S. Nie. 2002. Luminescent quantum dots for multiplexed biological detection and imaging. *Curr Opin Biotechnol* 13, no. 1: 40-6.

Check, E. 2002. A tragic setback. *Nature* 420, no. 6912: 116-8.

Chowdhury, N. R., C. H. Wu, G. Y. Wu, P. C. Yerneni, V. R. Bommineni, and J. R. Chowdhury. 1993. Fate of DNA targeted to the liver by asialoglycoprotein receptor-mediated endocytosis in vivo. Prolonged persistence in cytoplasmic vesicles after partial hepatectomy. *J Biol Chem* 268, no. 15: 11265-71.

Cornberg, M., H. Wedemeyer, and M. P. Manns. 2002. Treatment of chronic hepatitis C with pegylated interferon and ribavirin. *Curr Gastroenterol Rep* 4, no. 1: 23-30.

Cripe, L. D. and S. Hinton. 2000. Acute myeloid leukemia in adults. *Curr Treat Options Oncol* 1, no. 1: 9-17.

Cristiano, R. J., L. C. Smith, M. A. Kay, B. R. Brinkley, and S. L. Woo. 1993. Hepatic gene therapy: Efficient gene delivery and expression in primary hepatocytes utilizing a conjugated adenovirus-DNA complex. *Proc Natl Acad Sci U S A* 90, no. 24: 11548-52.

Cristiano, R. J., L. C. Smith, and S. L. Woo. 1993. Hepatic gene therapy: Adenovirus enhancement of receptor-mediated gene delivery and expression in primary hepatocytes. *Proc Natl Acad Sci U S A* 90, no. 6: 2122-6.

Cucinotta, F. A., W. Schimmerling, J. W. Wilson, L. E. Peterson, G. D. Badhwar, P. B. Saganti, and J. F. Dicello. 2001. Space radiation cancer risks and uncertainties for mars missions. *Radiat Res* 156, no. 5 Pt 2: 682-8.

Dautry-Varsat, A. 1986. Receptor-mediated endocytosis: The intracellular journey of transferrin and its receptor. *Biochimie* 68, no. 3: 375-81.

De Smedt, S. C., J. Demeester, and W. E. Hennink. 2000. Cationic polymer based gene delivery systems. *Pharm Res* 17, no. 2: 113-26.

Douglas, S. J., S. S. Davis, and L. Illum. 1987. Nanoparticles in drug delivery. *Crit Rev Ther Drug Carrier Syst* 3, no. 3: 233-61.

Dubertret, B., P. Skourides, D. J. Norris, V. Noireaux, A. H. Brivanlou, and A. Libchaber. 2002. In vivo imaging of quantum dots encapsulated in phospholipid micelles. *Science* 298, no. 5599: 1759-62.

Emery, D. W. and G. Stamatoyannopoulos. 1999. Stem cell gene therapy for the beta-chain hemoglobinopathies. Problems and progress. *Ann N Y Acad Sci* 872: 94-107; discussion 107-8.

Feray, C., L. Caccamo, G. J. Alexander, B. Ducot, J. Gugenheim, T. Casanovas, C. Loinaz, M. Gigou, P. Burra, L. Barkholt, R. Esteban, T. Bizollon, J. Lerut, A. Minello-Franza, P. H. Bernard, K. Nachbaur, D. Botta-Fridlund, H. Bismuth, S. W. Schalm, and D. Samuel. 1999. European collaborative study on factors influencing outcome after liver transplantation for hepatitis C. European concerted action on viral hepatitis (eurohep) group. *Gastroenterology* 117, no. 3: 619-25.

Fischer, A. 2001. Gene therapy: Some results, many problems to solve. *Cell Mol Biol (Noisy-le-grand)* 47, no. 8: 1269-75.

Flint, M., J. M. Thomas, C. M. Maidens, C. Shotton, S. Levy, W. S. Barclay, and J. A. McKeating. 1999. Functional analysis of cell surface-expressed hepatitis C virus e2 glycoprotein. *J Virol* 73, no. 8: 6782-90.

Flotte, T. R. 1993. Prospects for virus-based gene therapy for cystic fibrosis. *J Bioenerg Biomembr* 25, no. 1: 37-42.

Flotte, T. R. and B. J. Carter. 1995. Adeno-associated virus vectors for gene therapy. *Gene Ther* 2, no. 6: 357-62.

Forns, X., T. Allander, P. Rohwer-Nutter, and J. Bukh. 2000. Characterization of modified hepatitis C virus e2 proteins expressed on the cell surface. *Virology* 274, no. 1: 75-85.

Fraser, N. W. 1994. Herpes simplex virus-1 latency and its implications for gene therapy of the nervous system. *Gene Ther* 1 Suppl 1: S51.

Geller, A. I., K. Keyomarsi, J. Bryan, and A. B. Pardee. 1990. An efficient deletion mutant packaging system for defective herpes simplex virus vectors: Potential applications to human gene therapy and neuronal physiology. *Proc Natl Acad Sci U S A* 87, no. 22: 8950-4.

Ghobrial, R. M., D. G. Farmer, A. Baquerizo, S. Colquhoun, H. R. Rosen, H. Yersiz, J. F. Markmann, K. E. Drazan, C. Holt, D. Imagawa, L. I. Goldstein, P. Martin, and R. W. Busuttil. 1999. Orthotopic liver transplantation for hepatitis C: Outcome, effect of immunosuppression, and causes of retransplantation during an 8-year single-center experience. *Ann Surg* 229, no. 6: 824-31; discussion 831-3.

Ghosh, S. S., M. Takahashi, N. R. Thummala, B. Parashar, N. R. Chowdhury, and J. R. Chowdhury. 2000. Liver-directed gene therapy: Promises, problems and prospects at the turn of the century. *J Hepatol* 32, no. 1 Suppl: 238-52.

Gutfreund, K. S. and V. G. Bain. 2000. Chronic viral hepatitis C: Management update. *Cmaj* 162, no. 6: 827-33.

Hacein-Bey-Abina, S., C. von Kalle, M. Schmidt, F. Le Deist, N. Wulffraat, E. McIntyre, I. Radford, J. L. Villeval, C. C. Fraser, M. Cavazzana-Calvo, and A. Fischer. 2003. A serious adverse event after successful gene therapy for x-linked severe combined immunodeficiency. *N Engl J Med* 348, no. 3: 255-6.

Heng, G., L. Yongjun, Z. Yuehong, L. Changwei, Y. Jing, S. Cunxian, W. Pengyan, Z. Sanmei, W. Zongli, and S. Mingpeng. 2002. Nanoparticle as a new gene transferring vector in specific expression gene. *Chin Med Sci J* 17, no. 4: 220-4.

Herrmann, F. 1995. Cancer gene therapy: Principles, problems, and perspectives. *J Mol Med* 73, no. 4: 157-63.

Hino, K., S. Sainokami, K. Shimoda, H. Niwa, and S. Iino. 1994. Clinical course of acute hepatitis C and changes in hcv markers. *Dig Dis Sci* 39, no. 1: 19-27.

Ikeda, M., M. Yi, K. Li, and S. M. Lemon. 2002. Selectable subgenomic and genome-length dicistronic rnas derived from an infectious molecular clone of the hcv-n strain of hepatitis C virus replicate efficiently in cultured huh7 cells. *J Virol* 76, no. 6: 2997-3006.

Jaiswal, J. K., H. Mattoussi, J. M. Mauro, and S. M. Simon. 2003. Long-term multiple color imaging of live cells using quantum dot bioconjugates. *Nat Biotechnol* 21, no. 1: 47-51.

Kaiser, J. 2003. Gene therapy. Seeking the cause of induced leukemias in x-scid trial. *Science* 299, no. 5606: 495.

Kay, M. A., Q. Li, T. J. Liu, F. Leland, C. Toman, M. Finegold, and S. L. Woo. 1992. Hepatic gene therapy: Persistent expression of human alpha 1-antitrypsin in mice after direct gene delivery in vivo. *Hum Gene Ther* 3, no. 6: 641-7.

Kennedy, P. G. and I. Steiner. 1993. The use of herpes simplex virus vectors for gene therapy in neurological diseases. *Q J Med* 86, no. 11: 697-702.

Kotin, R. M. 1994. Prospects for the use of adeno-associated virus as a vector for human gene therapy. *Hum Gene Ther* 5, no. 7: 793-801.

Kuwabara, T., M. Warashina, S. Koseki, M. Sano, J. Ohkawa, K. Nakayama, and K. Taira. 2001. Significantly higher activity of a cytoplasmic hammerhead ribozyme than a corresponding nuclear counterpart: Engineered trnas with an extended 3' end can be exported efficiently and specifically to the cytoplasm in mammalian cells. *Nucleic Acids Res* 29, no. 13: 2780-8.

Latchman, D. S. 1994. Herpes simplex virus vectors for gene therapy. *Mol Biotechnol* 2, no. 2: 179-95.

Leary, J. F. 1994. Strategies for rare cell detection and isolation. *Methods Cell Biol* 42 Pt B: 331-58.

Lee, J. C., Y. F. Shih, S. P. Hsu, T. Y. Chang, L. H. Chen, and J. T. Hsu. 2003. Development of a cell-based assay for monitoring specific hepatitis C virus ns3/4a protease activity in mammalian cells. *Anal Biochem* 316, no. 2: 162-70.

Lee, P. A., L. M. Blatt, K. S. Blanchard, K. S. Bouhana, P. A. Pavco, L. Bellon, and J. A. Sandberg. 2000. Pharmacokinetics and tissue distribution of a ribozyme directed against hepatitis C virus rna following subcutaneous or intravenous administration in mice. *Hepatology* 32, no. 3: 640-6.

Lindsten, K., T. Uhlikova, J. Konvalinka, M. G. Masucci, and N. P. Dantuma. 2001. Cell-based fluorescence assay for human immunodeficiency virus type 1 protease activity. *Antimicrob Agents Chemother* 45, no. 9: 2616-22.

Lohmann, V., F. Korner, J. Koch, U. Herian, L. Theilmann, and R. Bartenschlager. 1999. Replication of subgenomic hepatitis C virus rnas in a hepatoma cell line. *Science* 285, no. 5424: 110-3.

Lvov, Y., A. A. Antipov, A. Mamedov, H. Mohwald, and G. B. Sukhorukov. 2001. Urease encapsulation in nanoorganized microshells. *Nano Letters* 1, no. 3: 125-128.

Lvov, Y. and F. Caruso. 2001. Biocolloids with ordered urease multilayer shells as enzymatic reactors. *Anal Chem* 73, no. 17: 4212-7.

Mamedov, A. A., A. Belov, M. Giersig, N. N. Mamedova, and N. A. Kotov. 2001. Nanorainbows: Graded semiconductor films from quantum dots. *J Am Chem Soc* 123, no. 31: 7738-9.

Mao, H. X., S. Y. Lan, Y. W. Hu, L. Xiang, and Z. H. Yuan. 2003. Establishment of a cell-based assay system for hepatitis C virus serine protease and its primary applications. *World J Gastroenterol* 9, no. 11: 2474-9.

Marshall, E. 1999. Gene therapy death prompts review of adenovirus vector. *Science* 286, no. 5448: 2244-5.

Martin, S. J. and D. R. Green. 1995. Protease activation during apoptosis: Death by a thousand cuts? *Cell* 82, no. 3: 349-52.

Maruyama, A., T. Ishihara, J. S. Kim, S. W. Kim, and T. Akaike. 1997. Nanoparticle DNA carrier with poly(l-lysine) grafted polysaccharide copolymer and poly(d,l-lactic acid). *Bioconjug Chem* 8, no. 5: 735-42.

McKenzie, R. C., J. R. Arthur, and G. J. Beckett. 2002. Selenium and the regulation of cell signaling, growth, and survival: Molecular and mechanistic aspects. *Antioxid Redox Signal* 4, no. 2: 339-51.

Mitchell, D. G. 1997. Mr imaging contrast agents--what's in a name? *J Magn Reson Imaging* 7, no. 1: 1-4.

Miyagishi, M., T. Kuwabara, and K. Taira. 2001. Transport of intracellularly active ribozymes to the cytoplasm. *Cancer Chemother Pharmacol* 48 Suppl 1: S96-101.

Mizutani, Y., Y. Okada, O. Yoshida, M. Fukumoto, and B. Bonavida. 1997. Doxorubicin sensitizes human bladder carcinoma cells to fas-mediated cytotoxicity. *Cancer* 79, no. 6: 1180-9.

Morgan, E. H. and E. Baker. 1988. Role of transferrin receptors and endocytosis in iron uptake by hepatic and erythroid cells. *Ann N Y Acad Sci* 526: 65-82.

Nakabayashi, H., K. Taketa, T. Yamane, M. Miyazaki, K. Miyano, and J. Sato. 1984. Phenotypical stability of a human hepatoma cell line, huh-7, in long-term culture with chemically defined medium. *Gann* 75, no. 2: 151-8.

Neutra, M. R., A. Ciechanover, L. S. Owen, and H. F. Lodish. 1985. Intracellular transport of transferrin- and asialoorosomucoid-colloidal gold conjugates to lysosomes after receptor-mediated endocytosis. *J Histochem Cytochem* 33, no. 11: 1134-44.

Nishikawa, M., S. Takemura, F. Yamashita, Y. Takakura, D. K. Meijer, M. Hashida, and P. J. Swart. 2000. Pharmacokinetics and in vivo gene transfer of plasmid DNA complexed with mannosylated poly(l-lysine) in mice. *J Drug Target* 8, no. 1: 29-38.

Ohnishi, T., A. Takahashi, and K. Ohnishi. 2001. Biological effects of space radiation. *Biol Sci Space* 15 Suppl: S203-10.

Paunesku, T., T. Rajh, G. Wiederrecht, J. Maser, S. Vogt, N. Stojicevic, M. Protic, B. Lai, J. Oryhon, M. Thurnauer, and G. Woloschak. 2003. Biology of tio2-oligonucleotide nanocomposites. *Nat Mater* 2, no. 5: 343-6.

Petersein, J., S. Saini, and R. Weissleder. 1996. Liver. Ii: Iron oxide-based reticuloendothelial contrast agents for mr imaging. Clinical review. *Magn Reson Imaging Clin N Am* 4, no. 1: 53-60.

Pfeifer, A. and I. M. Verma. 2001. Gene therapy: Promises and problems. *Annu Rev Genomics Hum Genet* 2: 177-211.

Pietschmann, T. and R. Bartenschlager. 2001. The hepatitis C virus replicon system and its application to molecular studies. *Curr Opin Drug Discov Devel* 4, no. 5: 657-64.

Pileri, P., Y. Uematsu, S. Campagnoli, G. Galli, F. Falugi, R. Petracca, A. J. Weiner, M. Houghton, D. Rosa, G. Grandi, and S. Abrignani. 1998. Binding of hepatitis C virus to cd81. *Science* 282, no. 5390: 938-41.

Poynard, T., V. Leroy, M. Cohard, T. Thevenot, P. Mathurin, P. Opolon, and J. P. Zarski. 1996. Meta-analysis of interferon randomized trials in the treatment of viral hepatitis C: Effects of dose and duration. *Hepatology* 24, no. 4: 778-89.

Prabha, S., W. Z. Zhou, J. Panyam, and V. Labhasetwar. 2002. Size-dependency of nanoparticle-mediated gene transfection: Studies with fractionated nanoparticles. *Int J Pharm* 244, no. 1-2: 105-15.

Qian, Z. M., H. Li, H. Sun, and K. Ho. 2002. Targeted drug delivery via the transferrin receptor-mediated endocytosis pathway. *Pharmacol Rev* 54, no. 4: 561-87.

Reynolds, A. R., S. Moein Moghimi, and K. Hodivala-Dilke. 2003. Nanoparticle-mediated gene delivery to tumour neovasculature. *Trends Mol Med* 9, no. 1: 2-4.

Rice, C. M. and C. H. Hagedorn, eds. 2000. *The hepatitis C viruses*. Current topics in microbiology and immunology ; 242. Berlin ; London: Springer.

Rijnbrand, R., P. J. Bredenbeek, P. C. Haasnoot, J. S. Kieft, W. J. Spaan, and S. M. Lemon. 2001. The influence of downstream protein-coding sequence on internal ribosome entry on hepatitis C virus and other flavivirus rnas. *Rna* 7, no. 4: 585-97.

Rogach, A. L., D. Nagesha, J. W. Ostrander, M. Giersig, and N. A. Kotov. 2000. "raisin bun"-type composite spheres of silica and semiconductor nanocrystals. *Chem Mater* 12: 2676-2685.

Romano, G., P. P. Claudio, H. E. Kaiser, and A. Giordano. 1998. Recent advances, prospects and problems in designing new strategies for oligonucleotide and gene delivery in therapy. *In Vivo* 12, no. 1: 59-67.

Sandberg, J. A., C. D. Sproul, K. S. Blanchard, L. Bellon, D. Sweedler, J. A. Powell, F. A. Caputo, D. J. Kornbrust, V. P. Parker, T. J. Parry, and L. M. Blatt. 2000. Acute toxicology and pharmacokinetic assessment of a ribozyme (angiozyme) targeting vascular endothelial growth factor receptor mrna in the cynomolgus monkey. *Antisense Nucleic Acid Drug Dev* 10, no. 3: 153-62.

Scherer, F., M. Anton, U. Schillinger, J. Henke, C. Bergemann, A. Kruger, B. Gansbacher, and C. Plank. 2002. Magnetofection: Enhancing and targeting gene delivery by magnetic force in vitro and in vivo. *Gene Ther* 9, no. 2: 102-9.

Schwartz, A. L. 1984. The hepatic asialoglycoprotein receptor. *CRC Crit Rev Biochem* 16, no. 3: 207-33.

Sjoquist, J., B. Meloun, and H. Hjelm. 1972. Protein a isolated from staphylococcus aureus after digestion with lysostaphin. *Eur J Biochem* 29, no. 3: 572-8.

Stewart, M., R. P. Baker, R. Bayliss, L. Clayton, R. P. Grant, T. Littlewood, and Y. Matsuura. 2001. Molecular mechanism of translocation through nuclear pore complexes during nuclear protein import. *FEBS Lett* 498, no. 2-3: 145-9.

Stockert, R. J. 1995. The asialoglycoprotein receptor: Relationships between structure, function, and expression. *Physiol Rev* 75, no. 3: 591-609.

Strauss, M. 1994. Liver-directed gene therapy: Prospects and problems. *Gene Ther* 1, no. 3: 156-64.

Sullenger, B. A. and E. Gilboa. 2002. Emerging clinical applications of rna. *Nature* 418, no. 6894: 252-8.

Teradaira, R., V. Kolb-Bachofen, J. Schlepper-Schafer, and H. Kolb. 1983. Galactose-particle receptor on liver macrophages. Quantitation of particle uptake. *Biochim Biophys Acta* 759, no. 3: 306-10.

Thomas, C. E., A. Ehrhardt, and M. A. Kay. 2003. Progress and problems with the use of viral vectors for gene therapy. *Nat Rev Genet* 4, no. 5: 346-58.

Thurnher, M., E. Wagner, H. Clausen, K. Mechtler, S. Rusconi, A. Dinter, M. L. Birnstiel, E. G. Berger, and M. Cotten. 1994. Carbohydrate receptor-mediated gene transfer to human t leukaemic cells. *Glycobiology* 4, no. 4: 429-35.

Tiefenauer, L. X., G. Kuhne, and R. Y. Andres. 1993. Antibody-magnetite nanoparticles: In vitro characterization of a potential tumor-specific contrast agent for magnetic resonance imaging. *Bioconjug Chem* 4, no. 5: 347-52.

Uzan, G., M. H. Prandini, and R. Berthier. 1995. Regulation of gene transcription during the differentiation of megakaryocytes. *Thromb Haemost* 74, no. 1: 210-2.

Vinceti, M., E. T. Wei, C. Malagoli, M. Bergomi, and G. Vivoli. 2001. Adverse health effects of selenium in humans. *Rev Environ Health* 16, no. 4: 233-51.

Violante, M. R. 1990. Potential of microparticles for diagnostic tracer imaging. *Acta Radiol Suppl* 374: 153-6.

Vrolijk, J. M., A. Kaul, B. E. Hansen, V. Lohmann, B. L. Haagmans, S. W. Schalm, and R. Bartenschlager. 2003. A replicon-based bioassay for the measurement of interferons in patients with chronic hepatitis C. *J Virol Methods* 110, no. 2: 201-9.

Wagner, E., K. Zatloukal, M. Cotten, H. Kirlappos, K. Mechtler, D. T. Curiel, and M. L. Birnstiel. 1992. Coupling of adenovirus to transferrin-polylysine/DNA complexes greatly enhances receptor-mediated gene delivery and expression of transfected genes. *Proc Natl Acad Sci U S A* 89, no. 13: 6099-103.

Wang, Y. X., S. M. Hussain, and G. P. Krestin. 2001. Superparamagnetic iron oxide contrast agents: Physicochemical characteristics and applications in mr imaging. *Eur Radiol* 11, no. 11: 2319-31.

Weigel, P. H. 1993. Endocytosis and function of the hepatic asialoglycoprotein receptor. *Subcell Biochem* 19: 125-61.

Wenk, J., P. Brenneisen, C. Meewes, M. Wlaschek, T. Peters, R. Blaudschun, W. Ma, L. Kuhr, L. Schneider, and K. Scharffetter-Kochanek. 2001. Uv-induced oxidative stress and photoaging. *Curr Probl Dermatol* 29: 83-94.

Wu, G. Y. and C. H. Wu. 1991. Delivery systems for gene therapy. *Biotherapy* 3, no. 1: 87-95.

Wu, X., H. Liu, J. Liu, K. N. Haley, J. A. Treadway, J. P. Larson, N. Ge, F. Peale, and M. P. Bruchez. 2003. Immunofluorescent labeling of cancer marker her2 and other cellular targets with semiconductor quantum dots. *Nat Biotechnol* 21, no. 1: 41-6.

Wunschmann, S., J. D. Medh, D. Klinzmann, W. N. Schmidt, and J. T. Stapleton. 2000. Characterization of hepatitis C virus (hcv) and hcv e2 interactions with cd81 and the low-density lipoprotein receptor. *J Virol* 74, no. 21: 10055-62.

Zauner, W., N. A. Farrow, and A. M. Haines. 2001. In vitro uptake of polystyrene microspheres: Effect of particle size, cell line and cell density. *J Control Release* 71, no. 1: 39-51.

Zhang, R., J. Durkin, W. T. Windsor, C. McNemar, L. Ramanathan, and H. V. Le. 1997. Probing the substrate specificity of hepatitis C virus ns3 serine protease by using synthetic peptides. *J Virol* 71, no. 8: 6208-13.

Zhu, M., W. G. Chapman, M. J. Oberley, W. W. Wasserman, and W. E. Fahl. 2001. Polymorphic electrophile response elements in the mouse glutathione s-transferase gsta1 gene that confer increased induction. *Cancer Lett* 164, no. 2: 113-8.

Zhu, M. and W. E. Fahl. 2000. Development of a green fluorescent protein microplate assay for the screening of chemopreventive agents. *Anal Biochem* 287, no. 2: 210-7.

Zhu, M., and Fahl, W. E. 2001. Functional characterization of transcription regulators that interact with the electrophile response element. *Biochem Biophys Res Commun* 289, no. 1: 212-9.

ABSTRACT

The present invention provides method, apparatus, and system to produce multifunctional and multi-step nanoparticle systems that follow a predictable and well defined sequence of events ("molecular programming") as laid out by a molecular chain of events. These events include, but are not limited to, events such as initial cell targeting, facilitation of cell entry, intracellular re-targeting, intracellular anchoring to the site of drug/gene delivery, drug or gene delivery, and controlled delivery of the drugs or genes within single cells through feedback loops facilitated by molecular biosensors and other molecules.

5

10

ABSTRACT:

To date, experiments with nanoparticle based gene delivery has only been possible in laboratories with considerable experience in the area of nanoparticle construction. We report a simple and cheap alternative to custom constructed nanoparticles for use in biological systems. Additionally, we show that magnetic nanoparticles can not only be used to deliver genes, but also that those same genes can be recovered from cells after expression for several days. We describe in detail the construction of layered nanoparticles that can be accomplished in minutes using commercially available components. Testing the nanoparticles for DNA bioconjugation is also discussed. These particles were able to deliver genes to a human hepatoma cell line, Huh-7. It was found that tethering orientation was relevant to gene expression. Several days after exposure to nanoparticles, the nanoparticle tethered genes could be recovered and amplified from populations. These data highlight the stability and biological usefulness of the DNA tethered to these nanoparticles. Finally, DNA tethered magnetic nanoparticles were capable of transfecting tethered genes in vivo.